

**Hydrological processes and impacts of climate change in  
the alpine catchment in the arid region—  
A case study on the Yarkant River basin in Karakoram**

**Jiao LIU  
May, 2017**

---



Faculty of Sciences  
Department of Geography

**Hydrological processes and impacts of climate change in  
the alpine catchment in the arid region—  
A case study on the Yarkant River basin in Karakoram**

Dissertation submitted in accordance with the requirement for  
the degree of doctor of science: Geography

Jiao Liu  
(Joint PhD of University of Chinese Academy of Sciences, China,  
and Ghent University, Belgium)

May, 2017

---

## **Members of Examination Committee**

Prof. dr. Veerle Van Eetvelde (co-chairman)

Department of Geography, Ghent University

Prof. dr. Xi CHEN (co-chairman)

Xinjiang Branch. Chinese Academy of Sciences

Prof. dr. Morgan De Dapper (secretaries)

Department of Geography, Ghent University

Prof. dr. Jean Bourgeois

Department of Archaeology, Ghent University

Prof. dr. Sidharta Gautama

Department of Telecommunication and Information, Ghent University

Prof. dr. Alishir Kurban

Xinjiang Institute of Ecology and Geography, Chinese Academy of Sciences

Prof. dr. Chi Zhang

Xinjiang Institute of Ecology and Geography, Chinese Academy of Sciences

Prof. dr. Geping Luo

Xinjiang Institute of Ecology and Geography, Chinese Academy of Sciences

Prof. dr. Anming Bao

Xinjiang Institute of Ecology and Geography, Chinese Academy of Sciences

## **Promoters**

Prof. dr. Tie Liu

Xinjiang Institute of Ecology and Geography, Chinese Academy of Sciences

Prof. dr. Philippe De Maeyer

Department of Geography, Ghent University

---

---

## Table of contents

---

Table of contents.....	I
List of figures.....	V
List of tables.....	VII
Acknowledgments.....	IX
<b>CHAPTER 1 .....</b>	<b>1</b>
Introduction.....	1
1.1 Overview .....	2
1.1.1 Hydrological processes .....	2
1.1.2 Hydrological model.....	4
1.1.3 Application of remote sensing.....	7
1.1.4 Climate change .....	8
1.2 Study area .....	10
1.2.1 Geographic features.....	10
1.2.2 Meteorological features .....	11
1.2.3 Hydrological features .....	13
1.3 Data sets.....	13
1.3.1 Station-based data .....	13
1.3.2 Remote sensing data.....	14
1.3.3 Climate change data .....	17
1.4 Rationale and synopsis .....	19
1.4.1 Research objectives and questions .....	19
1.4.2 Dissertation outline .....	21
1.4.3 Out of scope .....	23
References .....	24
<b>CHAPTER 2 .....</b>	<b>29</b>
Joint application of multiple models in hydrological processes study .....	29
ABSTRACT.....	30
2.1 Introduction .....	30
2.2 Study area .....	32
2.3 Hydrological model .....	32
2.3.1 SWAT.....	32
2.3.2 MIKE SHE .....	35

---

2.4 Methodology.....	36
2.4.1 Modeling .....	36
2.4.2 Calibration.....	38
2.5 Result and discussion.....	39
2.5.1 Simulation results.....	39
2.5.2 Runoff.....	41
2.5.3 Snow.....	42
2.5.4 Evapotranspiration .....	47
2.6 Summary and Conclusions .....	50
References .....	51
<b>CHAPTER 3 .....</b>	<b>55</b>
The responses of hydrological processes to the different input data .....	55
ABSTRACT.....	56
3.1 Introduction .....	56
3.2 Study area .....	58
3.3 Forcing data .....	58
3.3.1 Station data.....	58
3.3.2 TRMM.....	58
3.3.4 LST.....	60
3.3.4. PET.....	61
3.4. Methodology.....	61
3.4.1 Model programmes .....	61
3.4.2 Calibration.....	62
3.4.3 Hypothesis test .....	62
3.5 Results and discussion .....	64
3.5.1. Simulated discharges.....	64
3.5.2 Sensitivities of water components.....	66
3.5.3 Response of the hydrological processes.....	67
3.6 Conclusions .....	74
References.....	75
<b>CHAPTER 4 .....</b>	<b>79</b>
The effects of climate change on the hydrological processes.....	79
ABSTRACT.....	80
4.1 Introduction .....	80
4.2 Study area and data.....	83
4.3 Methodology.....	83



---

4.3.1 Modified QPM for precipitation .....	84
4.3.2 Delta method for temperature .....	86
4.3.3 Hydrological modeling.....	86
4.4 Future climate change.....	86
4.4.1 Precipitation .....	86
4.4.2 Temperature .....	90
4.5 Effects on hydrological processes .....	92
4.5.1 Variation in water components .....	92
4.5.2 Snow.....	93
4.5.3 Streamflow .....	98
4.5 Conclusions .....	101
References .....	102
<b>CHAPTER 5 .....</b>	<b>105</b>
General discussion .....	105
5.1 Summary and discussion of research questions .....	106
RQ1: How is hydrological processes described in different hydrological models?.....	107
RQ2: How do remote sensing data perform in hydrological modeling?...	110
RQ3: What are the responses of hydrologic components to forcing data?	111
RQ4: What are the effects of climate change on the hydrological processes? .....	113
5.2 Critical reflections on methodology .....	115
5.3 Recommendations for future work .....	117
5.3.1 Future work on model integration .....	117
5.3.2 Future work on diversified RSD .....	117
5.3.3 Future work on attribution analysis.....	117
References .....	118
<b>CHAPTER 6 .....</b>	<b>123</b>
General conclusion.....	123
Summary .....	127
Samenvatting (Dutch Summary).....	129
摘要 (Chinese Summary) .....	131
Curriculum Vitae (Bibliography).....	133

---

---

## List of figures

---

Figure 1.1 Hydrological flow chart of SWAT (a, Adapted from Arnold et al. 1998) and MIKE SHE (b, Adapted from Abbott et al. 1986a, 1986b). Boxes represent different hydrological processes, ellipses represent various water storage and arrows represent water flow directions.....	7
Figure 1.2. Locations of the Yarkant River basin and meteorological and hydrological stations .....	11
Figure 1.3 Land use types (a) in 2010 and elevation bands (b) in the Yarkant River basin .....	11
Figure 1.4 Monthly precipitation, pan-evaporation and temperature values at Tashkurgan station in 2000-2009 and discharge at Kaqun station in 2003-2009 .....	12
Figure 1.5 Outline of the dissertation .....	22
Figure 2.1 The observed and simulated discharges at Kaqun station during 2003~2009 in the daily scale (upper one) and monthly scale (under one) .....	40
Figure 2.2 The daily constitution of the simulation runoff from SWAT and MIKE SHE in Yarkant River basin .....	42
Figure 2.3 The simulated daily snowmelt from SWAT and MIKE SHE in the Yarkant River basin .....	43
Figure 2.4 The snow storage in the different elevation bands from SWAT and MIKE SHE in Yarkant River basin in 2003-2009 .....	44
Figure 2.5 Simulated snowpack of SWAT (1 <sup>st</sup> column), MIKE SHE in sub-basin(2 <sup>nd</sup> column) and MIKE SHE (3 <sup>rd</sup> column) in Yarkant River basin on 31 <sup>st</sup> Mar. (1 <sup>st</sup> row), 30 <sup>th</sup> Jun. (2 <sup>nd</sup> row), 30 <sup>th</sup> Sep. (3 <sup>rd</sup> row) and 31 <sup>st</sup> Dec. (4 <sup>th</sup> row) 2003 .....	46
Figure 2.6 Remotely sensed snow coverage (1 <sup>st</sup> row), simulated of MIKE SHE (2 <sup>nd</sup> row) in Yarkant River basin on 31 <sup>st</sup> Mar. (1 <sup>st</sup> column), 30 <sup>th</sup> Jun. (2 <sup>nd</sup> column), 30 <sup>th</sup> Sep. (3 <sup>rd</sup> column) and 31 <sup>st</sup> Dec. (4 <sup>th</sup> column) 2003.....	47
Figure 2.7 The daily average evapotranspiration of SWAT (1 <sup>st</sup> column), MIKE SHE in sub-basin(2 <sup>nd</sup> column) and MIKE SHE (3 <sup>rd</sup> column) in Yarkant River from Jan.~Mar. (first line), Apr.~Jun. (second line), Jul.~Sep. (third line), and Oct.~Dec (forth line) 2003 .....	49
Figure 3.1 Regression relation between the daily air temperature and LST at the Tashkurgan and Pishan station in 2000~2009 .....	61
Figure 3.2 The comparisons of daily discharge at Kaqun station between the TRMM (upper one), LST (middle one), GPET (under one) simulations and the STA simulation, observation.....	65

---

Figure 3.3 Boxplot of the mean monthly discharges at the outlet station derived from eight model programmes in 2003~2009 .....	66
Figure 3.4 Spatial distribution of the simulated mean annual snow storage by the STA, TRMM, LST and GPET model in the Yarkant River basin during 2003~2009. ....	68
Figure 3.5 The temporal distribution of snow storage in the different elevation bands. .	70
Figure 3.6 Spatial distribution of the mean annual precipitation for TRMM and SBD in the Yarkant River basin during 2003~2009 .....	70
Figure 3.7 Spatial distribution of the mean annual temperature between the station and TRMM data in the Yarkant River basin in 2003~2009.....	71
Figure 3.8 The spatial distribution of the simulated mean annual transpiration of the STA, TRMM, LST and GPET model in the Yarkant River basin during 2003~2009. ....	73
Figure 3.9 The temporal distribution of the mean monthly PET from SBD and RSD in the whole Yarkant River basin during 2003~2009.....	74
Figure 4.1 The mean frequency changes of the rainy days in each month of future periods relative to those of the history period determined by the 18 GCMs.....	87
Figure 4.2The mean quantile perturbations of precipitation intensity in each month of future periods relative to those of the history period determined by the 18 GCMs .	89
Figure 4.3 The amount change rates of the generated future monthly precipitation with respect to those observed in the history period.....	90
Figure 4.4 The mean monthly changes in temperature of future periods compared to those of the history period determined by the 18 GCMs.....	91
Figure 4.5 The monthly values of S/P in different periods in the Yarkant River basin...	94
Figure 4.6 The monthly volumes of snowpack change and snowmelt in each period in the Yarkant River basin in RCP4.5 .....	95
Figure 4.7 The monthly volumes of snowpack change and snowmelt in each period in the Yarkant River basin in RCP8.5 .....	96
Figure 4.8 The spatial distribution of the snowpack on August 31 <sup>st</sup> of the last year in each period under RCP4.5 (first row) and RCP8.5 (second row) .....	97
Figure 4.9 The distribution of permanent snow storage in the different elevation bands on August, 31 <sup>st</sup> of each period's last year.....	98
Figure 4.10 Average monthly discharge in each period at Kaqun station .....	99
Figure 4.11 Exceedance probabilities of the simulated discharge at Kaqun station in each period .....	100

---

## List of tables

---

Table 1-1 Development of the hydrological models.....	5
Table 1-2 Collected meteorological and hydrological data .....	14
Table 1-3 Detailed information on remote sensing data .....	15
Table 1-4 Detailed information on the 21 GCMs of CMIP5 .....	17
Table 1-5 Characteristics of different RCP datasets (Riahi et al, 2007; Van et al, 2007; Hijioka et al, 2008; Wise et al,2009) .....	18
Table 2-1 The PCG and TCG at different altitude groups of Yarkant River basin .....	38
Table 2-2 Statistical coefficients of the SWAT and MIKE SHE performances on daily and monthly scale .....	40
Table 2-3 The average annual values of the water components from SWAT and MIKE SHE inYarkant River basin in 2003-2009 .....	41
Table 2-4 The elevation ranges and area ratios of the elevation bands in Yarkant River basin parted in SWAT and MIKE SHE model.....	44
Table 3-1. Comparison between the raw and corrected TRMM precipitation .....	59
Table 3-2 Eight models in this research based on the different input data .....	61
Table 3-3 The formulation of the test's statistics and percentile of the F distribution of the main effects of three factors and their interaction .....	63
Table 3-4 The final values of the calibration parameters in different models .....	64
Table 3-5 Statistical coefficients of the performance of different models.....	66
Table 3-6 The probability $p$ values of the hypothesis $H_0$ test.....	67
Table 3-7 The snow covered area with a bigger depth than in STA and LST.....	71
Table 3-8 The amount of the mean annual transpiration for different land use types from four models in 2003~2009a.....	72
Table 4-1 The average, maximum/minimum values of the annual rainy days change factors in future periods relative to those of the history period determined by the 18 GCMs .....	88
Table 4-2 The increased rates of annual precipitation in future periods relative to the history period.....	90
Table 4-3 The average, maximum/minimum values of the annual rainy days change factors in future periods relative to those of the history period determined by the 18 GCMs .....	91

---

Table 4-4 The average yearly temperature determined the GCMs at Tashkurgan and Pishan station and the elevation lapse rates (EPR) were calculated based on these two stations. ....	92
Table 4-5 The annual amounts of the water balance components in the Yarkant River basin during each period.....	93
Table 5-1 Overview of the contents of this dissertation .....	108

---

## Acknowledgments

---

When this dissertation is coming to finish, my memory flashbacks and recalls all my experiences over the past four years. Many special moments bubble up, they are full of excited, cheerful, disappointed or stressful, and many emissions that I will never forget. However, at this moment, I am so grateful because all of these experiences have become priceless treasures in my life. During this doctoral program, I learned so much from the people around me, not only on the subject of my Ph.D. but also about the society in which we live. Without the guidance, assistance and support from people round me, this road would have been more difficult, colorless and boring. It is impossible to mention everyone here, but I would like to acknowledge the people who contributed in many ways to this academic work.

Above all, I would like to express my gratitude and appreciation to my co-promoter at Ghent University, Prof. Dr. Philippe De Maeyer. It was such a pleasant surprise when he accepted me to the joint Ph.D. program at UGent. Becoming his Ph.D. student was a turning point in my life. Since then, I have begun to know and understand how big this world is. Prof. De Maeyer's creative suggestion and wise guidance have enabled my progress toward this dissertation, and his extreme enthusiasm and patience have guaranteed that my study at UGent went well.

Many thanks are extended to my promoter at UCAS, Prof. Dr. Tie Liu. Four years ago, the choice enabled me to embark on my studies. When I came to Xinjiang, Prof. Liu helped me to open the gates of the academic world. Every step of progress in my study over the past four years has involved Prof. Liu's warm contributions. My every potential idea was encouraged by him, but when the flame of these ideas was going out, Prof. Liu always inspired me other new methods. With his kindness and approachability, the path of my PhD is clear and bright. Additionally, because of his tireless supervision, great passion, and intellectual inspiration, I found treasures and interests in the academic world and was given a perfect model for my future career.

I want show my appreciation to Prof. Dr. Anming Bao, the head of the GIS laboratory. Prof. Bao's support ensures that many potential possibilities of mine come to true and I can favorably finish this dissertation. His generous and enlightening advice have effectively enhanced my work. I thank Prof. Bao for creating such nice atmosphere for my study and work.

---

The special thanks given to Prof. Alishir Kurban must be mentioned. Thanks Prof. Kurban for his great help to my study in Ugent, and his suggestions are really implicational and available for my future life and job.

I also would like to thank my school colleagues in UGent, to Helga for the kind responses to any problems I have encountered, to Therese and Karine for the aiding my study, to Sabine for the earnest language corrections of this paper, to Soetkin and Ann for the recommendations given to each of my trip, to all members for the academic sharing on every Monday noon. I have received countless assistance from many people who I cannot list them all. However, to all of my dear colleagues, I will never forget your smiling faces that warm the heart of an international student. As well, I give my eternal thanks to Fang and Miao, whose company made everything more vivid and comfortable, in this way, sadness has been degraded and pleasures have been amplified.

Sincere thanks go to the people in Xinjiang Institute of Ecology and Geography who supported and happily participated in my study. Thanks to the teachers in the student office, namely, Chunhua Li, Bin Zhou and Ting Zou. Your work is a good foundation for my study. Additionally, to all the members of “Bao’s team”, I cannot count how many times we shared happiness with each other. I am especially thankful for Pengfei Zhang’s organization of many collegial gatherings. Additionally, I am thankful to Jinping Liu and Hao Guo for assistance with data processing. I wish you all the best in your future endeavors.

Finally, I offer the most sincere thanks to my parents, although they might not see this dedication. My parents are normal Chinese farmers with the characteristics of kindness, simplicity, strong work ethic and realism. They never imagine how I will be in future, but care if I am good or not at present. I know that they are proud of me, but they deserve to know that what I have accomplished thus far is meaningless without them.

Jiao Liu

22<sup>nd</sup> February 2017



# CHAPTER 1

## Introduction

---

*This chapter is divided into four sections. First, according to the theme of this dissertation, general background is introduced on the topics of hydrological processes, hydrological models, remote sensing data and climate change (Section 1.1). Second, detailed information on the Yarkant River basin is presented to establish why it was chosen as the case study (Section 1.2). and all of the datasets and sources used in this dissertation are also described (Section 1.3). Finally, the rationale and synopsis are discussed (Section 1.4)*

## **1.1 Overview**

With the persistently increased demands on water resources, related issues such as ecological degeneration, worsening environmental systems and aggravating water conflicts have been caused by a shortage of available water resources. These issues have attracted attentions of governments and scientists, and many studies have been conducted in response. Since effective water resource management is necessary to guarantee sustainability of ecological, economic and social system, understanding of hydrological processes is the foundation of water resources management. Currently, there is little study on the hydrological processes associated with the water cycle in the high alpine catchment. Consequently, the water system based on the water component cycle has become the most important topic in the water field in the 21<sup>st</sup> century (Xia, 2009).

### **1.1.1 Hydrological processes**

Hydrological processes are highly complex natural system that includes the interactions of many nature factors. Water movements in hydrological processes dominate the activities of natural life and even the evolutionary processes of the environment on earth. Indeed, human livelihood is confined to specific regions with appropriate water access. In the 1950s, a schematic framework of global water cycle was established, but the magnitude and distribution of the water components were still unclear. Since the 1970s, an increasing number of observational gauges for different hydrological components were installed in the field, and the measurement technologies were continually improved. Consequently, more and better observations were obtained. Based on quantitative analysis of these observations, clearer understandings of the water resource cycle processes and distribution were obtained on the global scale (Zhang et al, 2008). During this period, increasing attention was focused on investigation of water resources, but the physical characteristics of hydrological processes and mechanisms of water component interactions were still not understood unambiguously. Additionally, on the finer catchment scale, the density of gauges was not sufficient to describe the hydrological processes.

Until the 1990s, certain international organizations such as the World Climate Research Programme (WCRP), the International Geosphere Biosphere Programme (IGBP) (WMO, 1987) and the Biospheric Aspects of the Hydrological Cycle (BAHC) (Gao et al., 2000) began to focus on the characteristics of hydrological processes and the evolving rules of

water resources under global change, and all of these studies on the effects of spatial scales. During this period, with the development of the physically based distributed hydrological model, the hydrological models became the most popular and primary tools in the study of hydrological processes on the catchment scale. The hydrological modelling is based on a universal understanding of interactions among hydrological components, but the features of hydrological processes on catchment scale always vary from watershed to watershed. Therefore, in-depth studies of hydrological processes based on modeling are still necessary, especially in certain characteristic regions.

The arid regions add up to 40% of the global land area, and 38% of the world population lives in these places and faces a highly fragile environmental system. Even worse, the arid areas are predicted to expand to 50% under the high emission scenario of global change, and this expansion will pose a more severe challenge to human habitats (Huang et al., 2015). The Xinjiang Uygur Autonomous Province in northwest China is located in the Eurasian hinterland. Xinjiang is an emblematic arid region located far away from ocean and surrounded by high mountains. The average annual precipitation is approximately 150 mm, but pan-evaporation reaches 2800 mm in this region. Comparing its vast area, the limited water resources strongly restrict the local economic development and threaten the security of the ecosystem. Mountains, oases and deserts are the three basic ecological entities in nature, and the water cycle is strongly tied to the local geographical characteristics (Chen et al, 2012). Generally, rainfall and melt water in mountains are the main runoff-producing sources. The runoff is transported to the piedmont area and supports the development of oases, where most population is situated and most water is consumed. Due to the harsh climate, the rivers finally dry out and disappear in the plains area. The dominate landscapes are desert and bare land with sparse vegetation, which is a notably fragile ecological system.

In the arid region, most water resources are distributed in the independent inland river basin and with the domination of melt water in the mountain area, and development of the piedmont oasis mostly depends on the volumes of runoff derived from the mountain region whose hydrological system is particularly tied to the unequal characteristics of different seasons (Kang, 1998). The Consortium of Universities for the Advancement of Hydrological Science Inc. (CUAHSI) (Roger et al. 2004) also indicated the importance of mountainous hydrological processes and reported that the hydrological processes determine the water availability, land cover and influence the local climate in inland river basins. Therefore, a comprehensive understanding of the water resources in the mountain region is the foundation of water resources management for the downstream

oasis. However, the complex hydrological processes and extreme heterogeneity of response units in the high alpine catchment make the catchment modeling more difficult.

### **1.1.2 Hydrological model**

The hydrological model is a simplification of complex hydrological phenomena and an important tool used to study these hydrological processes (Beven, 2001). The development of the hydrological models during different periods is presented in Table 1-1. The mathematical equations used to describe one certain water movement were taken as the origins of the hydrological model (Chow et al, 1988), such as the Saint-Venant equation for surface runoff, the Richard equation for soil interflow in the unsaturated zone and the MacCarthy equation for channel flow. Since the 1950s, different water movements were joined from a systematic perspective, and the model focused on the processes of rainfall-runoff that established in this period. However, the physical relationships among water components were replaced by statistical relationships, and thus the models were referred to as “black-box models” in this period.

During the 1960s to the 1980s, the physically based model was developed, including the interactions of hydrological components and routing scheme for generating the final hydrography at the outlet. In this period, a number of lumped conceptual models were widely developed, such as the Stanford Watershed Model (Crawford and Linsley 1966), the Hydrologiska Fyrans Vattenbalans model (abbreviated as HBV) (Bergstrom 1972), the Nedbør-Afstrømnings Model (abbreviated as NAM) (Nielsen and Hansen 1973) and the Snowmelt Runoff Model (abbreviated as SRM) (Martinec 1975). These models have improved simulations of hydrological progresses on a catchment scale. Because they are simple and less data-intensive, the lumped conceptual models still have practical value in current hydrological studies. However, applications of these models also have been strongly restricted because they cannot reflect the heterogeneity of the catchment.

After the 1980s, improvements in computational power and spatial technology made it possible to implement heterogeneous simulations for the hydrological response units. Contemporary, the concerning of hydrology study also had been extended to the related issues, such as water quality, catchment ecological system, local climate change and human activities, these issues required to consider the differences of catchment hydrological processes. In this manner, the distributed hydrological models, which generally include a more strict and detailed physical foundation and development of a distributed parameter set, that differences in the hydrological response units can be reflected in the distributed hydrological models. Compared with other types of

hydrological models, the advantages of the distributed hydrological models include the following: i) more accurate and stricter describing in the physical mechanism of hydrological processes; ii) ease of simulating the response of hydrological processes to changes in an underlying surface (land use/cover change); iiv) ability to reflect the spatial heterogeneity of catchment; iv) ease of combination with geographic information and remote sensing data; and v) utility in assessment of ecology, climate change and water resources management strategies via coupling with other models.

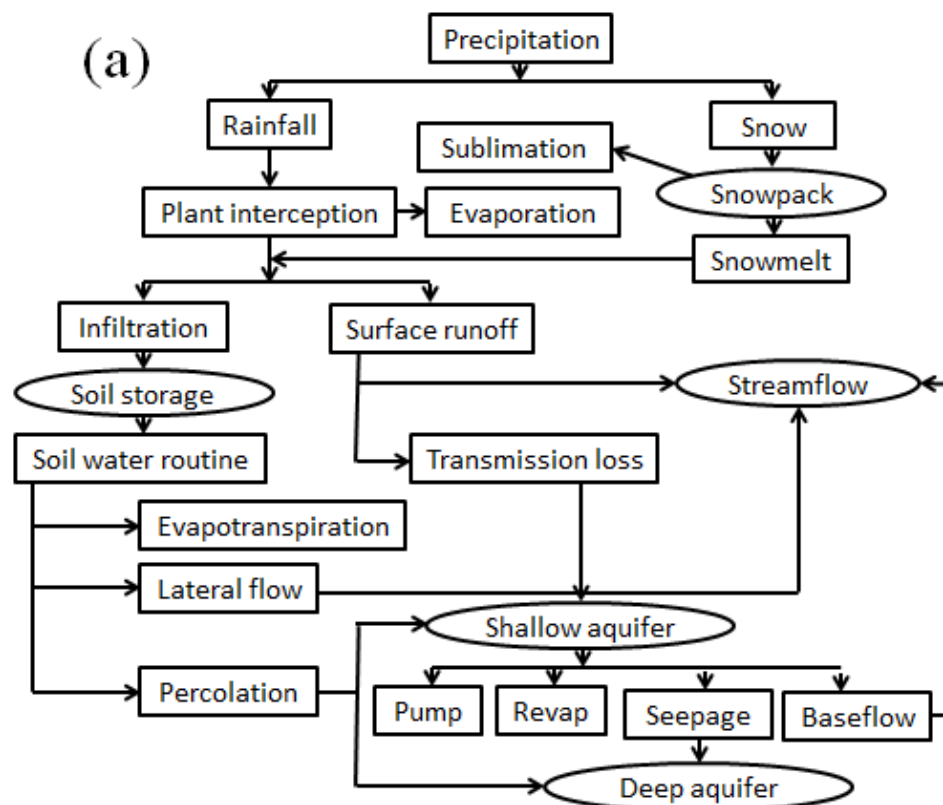
**Table 1-1 Development of the hydrological models**

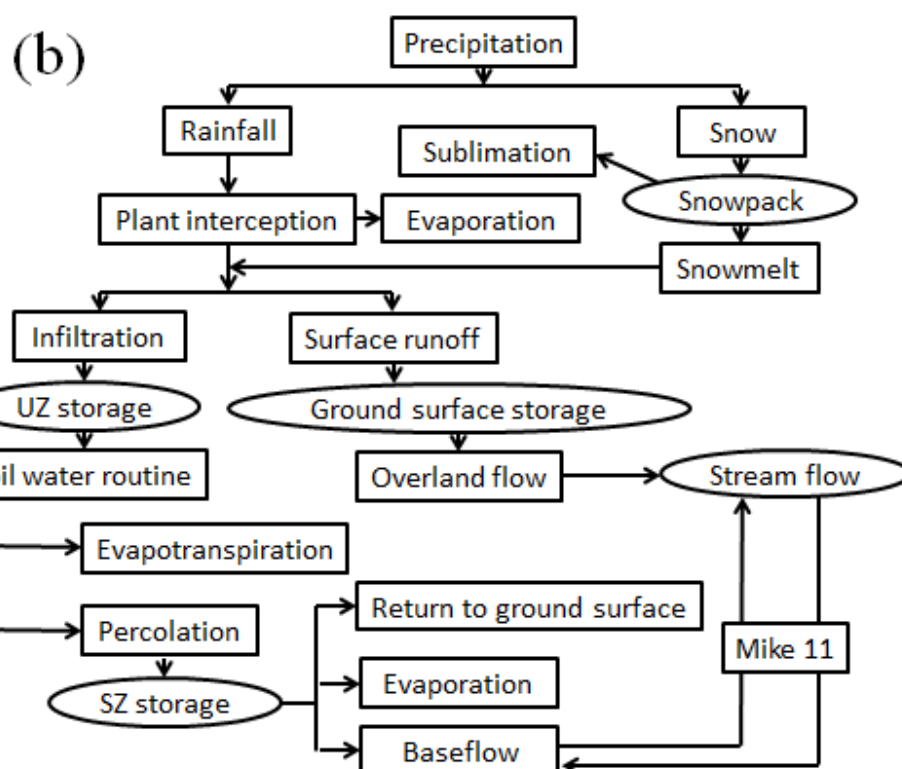
Period	Development	Explanation	Issues of concern
1930s-1950s	Establishment of related concepts and theories	Basic laws of water movement	Flood
1950s-1960s	Modeling of hydrological components	Relationship of rainfall-runoff	Flood
1960s-1980s	Lumped hydrological model	Hydrological processes on the catchment	Flood and water resources management
1980s~present	Distributed model and coupling of multiple models	Heterogeneity of the hydrology responses	Flood and water resources management, climate change, etc.

The Soil and Water Assessment Tool (SWAT) (Arnold, 1998) and the European Hydrological System (MIKE SHE) (Abbott, 1986a, 1986b) are currently the two most popular physically distributed hydrological models, which represent two distinct approach of hydrological modeling. In hydrological simulation of these two models, the water balance theory is used as the overall governing equation, and most hydrological processes are included. The hydrological flow charts are illustrated in Figure 1.1. These two models have been successfully applied in various fields world-wide, such as irrigation planning (Dechmi et al., 2012; Jayatilaka and Storn, 1998), flood forecasting (Zhang et al., 2014; Sahoo et al., 2006), influence of climate change on water resources (Najafi et al., 2011; Lirong et al., 2012), water pollution (Galván et al., 2009; Pisinaras et al., 2010), and exchange between surface and ground water (Bosson et al., 2012; Thompson et al., 2004) and so on.

Fontaine et al. (Fontaine, 2002) incorporated a modified snowfall-snowmelt routine using elevation bands in the SWAT model, and this improvement allowed the SWAT model to be used in mountainous catchments (Robert, 2008; Debele et al., 2009; Rahman et al., 2012). MIKE SHE is a determinate hydrological model in which the catchment is split into a number of square grids with elevation information, and the

meteorological data can be imported into each grid independently (DHI, 2007) such that the variation of precipitation and temperature with elevation can be reflected. The MIKE SHE model has been successfully applied in mountain terrains (Smerdon et al., 2009; Liu et al., 2012). Most studies in mountain watersheds with the SWAT or MIKE SHE model were primarily focused on snowmelt by a single model. The accuracy of a single model spatially applied in hydrological processes simulation seems incredulous (Sefton, 1997).





\*UZ: unsaturated zone, SZ: saturated zone

**Figure 1.1** Hydrological flow chart of SWAT (a, Adapted from Arnold et al. 1998) and MIKE SHE (b, Adapted from Abbott et al. 1986a, 1986b). Boxes represent different hydrological processes, ellipses represent various water storage and arrows represent water flow directions.

### 1.1.3 Application of remote sensing

The establishment and application of distributed hydrological models have higher requirements for forcing data relative to lump models. Furthermore, to produce a more accurate simulation, abundant and accurate data are also required for model's multiple calibrations. However, the gauged observations are hard to satisfy the complete requirements of hydrological modelling in mountainous regions, not matter in forcing or calibrating. In Xinjiang, the density of meteorological stations is quite low with one station per every 4000 km<sup>2</sup>. Even worse, most of gauged stations are located in front of the mountains, and the representativeness of these stations for the mountainous area is quite deficient. Therefore, scarcity of data further increases difficulties to apply the distributed hydrological models in high alpine catchment.

With respect to the ungauged and insufficiently gauged catchment, the International Association of Hydrological Sciences (IAHS) has specifically drawn up a key study plan known as Prediction in Ungauged Basins (PUB) (Sivapalan, 2003). The PUB plan

focuses on estimation of the predictive uncertainty and its subsequent reduction. According to this central theme, certain programs were suggested: 1) establishment of interpretation by reanalysis of previous data and comparison of different catchments; 2) development of catchment modeling based on selected new data sources such as remote sensing data; 3) improvement in the accuracy of hydrological process simulation through uncertainty analysis.

Remote sensing data offer the features of timely updates, wide coverage range, spatial distribution, abundant information and low costs (Bi et al., 2002). Applications of remote sensing data in the studies of hydrological process have greatly reduced the uncertainty related to forcing data and parameter estimation. In results, the simulations in ungauged or insufficiently gauged catchments have been improved. Generally, the application of remote sensing in hydrology can be summarized based on two aspects: i) the direct application as the measurement of hydrological data and parameters, such as snow-covered areas, land use types and precipitation, etc.; and ii) the indirect application in calculation of hydrological variables based on remote sensing spectrum, such as evapotranspiration and soil moisture content.

In the distributed hydrological model, the catchment is divided into grids or sub-basins that can be easily coupled with the grid remote sensing data. However, the scale matching between remote sensing data and the hydrology calculated units, and the precision of the remote sensing data are still two challenging issues. Consequently, due to the spatial resolution and accuracy of remotely sensed data, the necessary downscaling and bias correction has to be appropriately considered.

#### **1.1.4 Climate change**

There is not any doubt for the effects of climate change on water resources system in the world. The climate system is a complex system that scientists intend to describe the interactions of ocean, land and atmosphere, by combining a series of equations. In the past several decades, the world's meteorologists have made significant progress in building a dynamic framework that includes application of the semi-Lagrangian method, incorporation of a reference atmosphere, construction of an energy balance and improvement of the land surface model (Dai et al., 2003) as well as better computing techniques. After continuous development, the GCM that explains the climate system using mathematic-physical equations has been viewed as the main tool in studies of the interactive factors (Edwards, 2010). Indeed, a climate model is a mathematical tool used



to represent the physical and chemical processes via computer code such that climate-related scenario simulations can be run and future trends predicted at certain space and time scales (Lynch, 2008).

The United Nations Intergovernmental Panel on Climate Change (IPCC) Fifth Assessment Report (AR5) uses the Coupled Model Intercomparison Project Phase 5 (CMIP5) to forecast future climate change (IPCC, 2013). The average temperatures have increased by approximately 0.74 °C from 1906 to 2005, and on a global scale, these warming values are expected to continually increase by 0.3-4.8 °C at the end of the 21<sup>st</sup> century. Climate change could place greater pressures on the water system (Christierson et al., 2012), agriculture (Rosenzweig et al., 2014), forestry (Hanewinkel et al., 2013), ecological balance (Bellard et al., 2012), human health (Martens, 2014) and other related aspects. These issues have been of high concern to the scientific community, the public, and governments since the 1970s. In the mid-1980s, changes in hydrological cycling due to climate change became one of the hottest topics and issues of widest concern by scholars and scientists (Milly, 2007; Vorosmarty et al., 2000).

Water is a primary factor in atmospheric circulation, and the impact of climate change on hydrological processes is strong, including many aspects of precipitation, stream runoff, evapotranspiration, soil water contents and so on. These changes could result in temporal and spatial re-distribution of water resources and might drive a greater frequency and stronger intensity of extreme floods and droughts. All of these evidences pose serious challenges to water resources management and sustainable development of society and ecosystem in the future. In addition, agricultural water requirements have also increased with global warming (Roosmalen et al., 2016). In short, the impact of climate change on water resources is profound and has great significance.

For inland river basins in arid region, snowpack and glacier melt water contribute a great proportion to their total stream runoff. Glaciers are also known as “solid reservoirs” and “water towers” in arid regions, and their melt water is highly sensitive to climate change. IPCC (2013) stated that global glaciers and spring snow coverage in the northern hemisphere have already decreased in area by 15-85% and 7-15%, respectively, because of global warming. Arid regions with fragile ecological systems and weak stability are highly sensitive to climate change. The availability of water resources are so important that it literally means life for human, livelihood and ecosystem security. Climate change has strongly affected the hydrothermal conditions in mountain regions in terms of the runoff producing. In the background of global warming, the adjustment capacity of

glaciers to water resources is decreasing that reduction corresponds to shrinking of these “solid reservoirs”. In this manner, the uncertainties in the water cycle have increased in mountain regions. The stability of ecological systems in downstream oases has been threatened under the current climate change situation due to the uncertainty of water resources.

## **1.2 Study area**

### **1.2.1 Geographic features**

The Yarkant River (Figure 1.2) located in the southwestern margin of Xinjiang province is the longest headstream of the Tarim River, which is the largest inland river in the world. The Tarim River basin is one of the largest closed hydrological drainage systems and is ideal land for agriculture. No runoff contributes to the main channel of the Tarim River, and all of the water consumption comes from the headstreams. The Yarkant River is located between 74°28'-80°54' E and 34°50'-40°31' N, the length of main channel is near 1097 km, and the total area is approximately  $9.89 \times 10^4 \text{ km}^2$ . The mountainous area is approximately  $6.08 \times 10^4 \text{ km}^2$  and accounts for 61.5% of the region. The Yarkant River originates from the north slope of Karakoram, which contains an irrigated district, the Yarkant River oasis, with an area of  $2.5 \times 10^4 \text{ km}^2$  in the downstream of outlet hydrological station Kaqun. After outflow from this oasis, the Yarkant River passes by the Taklimakan desert and turns to the northeast. Finally, the Yarkant River converges with the Kashgar River, Aksu River and Hetian River to the south of Aksu oasis, and these streams flow into the Tarim River together.

In this paper, the mountain area upstream of Kaqun station is chosen as the study area (Figure 1.2). This region is located in the southern portion of Central Asia and the northwest Tibetan Plateau, far away from the ocean and the typical arid regions of the world. The area of this study region covers approximately  $50,248 \text{ km}^2$ . The study catchment has highly complex terrain, and generally, the southern portion is much higher in elevation than the northern portion. The topography varies from 8611 m (Chogori peak, the second highest peak in the world) to 1450 m with an average elevation of 4450 m. Mountains, gorges and basins are staggered in this region. The land cover types in this study area maintain a close relationship with the altitude distribution and present a strong spatial heterogeneity (Figure 1.3). Snowpack and glaciers are the uppermost land use type, contributing 26.14% and mainly situated in the region above 5000 m. The other major land cover types are closed-open herbaceous, bare land and

sparse herbaceous areas normally located at less than 5000 m, with contributions of 29%, 20% and 19.1%, respectively. Small closed open shrubs and evergreen needle-leaved trees are distributed around the outlet district.

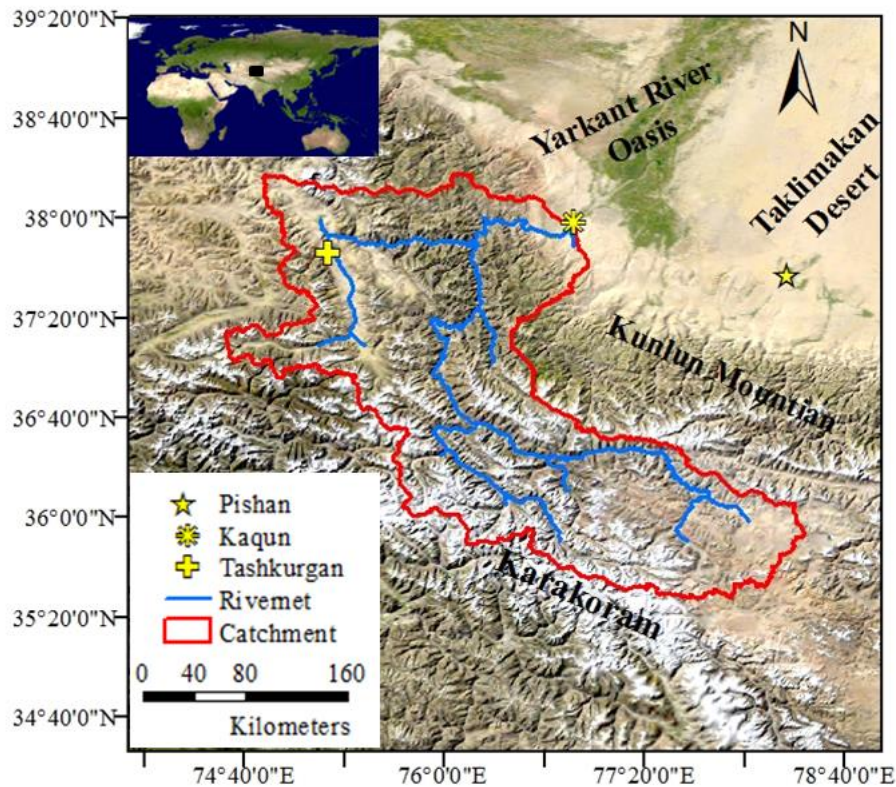


**Figure 1.2.** Locations of the Yarkant River basin and meteorological and hydrological stations

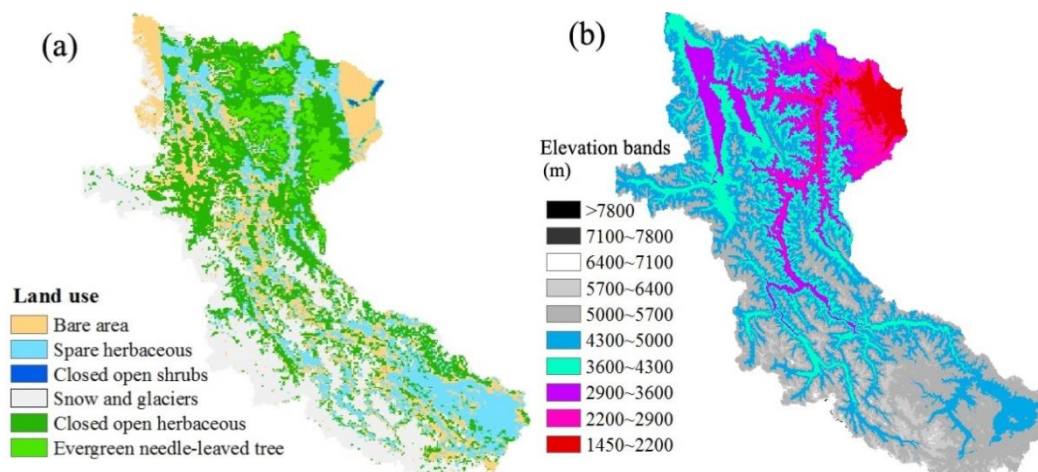


**Figure 1.3** Land use types (a) in 2010 and elevation bands (b) in the Yarkant River basin

### 1.2.2 Meteorological features

The Yarkant River basin is primarily controlled by the westerly airflow, and a small

proportion area is affected by the Indian Ocean southwest monsoon. According to the geographic location and terrain, the Yarkant River basin can be divided into five climatic regions: Kunlun Mountain region, Pamirs region, low mountain and hill region, plain region and desert region (Sun et al. 2006). In the mountain region, the winter is lengthy and cold, spring and autumn are short and windy, and summer is not evident. Because of the great entrapment capacity of the high mountains for water vapor at high altitude, the precipitation increases and the temperature decreases significantly with increasing elevation. The heterogeneity of precipitation and temperature is quite large in spatial distribution. The annual precipitation is approximately 450 mm in the high altitude areas (higher than 5000 m) and only 100 mm in the lower region (approximately 3000 m). The mean temperature near the snowline (approximately 5500 m) is approximately  $-10.5^{\circ}\text{C}$ , and this value is near  $11.8^{\circ}\text{C}$  in the plains region (Kang, 2009; Wang et al, 2009; Gao et al., 2010).

The study area is a rarely observable catchment with only one internal meteorological station (Tashkurgan) and two adjacent stations (Shache and Pishan). Based on the records of the Tashkurgan station in 2000-2009, with an annual mean value of 1516.2 mm, the pan-evaporation is much higher than the precipitation, which has an annual mean value of only 93.4 mm. The average temperature is  $3.84^{\circ}\text{C}$ . The monthly distributions of these characteristics are shown in Figure 1.4.

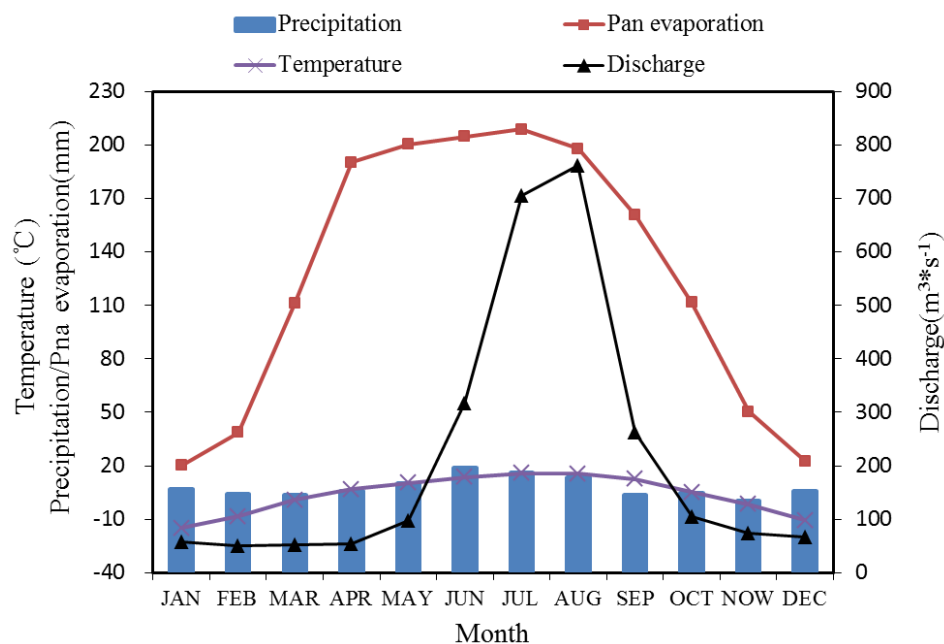


**Figure 1.4 Monthly precipitation, pan-evaporation and temperature values at Tashkurgan station in 2000-2009 and discharge at Kaqun station in 2003-2009**

### 1.2.3 Hydrological features

Due to storage of cold air in the mountainous region and the abundant precipitation, valley glaciers are highly developed in the Yarkant River basin. Based on the second Chinese glacier inventory (Feng et al. 2015), the total number of glaciers is 3247, and the estimated amount of ice storage is  $642.1 \text{ km}^3$ . 10 glaciers with a length of more than 20 km and a covered area larger than  $70 \text{ km}^2$ , the largest glacier is found in the Insulati Valley with a length of 42 km and an area of  $380 \text{ km}^2$ . Chogori (8611 m) and Muztaga (7546 m) mountain peaks, and dozens of snow-covered mountains at an altitude of more than 6000 m are also developing in this region. Because of the melt water in the mountain region, a rich volume of average annual stream runoff with a value of  $6.87 \times 10^{10} \text{ m}^3$  is observed at Kaqun Station. The temporal distribution of discharge is non-uniform during the year, and the proportion from June to September is nearly 80% of the total annual runoff (Figure 1.4).

The water resources from the mountain area support the development of the Yarkant River oasis. In this oasis, the dominant economy is irrigated agriculture that is highly dependent on the available water derived from the mountain area. This irrigated district is a major grain- and cotton-producing region and the largest agricultural irrigation region in Xinjiang (Tang et al., 2013). A population of 2 million lives in the Yarkant River oasis. However, this oasis is situated at the eastern edge of the Tahlimak Desert. Because of the harsh climate conditions, the ecological system of this oasis is highly vulnerable and strongly restricted by the water resources from the study area.

## 1.3 Data sets

The two most popular spatially distributed hydrological models, SWAT and MIKE SHE, were implemented in this research. Due to the problem of low density of gauging stations, traditional station-based data (SBD) and remote sensing data (RSD) were used to drive and verify the models. Furthermore, 21 GCMs productions in CMIP5 were chosen as the data resources in the climate change study.

### 1.3.1 Station-based data

The gauged meteorological data were obtained from the China Meteorological Data Sharing Service System (<http://cdc.cma.gov.cn/home.do>), and the necessary meteorological factors were collected from the three stations with available long-term

records. The records from internal station Tashkurgan were used to drive the model. Alternatively, two other adjacent station records from Shache and Pishan were mainly used to calculate the lapse rate of precipitation and temperature and to verify bias corrections of remote sensing data. The data for 1986-2005 were used in the climate change study, and data from 2003-2009 were used to set up the hydrological models. The Tarim Water Resources Management Bureau supported the discharges records at the Kaqun hydrological station. This bureau is a local governmental agency that oversees all affairs related to water resources in the Tarim River basin. The achieved discharge data were the only observations that can be used to calibrate the model outputs. The detailed information on the stations and collected data is listed in Table 1-2.

**Table 1-2 Collected meteorological and hydrological data**

Station	Location	Elevation	Data	Period
Tashkurgan	75.14E, 37.46N	3090.1 m	Daily precipitation, maximum/minimum/ average temperature, wind speed, relative humidity, solar radiation	1986-2009
Pishan	78.17E, 37.37N	1375.4 m		
Shache	77.16E, 38.26N	1231.2 m		
Kaqun	76.90E, 37.98N	1450.0 m	Daily discharge	2003-2009

### 1.3.2 Remote sensing data

Except for the necessary geodata, to overcome the problem of the weak SBD representativeness, spatially distributed RSD including precipitation, temperature, and potential evapotranspiration (PET) were obtained to replace the corresponding SBD and analyze the effects of different input data sources on the hydrological processes. Considering the importance of snow in the study area, remotely sensed snow cover area data were applied to verify the model outputs. The spatially distributed RSDs and their included properties are given in Table 1-3.

### DEM

The Digital Elevation Model (DEM) is sourced from the Shuttle Radar Topography Mission (STRM) (<http://srtm.csi.cgiar.org/>), originally produced by the National Aeronautics and Space Administration (NASA). The DEM acts as the primary geodata for the hydrological model, and both the basic geomorphologic factors including elevation, slope gradient and direction et al. were given in the DEM as well as the catchment boundary, river network and depression information.

## Land use

Based on the Landsat Thematic Mapper (TM) data, the land use is supported by the Xinjiang Institute of Ecology and Geography, Chinese Academy of Sciences. According to the plant cover types, parameters such as leaf area index (LAI), root depth (RD), crop coefficient ( $K_c$ ) and growth cycle were obtained.

**Table 1-3 Detailed information on remote sensing data**

Data	Resource	Resolution	Property
DEM	SRTM	90 m $\times$ 90 m	Elevation
Land use	Based on the Landsat TM	.shp file	Ground surface covering types
Soil types	HWSD	500 m $\times$ 500 m	Soil types and physical characters
Precipitation	TRMM	0.25° $\times$ 0.25°	Daily precipitation
Temperature	MODIS 11C1	0.05° $\times$ 0.05°	Daily average land surface temperature
PET	FEWS NET Data Portal	1° $\times$ 1°	Daily PET
Snow coverage	MODIS 10A2	500 m $\times$ 500 m	Largest snow covered area in 8 days

## Soil

Using the data from the Harmonized World Soil Database (HWSD) archived by the Flood and Agriculture Organization (FAO) and the International Institute for Applied Systems Analysis (IIASA), the different soil types were obtained, and the corresponding physical characteristics were calculated.

## Precipitation

The remotely sensed precipitation data were sourced from the Tropical Rainfall Measuring Mission (TRMM), a joint mission between NASA and the Japan Aerospace Exploration (JAXA) Agency intended to study rainfall for weather and climate research. Although the TRMM satellites stopped collecting data on April 15, 2015, the 17-year TRMM dataset is still an important space standard for measuring precipitation. The initial purpose of the TRMM was to measure the rainfall throughout the tropics, where most of the world's rain of the word, and the products covered from 35 degrees south to 35 degrees north in latitude. After August 2001, the orbital altitude was shifted to 403 km from 350 km, and larger ranges could be detected by the TRMM. Finally, the spatial coverage extended from 50 degrees south to 50 degrees north in latitude in the production of 3B42 and 3B43. Therefore, the TRMM products can be used in the study area. Important changes in 3B42 included the algorithm and verification, the algorithm

was improved by adjusting the merged-infrared precipitation rate and root-mean-square precipitation-error, and based on the 3B42 and gauged rainfall from the Global Precipitation Climatology Centre (GPCC), a monthly best-estimate precipitation rate was achieved using inverse-error-variance weighting (Huffman et al., 2001; 2007).

### **Temperature**

The Moderate Resolution Imaging Spectroradiometer (MODIS) land surface temperature (LST) was chosen as the data source for the required temperature calculation. The MODIS LST products contain global attributes (metadata) and scientific data sets (SDSs) (arrays) with local attributes, and they were validated with in situ measurements in more than 50 clear-sky cases over a temperature range from -10 °C to 58 °C (Wan et al., 2002; 2004; Coll et al., 2005). MODIS 11C1 is the fifth product in level 3 and is a daily global LST product in a geographic projection. This product is created by assembling the MOD11B1 daily tiles and resampling the SDSs at 6 km grids to a 0.05-degree spatial resolution.

### **Potential evapotranspiration**

The daily global PET derived from the United States Geological Survey (USGS) FEWS NET Data Portal (<http://earlywarning.usgs.gov/fews/>) was calculated from climate parameter data extracted from the Global Data Assimilation System (GDAS) analysis fields. The GDAS data were generated every 6 hours by the National Oceanic and Atmospheric Administration (NOAA). The GDAS fields used as input to the PET calculation include air temperature, atmospheric pressure, wind speed, relative humidity, and solar radiation (longwave, shortwave, outgoing and incoming). PET was computed for each 6-hour period and summed to obtain the daily totals.

The daily PET was calculated on a spatial basis using the Penman-Monteith equation (the formulation of Shuttleworth (1992) for reference crop evaporation is used). These equations were standardized in accordance with FAO publication 56 for the 6-hour calculations (Allen et al, 1998). These PET data have a 1-degree ground resolution and are global in spatial extent (-180 to +180 longitude by -90 to +90 latitude).

### **Snow coverage**

The snow coverage data were sourced from the MODIS product. Because snow-covered land typically has a notably high reflectance in the visible bands and rather low reflectance in the shortwave infrared band, the Normalized Difference Snow Index (NDSI) was used to detect the snow cover. If a cell's NDSI was larger than 0.4 and the



reflectivity in channel 2 was greater than 11%, this grid was identified as snow covered. If the snow and cloud could not be differentiated, the cloud mask was applied to correct the snow coverage data.

The maximum snow cover extent was generated by readings over 8 days. If snow was observed in a cell on any day in the period, the cell was mapped as snow. If no snow was found, the cell was filled with the clear-view observation that occurred most often (e.g., snow-free land, lake, etc.). Cloud cover was only reported if the cell was obscured by clouds for all eight days in the period. Each cell's snow/no snow chronology was recorded using bit flags and delivered as a separate variable.

### 1.3.3 Climate change data

GCMs have been developed based on mathematical modeling of the general circulation of the planetary atmosphere, land, oceans and the Navier-Stokes equations on a rotating sphere with thermodynamic terms for various energy sources such as radiation and latent heat. The IPCC was cofounded by the World Meteorological Organization (WMO) and the United Nations Environment Programme (UNEP) in 1988 and is a scientific intergovernmental body tasked with evaluating the risk of climate change caused by human activity. To develop improved methods and tools for diagnosis and comparison of general circulation models that simulate the global climate, 20 climate modeling groups from around the world decided to promote a new set of coordinated climate model experiments what is known as CMIP5 in 2008. According to this work, a total of 21 GCMs of CMIP5 were downloaded in this dissertation to study local climate change at an average ensemble level. Their information is listed in Table 1-4.

**Table 1-4 Detailed information on the 21 GCMs of CMIP5**

Order	Name	Institute	Resolution
1	BCC-CSM1.1-m	Beijing Climate Center, China Meteorological Administration	1.12°× 1.12°
2	CanESM2	Canadian Centre for Climate Modeling and Analysis	2.79°× 2.82°
3	CMCC-CM	Centro Euro-Mediterraneo per I Cambiamenti Climatici	0.75°× 0.75°
4	CNRM-CM5	Centre National de Recherches Meteorologiques / Centre Europeen de Recherche et Formation Avancees en Calcul Scientifique	1.4°× 1.4°
5	ACCESS1.3	CSIRO (Commonwealth Scientific and Industrial Research Organisation, Australia), and BOM (Bureau of Meteorology, Australia)	1.25°× 1.87°
6	CSIRO-Mk3.6.0	CSIRO (Commonwealth Scientific and Industrial	1.87°× 1.87°

		Research Organisation) in collaboration with the Queensland Climate Change Centre of Excellence	
7	BNU-ESM	College of Global Change and Earth System Science, Beijing Normal University	2.77°× 2.81°
8	INM-CM4	Institute for Numerical Mathematics	2.0°× 2.0°
9	IPSL-CM5B-LR	Institute Pierre-Simon Laplace	1.9°× 3.75°
10	FGOALS-g2	LASG, Institute of Atmospheric Physics, Chinese Academy of Sciences; and CESS, Tsinghua University	2.79°× 2.81°
11	MIROC5	Atmosphere and Ocean Research Institute (The University of Tokyo), National Institute for Environmental Studies, and Japan Agency for Marine-Earth Science and Technology	1.4°× 1.4°
12	MIROC-ESM	Atmosphere and Ocean Research Institute (The University of Tokyo), National Institute for Environmental Studies, and Japan Agency for Marine-Earth Science and Technology	2.79°× 2.81°
13	HadGEM2-ES	Met Office Hadley Centre	1.875°× 2.5°
14	MPI-ESM-LR	Max Planck Institute for Meteorology (MPI-M)	1.87°× 1.87°
15	MRI-ESM1	Meteorological Research Institute	1.125°× 1.125°
16	GISS-E2-R	NASA Goddard Institute for Space Studies	2°× 2.5°
17	CCSM4	National Center for Atmospheric Research	1.25°× 1.87°
18	NorESM1-M	Norwegian Climate Centre	1.9°× 2.5°
19	GFDL-CM3	Geophysical Fluid Dynamics Laboratory	2.0°× 2.5°
20	GFDL-ESM2G	Geophysical Fluid Dynamics Laboratory	2°× 2.5°
21	CESM1(BGC)	National Science Foundation, Department of Energy, National Center for Atmospheric Research	0.94°× 1.25°

**Table 1-5 Characteristics of different RCP datasets** (Riahi et al, 2007; Van et al, 2007; Hijioka et al, 2008; Wise et al, 2009)

RCP	Emission pathway	Radiative forcing	Concentration of CO <sub>2</sub>
RCP2.6	Low emission Reduce after peaking	2.6 W/m <sup>2</sup> in 2100	490 ppm in 2100
RCP4.5	Sustainable emission Steady under critical level	Less than 4.5 W/m <sup>2</sup> in 2100	650 ppm in 2100
RCP6.0	Sustainable emission Steady under critical level	Less than 6 W/m <sup>2</sup> in 2100	860 ppm in 2100
RCP8.5	High emission Continuous increase	8.5 W/m <sup>2</sup> in 2100	1370 ppm in 2100

Based on CMIP5, the AR5 of IPCC was issued in 2013. The Four Representative Concentration Pathways (RCP2.6, RCP4.5, RCP6, RCP8.5) database aimed to document

the emissions, concentrations, and land-cover change projections were provided to public. The RCPs dataset contained individual scenarios with common themes according to their 2100 radiative forcing level. The radiative forcing estimates were based on the forcing of greenhouse gases and other forcing agents but did not include direct impacts of land use (albedo) or forcing of mineral dust. The characteristics of different RCP datasets are listed in the following table. The RCP4.5 and RCP8.5 dataset were used in this study. In this dissertation, the RCP4.5 (an average emission level) and RCP8.5 (an extremely high emission level) were investigated to “average” and “extreme high” influence of climate change, and help us to know the “average” and “extreme” situations of hydrological processes in the future.

## **1.4 Rationale and synopsis**

### **1.4.1 Research objectives and questions**

Shortage of water resources is a prime restriction factor for the sustainable development of an arid region, and the stream runoff generated in the mountains and transferred to the piedmont supports the water resources demands of oasis in downstream. This dissertation is based on the perspective of the water cycle system and aims to offer an accurate understanding of the hydrological processes in the mountain catchment of an arid region, and provide the scientific supporting to water resources management in the downstream region. As the basic and important tool, hydrological models' performances in mountainous hydrological processes must be clarified. Firstly, the uncertainties derived from structure, algorithm input data and their effects on hydrological processes must be understood. This understanding is applicable not only for the current situation but also for variations under different climate change scenarios to predict future variances. In order to achieve this goal, the following questions must be answered.

***Question 1: How is the hydrological processes described in different hydrological models?***

Prompt development of the physically distributed hydrological models has made the hydrological model to be the most convenience tool for the studies of hydrological processes. While, the performances differ from region to region since the catchment conditions, and differ from model to model since the model structure and algorithm. For the particular catchment such as the Yarkant River basin in Karakoram, the extreme topographical and meteorological changes had made it difficult to correctly understand water cycle processes. The multiple calibrations of hydrological models in this

catchment should be basic efforts for simulated performances in hydrological processes (Refsgaard, 1997; Madsen, 2003), whereas insufficiently gauged observations in mountain catchment cannot support the multiple calibrations and a single-calibrated objective might negatively impact the other outputs of water components. Therefore, how is the performance of the hydrological models in such particular catchment? The model's performances decide the understanding of hydrological processes, accurate evaluation of model's simulation is a fatal problem for understanding of the hydrological processes. In this study, the joint application of multiple models based on the same input data set is used to address this challenge. The hydrological components are compared based on the multiple models' output, on the one hand, the effects of the model structure and algorithm on hydrological processes can be quantitatively analyzed; on the other hand, the simulated performances can be cross-validated based on the multiple outputs to improve understanding the hydrological processes in the mountain catchment.

***Question 2: How do remote sensing data perform in hydrological modeling?***

The distributed hydrological model has higher requirement for input data rather than lumped conceptual model. As results, the scattered climate stations in the piedmont alluvial plain are not capable of representing the climate environment for entire watershed. Before the issues of low density of gauging stations can be solved, the accuracy and reliability of hydrological modelling in the alpine catchment have always been strongly restricted by this kind of problem. The spatial RSD are easy to couple with the distributed hydrological model and can enrich the data sources of the hydrological process study. The problems of scale matching and bias correction are new challenges in RSD application. Therefore, accuracy test and appropriate bias corrections are preconditions for modeling applications. Or else, the performance of the model simulation forced by RSD is still confusing. In this study, the remotely sensed precipitation, temperature and PET are processed, and their performances are studies by comparison with observations and benchmark modeling.

***Question 3: What are the responses of hydrologic components to different forcing data?***

Besides the effect of model structures and algorithms, the responses of the hydrological processes to the different input data sources based on the hydrological model driven by SBD and RSD has drawn people's attention. Because of the complex relationships between the causal and resulting factors in hydrological processes, the uncertainty of input data take the different levels of influences on each output components. one

question must be answered firstly before study on the effect of input data: Which output of hydrological components should be used in analyzing the effect of input data? In this dissertation, the SDB of precipitation, temperature and PET is replaced by the corrected RSD in the fully distributed MIKE SHE model, and the analysis of variation (ANOVA) model is designed to test the significant effect of input data on different water components. Based on the significant relationship between input and output, the effect of input data's uncertainties on the hydrological processes can be investigated.

***Question 4: What are the effects of climate change on the hydrological processes?***

Little doubt remains related to the strong effects of climate change on water resources, but how are these effects progressing? What are the changes in the different forms of water resources and redistribution? From the method of extracting the change signals of meteorological variables, how to obtain the all-sided and accurate signals is the first challenge. Based on the GCMs, in order to reduce the uncertainty of future meteorological data, the modified method of signal extraction was applied to understand the climate change trends. Combined with the well-calibrated hydrological model and the full understanding of uncertainties, the effects of climate change on the hydrological processes were obtained from a water balance perspective at the catchment scale.

Question 1 is aimed at the model performance in hydrological processes, including the effects of model structure and module algorithm. Question 2 focuses on the performance of RSD applications in modeling. Question 3 analyzes the responses of the hydrological components to input data and determines how to define the significant relationships. According to the first three questions, the correct hydrological processes in the study area can be well understood. And based on this understanding, the variations in the climate change are addressed in Question 4. Consequently, a scientific assessment for hydrological processes in alpine catchment is created to support decision makers and relevant studies.

## **1.4.2 Dissertation outline**

The research questions stated above are addressed in the following chapters of this dissertation. All the chapter are not independent, but are connected by the logical relationship diagrammed in a framework (Figure 1.5). The chapter design corresponds to the research questions, and several chapters contribute together to clarify the primary objective. The hydrological models set up in Chapter 2 (driven by SBD) and Chapter 3 (driven by RSD) are the foundations for the following questions addressed in Chapter 4.

Chapters 2 through 4 correspond to papers published or prepared for publication in international peer-reviewed journals.

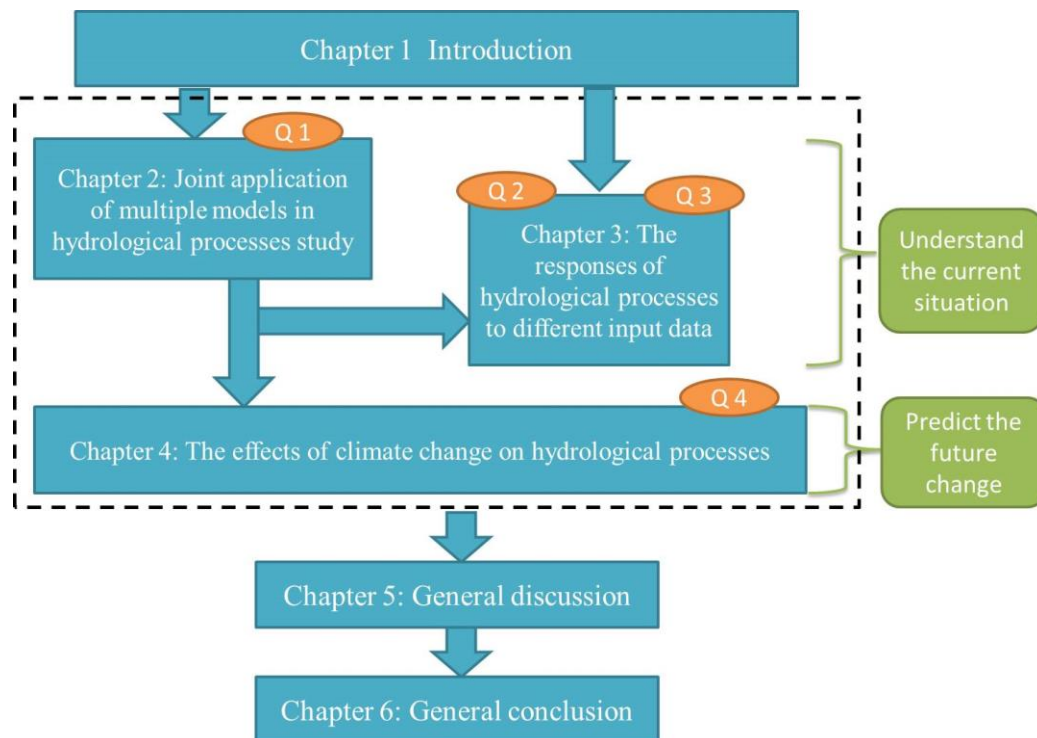


**Figure 1.5 Outline of the dissertation**

### ***Chapter 2. Joint application of multiple models in the hydrological process study***

This chapter, which work was published in *Water Resources Management* (Liu et al, 2016), describes the joint application of the SWAT and MIKE SHE models in hydrological processes simulation. Because of the uncertainties from their model structure and algorithm, a single model is not capable of accurately presenting the entire hydrological process, and if additional observations cannot be used in multiple objectives calibrations, this program's performance could worsen. Two physically based and distributed hydrological models are chosen for hydrological modelling. Subsequently, the differences in the same water component outputs are analyzed basing on their model structures and algorithms. Due to the importance of snow in the alpine catchment, the remotely sensed snow coverage data were chosen as the validation data to test the output of snow storage. Additionally, one integrated description of hydrological processes is stated based on the model output of two representative models.

### ***Chapter 3. Responses of hydrological processes to the different input data***

Chapter 3, which was published in *Water* (Liu et al, 2016), reveals the effects of different input data on the hydrological processes. Due to the limitations of the satellite

data in terms of physical sensors, space-time coverage and spatial resolution (Prigent, 2010), the results of raw RSD application has showed certain controversial results and been criticized. The appropriate bias correction methods have been used in this study to improve the precision of remotely sensed precipitation and temperature data. Based on the MIKE SHE model set up in Chapter 2, the corrected RSDs of precipitation, temperature and PET were applied to replace the corresponding SBD, and eight MIKE SHE models were established. Based on these model outputs, an innovative ANOVA model was implemented to define the significant effect of input data on water components. Finally, the spatial and temporal distinctions of sensitive water components were used to analyze the response to the corresponding input data.

#### ***Chapter 4. Effects of climate change on the hydrological processes***

This chapter (Liu et al, 2016, submitted) investigated the variations of hydrological processes under future climate change scenarios. According to the 21GCMs of CMIP5, a modified quantile perturbation method (QPM) and the delta method were used for precipitation and temperature to extract the variable signals, respectively. These change signals were added to the historical observations to obtain future climate factors. After coupling the models, which were well calibrated in Chapters 2 and 3, the readjustment of future hydrological processes can be quantitatively known.

Chapter 5 and Chapter 6 summarize and discuss the results of the previous chapters and also present important points for future research. A general discussion on the initial research questions and their results is given in Chapter 5. Chapter 6 summarizes the main conclusions of this dissertation and offers selected prospects for evaluation of hydrological processes in the alpine catchment of arid regions.

#### **1.4.3 Out of scope**

Not all aspects of this topic can be included in a given research study, and this gap always drives future investigations. Hydrological processes are complex natural phenomena, and in most catchment hydrological models, many natural processes are still not included in hydrological modeling or they are simplified due to difficulties of quantification or validation. It is a pity that snow and ice are not distinguishable in the SWAT and MIKE SHE model, and thus, the glacier simulation uses the same principle as a snow process in the two models, which is not an ideal approach. Moreover, in certain peak regions, snowdrifts and snow slides would be the dominant movement.

Unfortunately, these movements have not been included in the hydrological model, and thus, an aberrant phenomenon of ever-increasing snow storage was found in the simulation.

In addition, more numerous gauged observations would be definitely better to carry out the simulation work of natural processes. The Yarkant River Basin is a catchment that is difficult to physically reach due to the precipitous topography conditions. Limited observations reduce our grasp of the physical realities, which potentially adds uncertainty to the hydrological modeling.

## References

- Abbott, M. B., Cunge, J. A., O'Connell, P. E., Rasmussen, J. (1986a). An introduction to the European Hydrologic System — Systeme Hydrologique Europeen, "SHE", 2: Structure of a physically-based, distributed modeling system. *Journal of Hydrology*. 87: 61-77.
- Abbott, M. B., Cunge, J. A., O'Connell, P. E., Rasmussen, J. (1986b). An introduction to the European Hydrologic System — Systeme Hydrologique Europeen, "SHE", 1: History and philosophy of a physically-based, distributed modeling system. *Journal of Hydrology*. 87: 45-49.
- Allen, R. G., Pereira, L., Raes, D., Smith, M. (1998). Crop Evapotranspiration. Food and Agriculture Organization of the United Nations, Rome, Italy. FAO publication 56. ISBN 92-5-104219-5. 290p.
- Arnold, J. G., Muttiah, R. S., Williams, J. R. (1998). Large area hydrologic modeling and assessment part 1: Model development. *Journal of American Water Resources Association*. 34: 73-89.
- Bellard, C., Bertelsmeier, C., Leadley, P., Thuiller, W., Courchamp, F. (2012). Impacts of climate change on the future of biodiversity. *Ecology letter*. 15(4): 365-377.
- Bergstrom, S. (1972). Development and application of a digital runoff model (in Swedish), serie HYDROLOGI, No. 22, Norrkoping.
- Beven, K. J. (2001). *Rainfall Runoff Modeling: The Primer*. New York: John Wiley and Sons Ltd, 1-355.
- Bi, H. X., Zhong, B. L. (2002). Review on integrating of RS and GIS with hydrology. *Journal of Soil and Water Conservation*. 16(2):45-50.
- Bosson, E., Selroos, J. O., Stigsson, M., Gustafsson, L. G., Destouni, G. (2012). Exchange and pathways of deep and shallow groundwater in different climate and permafrost conditions using the Forsmark site, Sweden, as an example catchment. *Journal of Hydrology*. 21: 225-237. doi: 10.1007/s10040-012-0906-7.
- Chen, Y. N., Yang, Q., Luo, Y., Shen, Y. J., Pan, X. L., Li, L. H. (2012). Ponder on the issues of water resources in the arid region of northwest China. *Arid Land Geography*. 35(1): 1-9.
- Chow V. T., David R. M., Mays L. W. (1988). *Applied Hydrology*. McGraw-Hill, New York.



- Christierson, B., Vidal, J.-P., Wade, S. D. (2012). Using UKCP09 probabilistic climate information for UK water resource planning. *Journal of Hydrology*. 424: 8-67.
- Coll, C., Caselles, V., Galve, J.M., Valor, E., Niclos, R., Sanchez, J. M., Rivas, R. (2005). Ground measurements for the validation of landsurface temperatures derived from AATSR and MODIS data. *Remote Sensing Environmeng*. 97: 288-300.
- Crawford, N. H., and Linsley R. K. (1966). Digital simulation in hydrology: Stanford watershed model IV, Technichal Report no. 39. Department of Civil Engineering, Stanford University.
- Dai, Y., Zeng, X., Dickinson, R. E., Baker, I., Bonan, G. B., Bosilovich, M. G., Niu, G. (2003). The common land model. *Bulletin of the American Meteorological Society*. 84(8), 1013-1023.
- Debele, B., Srinivasan, R., Gosain, A. K. (2009). Comparison of Process-Based and Temperature-Index Snowmelt Modeling in SWAT. *Water Resources Management*. 24: 1065-1088. doi: 10.1007/s11269-009-9486-2.
- Dechmi, F., Burguete, J., Skhiri, A. (2012). SWAT application in intensive irrigation systems: Model modification, calibration and validation. *Journal of Hydrology*. 470-471: 227-238. doi: 10.1016/j.jhydrol.2012.08.055.
- DHI (2007): MIKE SHE user manual volime2: Reference Guide, DHI water & Environment.
- Edwards, P. N. (2010). *A vast machine: Computer models, climate data, and the politics of global warming*: Mit Press.
- Feng, T., Liu, S. Y., Xu, J. L., Guo, W. Q., Wei, J. F., Zhang, Z. (2015). Glacier change in Yarkant River basin from 1968 to 2009 derived from the first and second glacier inventories of China. *Journal of Glaciology and Geocryology*. 29: 808-814. 37(1): 1-13.
- Fontaine, T. A., Cruickshank, T. S., Arnold, J. H., Hotchkiss, R. H. (2002). Development of a snowfall-snowmelt routine for mountainous terrain for the soil water assessment tool(SWAT). *Journal of Hydrology*. 262: 209-223.
- Galván, L., Olías, M., Fernandez, V. R., Domingo, J. M., Nieto, J. M., Sarmiento, A. M., Cánovas, C. R. (2009). Application of the SWAT model to an AMD-affected river (Meca River, SW Spain). Estimation of transported pollutant load. *Journal of Hydrology*. 377: 445-454. doi: 10.1016/j.jhydrol.2009.09.002.
- Gao X., Zhang, S. Q., Ye, B. S., Jiao, C. J. (2010). Glacier Runoff Change in the Upper Stream of Yarkant River and Its Impact on River Runoff during 1961~2006. *Journal of Glaciology and Geocryology*, 32: 445-453.
- Gao, Y. C., Wang, C. Y. (2000). Biospheric aspects of hydrologic cycle BAHC plan and its research progress. *Progress in Geography*. 19(2): 97-103.
- Hanewinkel, M., Cullmann, D. A., Schelhaas, M.-J., Nabuurs, G.-J., Zimmermann, N. E. (2013). Climate change may cause severe loss in the economic value of European forest land. *Nature Climate Change*. 3(3): 203-207.
- Hijioka, Y., Matsuoka, Y., Nishimoto, H., Masui, M., Kainuma, M. (2008). Global GHG emissions scenarios under GHG concentration stabilization targets. *Journal of Global Environmental*

- Engineering. 13: 97-108.
- Huang, J. P., Yu, H. P., Guan, X. D., Wang, G. Y., Guo, R. X. (2015). Accelerate dryland expansion under climate change. *Nature Climate Change*. DOI:10.1038/nclimate2837.
- Huffman, G. J., Adler, R. F., Bolvin, D. T., Gu, G., Nelkin, E. J., Bowman, K. P., Hong, Y., Stocker, E. F., Wolff, D. B. (2007): The TRMM Multi-satellite Precipitation Analysis: Quasi-Global, Multi-Year, Combined-Sensor Precipitation Estimates at Fine Scale. *Journal of Hydrometeorology*. 8(1): 38-55.
- Huffman, G. J., Adler, R. F., Morrissey, M., Bolvin, D. T., Curtis, S., Joyce, R., McGavock, B., Susskind, J. (2001). Global Precipitation at One-Degree Daily Resolution from Multi-Satellite Observations. *Journal of Hydrometeorology*. 2(1): 36-50.
- IPCC. (2013). The Physical Science Basis. Working Group I Contribution to the Fifth Assessment Report of the Intergovernmental Panel on Climate Change. Cambridge, United Kingdom and New York, USA.
- Jayatilaka, C. J. and Storn, B. (1998). Simulation of water flow on irrigation bay scale with MIKE-SHE. *Journal of Hydrology*. 208: 108-130.
- Kang, E. S. (1998). Review and prospect of hydrology study on cold and dry region in China. *Journal of Glaciology and Geocryology*. 20(3): 238-245.
- Kang, J. C., Yang, H. (1991). Characteristic at Boundary Face of Ice-Bedrock on the Upper Region of Shaksam Valley, Karakoram. *Journal of Glaciology and Geocryology*. 13: 331-336.
- Liu, T., Willems, P., Feng, X. W., Li, Q., Huang, Y., Bao, A. M., Chen, X., Veroustraete, F., Dong, Q. H. (2012). On the usefulness of remote sensing input data for spatially distributed hydrological modeling: case of the Tarim River basin in China. *Hydrological processes*. 26: 335-344. doi: 10.1002/hyp.8129.
- Lirong, S., Jianyun, Z. (2012). Hydrologic Response to Climate Change in Beijiing River Basin Based on the SWAT Model. *Procedia Engineering*. 28: 241-245. doi: 10.1016/j.proeng.2012.01.713.
- Lynch, P. (2008). The origins of computer weather prediction and climate modeling. *Journal of Computational Physics*. 227(7): 3431-3444. doi:10.1016/j.jcp.2007.02.034.
- Madsen, H. (2003). Parameter estimation in distributed hydrological catchment modelling using automatic calibration with multiple objectives. *Advances in Water Resources*, 26: 205-216.
- Martinec, J. (1975). Snowmelt - runoff model for stream flow forecasts. *Nordic Hydrology*. 6: 145-154.
- Martens, P. (2014). Health and climate change: modeling the impacts of global warming and ozone depletion: Routledge.
- Milly, P. (2007). Global warming and water availability: the "big picture". Paper presented at the 21st Conference on Hydrology.
- Najafi, M. R., Moradkhani, H., Jung, I. W. (2011). Assessing the uncertainties of hydrological model selection in climate change impact studies. *Hydrologic. Processes*. 25: 2814-2826. doi: 10.1002/hyp.8043.

- Nielsen, S. A., and Hansen E. (1973). Numerical Simulation of the Rainfall-runoff Process on a Daily Basis. *Nordic Hydrology*. 4, 171-190.
- Prigent, C. (2010). Precipitation retrieval from space: An overview. *Comptes Rendus Geoscience* 342(4-5): 380-389.
- Prigent, C. (2011) Precipitation retrieval from space: An overview. *CR. Geosci.* 342: 380-389. DOI: 10.1016/j.crte.2010.01.004.
- Pisinaras, V., Petalas, C., Gikas, G. D., Gemitzi, A., Tsihrintzis, V. A. (2010). Hydrologic and water quality modeling in a medium-sized basin using the Soil and Water Assessment Tool (SWAT). *Desalination*. 250: 274-286. doi: 10.1016/j.desal.2009.09.044.
- Rahman, K., Maringanti, C., Beniston, M., Widmer, F., Abbaspour, K., Lehmann, A. (2012). Streamflow Modeling in a Highly Managed Mountainous Glacier Watershed Using SWAT: The Upper Rhone River Watershed Case in Switzerland. *Water Resources Management*. 27: 323-339. doi: 10.1007/s11269-012-0188-9.
- Refsgaard, J. C. (1997). Parameterisation, calibration and validation of distributed hydrological models. *Journal of Hydrology*, 198: 69-97.
- Riahi, K. Gruebler, A. and Nakicenovic N. (2007). Scenarios of long-term socio-economic and environmental development under climate stabilization. *Technological Forecasting and Social Change*. 74(7): 887-935.
- Robert S. A., Scott, W. W., Hans R. Z. (2008). Hydrologic Calibration and Validation of SWAT in a Snow-Dominated Rocky Mountain Watershed, Montana, USA. *Journal of American Water Resources Association*. 44: 1411-1430.
- Roger, C. B., Jeff, D., Noah, P. M. (2004). Mountain hydrology of the semi-arid weater US. *News and Technology Reports*
- Roosmalen, L. V.; Sonnenborg, T. O.; Jensen, K. H. (2009). Impact of climate and land use change on the hydrology of a large-scale agricultural catchment. *Water Resources Research*, 45, 150-164.
- Rosenzweig, C., Elliott, J., Deryng, D., Ruane, A. C., Müller, C., Arneth, A., Khabarov, N. (2014). Assessing agricultural risks of climate change in the 21st century in a global gridded crop model intercomparison. *Proceedings of the National Academy of Sciences*. 111(9): 3268-3273.
- Sahoo, G. B., Ray, C., De Carlo, E. H. (2006). Calibration and validation of a physically distributed hydrological model, MIKE SHE, to predict streamflow at high frequency in a flashy mountainous Hawaii stream, *Journal of Hydrology*. 327: 94-109. doi: 10.1016/j.jhydrol.2005.11.012.
- Sefton, C. E. M., Boorman, D. B. (1997). Recognizing the uncertainty in the quantification of the effects of climate change on hydrologic response. *Climatic Change*. 35: 415-434.
- Shuttleworth, W.J. (1992). Evaporation. In D. Maidment, *Handbook of Hydrology*. McGraw-Hill.
- Smerdon, B. D., Allen, D. M., Grasby, S. E., Berg, M. A. (2009). An approach for predicting groundwater recharge in mountainous watersheds. *Journal of Hydrology*. 365: 156-172. doi: 10.1016/j.jhydrol.2008.11.023.

- Smith, M. (1992). Expert consultation on the revision of FAO methodologies for crop water requirements. FAO, Rome, Italy. 60pp.
- Sivapalan M. (2003). Prediction in ungauged basins: a grand challenge for theoretical hydrology. *Hydrological processes*. 17(15): 3163-3170.
- Sun, B. G., Mao, W. D., Feng, Y. R., Chang, T., Zhang, L. P., Zhao, N. (2006). Study on the changes of air temperature, precipitation, and runoff volumn in the Yarkant River basin. *Arid Zone Research*. 23(2): 203-209.
- Tang, H., Yang, D. G., Zhang, Y. F. (2013) Food security and agricultural structural adjustment in Yarkant River Basin, northwest China. *Journal of Food, Agriculture and Environment*, 11: 324-328.
- Thompson, J. R., Sørensen, H. R., Gavin, H., Refsgaard, A. (2004). Application of the coupled MIKE SHE/MIKE 11 modeling system to a lowland wet grassland in southeast England. *Journal of Hydrology*. 293: 151-179. doi: 10.1016/j.jhydrol.2004.01.017.
- Van Vuuren, D., M. den Elzen, P. Lucas, B. Eickhout, B. Strengers, B. van Ruijven, S. Wonink, R. van Houdt (2007). Stabilizing greenhouse gas concentrations at low levels: an assessment of reduction strategies and costs. *Climatic Change*. doi:10.1007/s10584-006-9172-9.
- Vorosmarty, C. J., Fekete, B. M., Meybeck, M., Lammers, R. B. (2000). Geomorphometric attributes of the global system of rivers at 30-minute spatial resolution. *Journal of Hydrology*. 237(1-2): 17-39. doi:10.1016/S0022-1694(00)00282-1.
- Wan, Z., Zhang, Y., Zhang, Q., Li, Z. L. (2002). Validation of the land-surface temperature products retrieved from Terra Moderate Resolution Imaging Spectroradiometer data. *Remote Sensing Environmeng*. 83: 163-180.
- Wan, Z., Zhang, Y., Zhang, Q., Li, Z. L. (2004). Quality assessment and validation of the MODIS landsurface temperature. *International Journal of Remote Sensing*. 25: 261-274.
- Wang, D., Liu, S. J., Hu, L. J., Zhang, M. X. (2009). Monitoring and Analyzing the Glacier Lake Outburst Floods and Glacier Variation in the Upper Yarkant River, Karakoram. *Journal of Glaciology and Geocryology*. 29: 808-814.
- Wise, M. A, Calvin, K. V., Thomson, A. M., Clarke, L. E., Bond-Lamberty, B., Sands, R. D., Smith, S. J., Janetos, A. C., Edmonds, J. A., (2009). Implications of Limiting CO<sub>2</sub> Concentrations for Land Use and Energy. *Science*. 324:1183-1186. May 29, 2009
- Word Meteorological Organization (WMO), Report of the third session of JSC Working Group on the Land Surface Processes and Climate (1987). Manhatan, Kamsas. WMO/TD-No.232.
- Xia, J. (2009). Impact of water diversion project across basins on land water cycle and water security. *Journal of Basic Science and Engineering*. 17(6): 831-842.
- Zhang, Q., Zhao, Y. D., Zhang, C. J., Li, Y. H., Sun, G. W. (2008). Issues about hydrologic cycle and water resources in the arid region of Northwest China. *Arid Meteorology*, 26(2): 1-8.
- Zhang, X., Xu, Y. P., Fu, G. (2014). Uncertainties in SWAT extreme flow simulation under climate change. *Journal of Hydrology*. 515: 205-222. doi: 10.1016/j.jhydrol.2014.04.064.

# CHAPTER 2

## **Joint application of multiple models in hydrological processes study**

---

*Modified from: Liu, J., Liu, T., Bao, A. M., De. Maeyer, P., Feng, X. W., Scoot, N. M., Chen, X. (2016). Assessment of Different Modeling Studies on the Spatial Hydrological processes in an Arid Alpine Catchment. Water Resources Management. 30: 1757-1770. dio: 10.1007/s11269-016-1249-2.*

## ABSTRACT

To assess the accuracy of the modeling description of the spatial hydrology process in a high-altitude and arid mountainous catchment, and then support the scientific basis for the regional water resources management, a typical catchment Yarkant River basin located in northwest China have been chosen, and the constitution and spatial-temporal distribution of the multiple hydrology elements from the outputs of SWAT and MIKE SHE are analysed based on the modules' structure and algorithm. In generally, the simulated daily discharges both from two models matched the observation well at the outlet, but didn't reflect the different characteristics of SWAT and MIKE SHE, furthermore, the otherness of modules' structure and algorithm have presented on the sub-processes including snow melt, runoff and evapotranspiration are disparate. The consideration of the accumulation temperature, the changing snowmelt factor and the snowmelt feature of the temporal distribution in SWAT is related to the generation of flow discharges; the spatial distribution of the snow storage is much clearer in MIKE SHE due to its fully distributed structure based on grids. The subsurface lateral flow has a significant contribution to the stream in SWAT, while the base flow to the stream in MIKE SHE is more closed to actuality. The MIKE SHE model leads to more soil and open water evaporation due to the Kristensen-Jense approach and overland water storage, while SWAT has three options to calculate the evapotranspiration in different ranges to meet the local water balance in a less spatially distributed approach.

**Key words:** spatial process; hydrology elements distribution; model structure; modules' algorithm; Yarkant River basin

### 2.1 Introduction

Hydrological models are essential to understand hydrological processes, for quantifying interactions among natural physical factors (Boorman, 1997) and assessing management strategies (Loukas, 2007). However, with the same input data, different hydrological models that are applied in same study basin might generate dissimilar simulation results. Even the correct global trend can be attained together, but otherness was still existed in the processes and spatial interactions (Ferrant et al., 2011). So the model selection becomes a priority for a successful hydrology studies in special region (Maurer et al., 2010; Vansteenkiste et al., 2013).

In practice, the selection of a model for a study area relies on many factors (Gan, 1997; Xu, 1999), including the catchment characteristics and the data availability. It is rare that

an objective model selection approach is authentic, but mostly depend on the common practice of modellers (Najafi et al., 2011; Nasr et al., 2007), which causes trouble for water resources decision makers in continuing water resource management (Wood, 2004). Therefore, it is important to understand and quantify the impacts due to various conceptualizations and parameterizations in hydrological models and their simulation outputs in order to offer suggestions for water resource planners and managers.

In the phase 2 of the Distributed Model Intercomparison Project (DMIP2) (Smith et al., 2012; 2013), several distributed models was mixed compared to lumped benchmark, results indicated there was none single model can perform best in all cases. DANUBIA component (Barthel et al., 2012) comprised of 17 model components and discussed the integrated simulation of global change influence on agriculture and groundwater. Najafi et al. (2011) farther suggested that joint application of different models would be significant for water resource management after using four hydrological models in Tualatin River basin. Maurer et al. (2010) also demonstrated that the model structure is the essential factor for extreme flow by applying the Sacramento Soil Moisture Accounting (SacSMA) and Variable Infiltration Capacity (VIC) models for climate change investigation in the Sierra River basin. Similar phenomena were observed by Shi et al. (2011) in the Huaihe River from the modelled results of the SWAT and Xin'Anjiang models. These previous studies emphasized the importance of model selection and combined application of multiple models, however, there is little focus on the model performance of spatial hydrological processes, but only the discharges, and did not give detail interpretations of output deviations among different models.

Since SWAT and MIKE SHE can fulfil their modelling tasks independently, there are only small numbers of studies intended to quantify the differences between two of them. Furthermore, most attentions focused on the goodness of fit indices for the modelled discharges at outlet (El-Nasr et al., 2005; Golmohammadi et al., 2014). While, the calibration solely at basin outlets alone and ignoring other hydrologic components was not able to greatly improve model's reliability and accuracy (Smith et al., 2013).

Mountainous watersheds, headstream of most river basins in arid region, play an important role in water resource management for the downstream region (Rahman et al., 2012). Tarim River basin, which is the longest inland river in world, is located in Xinjiang Province in northwest China. The limited water resources have severely affected sustainable development of this region and caused a vulnerable ecological environment (Chen et al., 2006; Liu et al., 2011). Yarkant River is the largest tributaries

and primary water sources of Tarim River. Since most studies of Yarkant River basin have focused on the single effect of snow and glacier melt variation (Chen et al., 2006; 2010; Gao et al., 2010; Zhang et al., 2012), it would be meaningful to perform an integrated modelling study and understand the simulation effect in such region.

The study on hydrologic cycle process is the important foundation of the water resources utilization and management, especially in the arid region. In this paper, because of the extreme topographical condition, there is a strong spatial heterogeneity in Yarkant River basin, so two classical distributed models SWAT and MIKE SHE are chosen to apply jointly to assess the accuracy of modelling on the spatial hydrology process, additionally, the remotely sensed snow coverages are used for crossing-verifying. Excepting the analysis of simulated discharges at the outlet station, the spatial and temporal distribution of dominative sub-processes, including snowmelt, runoff and evapotranspiration, in the two models are compared and analysed regarding their arithmetic and structures to understand the model's response in the mountainous region.

## **2.2 Study area**

The Yarkant River basin (shown as Figure 1.2) was chosen in this study. More detailed information can be seen in Section 1.2.

## **2.3 Hydrological model**

### **2.3.1 SWAT**

SWAT is a continuous-time, semi-distributed, and physically based model. The catchment is subdivided into sub-basins that are connected with the river network; the non-homogeneity of every sub-basin is taken into account, and the sub-basin is further subdivided into specific soil/land use/slope characteristic units that are called hydrologic response units (HRUs). There is no spatial relationship or interaction among HRUs (Neitsch, 2011), and HRUs are the smallest computed unit in the SWAT model. The meteorological data, including rainfall, highest/lowest temperature, wind speed, solar radiation and relative humidity, are used as driving factors and to compute the variation in the water yield, including snow storage, evapotranspiration, water content in the soil, etc. Then, the runoff contribution to the channel is achieved through water balance control. In the channel, the variable storage approach or Muskingum methods can be used to compute the channel flow. Finally, the evaporation, transmission loss and water



leakage from the river are subtracted to obtain the discharges in the outlet profile.

### Runoff

In the SWAT model, the Soil Conservation Service (SCS) approach is used to calculate the surface flow. When the infiltration is calculated, the dynamic change process of the soil storage follows the change in the soil moisture content and transpiration and a comprehensive parameter Curve Number (CN) that represent the influence of the soil permeability, land use and field management on the infiltration. The CN is an experiential parameter, and the applicability of this value is different from HRU to HRU.

The water that enters the soil may do so in three different ways in SWAT model. First, the water may be removed because of plant uptake or evaporation; furthermore, water may enter streams by moving laterally in the profile. The final option is that water percolates past the bottom of the soil profile and recharges the aquifer, which may also contribute to the stream flow. In fact, according the definition of SWAT model, the superimposed contribution water to streams from two last ways called base flow.

### Snowmelt

In the SWAT model, the snowfall is stored as an accumulating snow pack, and the degree-day approach is used for snowmelt estimation. Because the density of the snowpack differs over time, when the snowpack is palled up with increasing snowfall or reduced by snow melt or sublimation, the amount of water is reported as the snow water equivalent. The mass balance of snow is expressed as

$$SNO_{day} = SNO_{day-1} + R_{day} - SNO_{sub} - SNO_{mel} \quad (2-1)$$

Where  $SNO_{day}$  and  $SNO_{day-1}$  are the water content of pack on a given day and the before day (mm H<sub>2</sub>O), respectively;  $R_{day}$  is the amount of snowfall on a given day (mm H<sub>2</sub>O);  $SNO_{sub}$  is the amount of sublimation on a given day (mm H<sub>2</sub>O); and  $SNO_{mel}$  is the amount of snow melt on a given day (mm H<sub>2</sub>O).

The influence of the accumulated temperature on snowmelt is considered, and the snowmelt temperature is determined by the snowpack temperature  $T_{snow}$  and the highest air temperature  $T_{max}$  on a given day. The snowpack temperature is determined by the mean daily air temperature on a given day  $T$  and the snowpack temperature on the previous day  $T_{snow-1}$ ; the influence of the two factors is adjusted by the lagging factor  $TIMP$ , and the snowpack temperature is calculated by

$$T_{snow} = T_{snow-1} * (1 - TIMP) + T * TIMP \quad (2-2)$$

In addition, the melt factor change follows the seasons, with the maximum and the minimum values occurring on the summer and winter solstices. The calculated equation is written below.

$$b_{mel} = \frac{SMFMX + SMFMN}{2} + \frac{SMFMX - SMFMN}{2} * \sin \left[ \frac{2\pi}{365} * (day - 81) \right] \quad (2-3)$$

Where  $b_{mel}$  is the melt factor;  $SMFMX$  is the maximum value for June 21 (mm H<sub>2</sub>O/day-°C);  $SMFMN$  is the minimum value for December 21 (mm H<sub>2</sub>O/day-°C); and  $day$  is the day number of the year.

Finally, the snowpack and maximum air temperature are considered in the snowmelt calculation as follows

$$SNO_{mel} = b_{mel} * SNO_{cov} * \left( \frac{T_{snow} + T_{max}}{2} - T_{mel} \right) \quad (2-4)$$

Where  $SNO_{mel}$  is the amount of snowmelt on a given day (mm H<sub>2</sub>O),  $SNO_{cov}$  is the fraction of the HRU area that is covered by snow,  $T_{max}$  is the maximum air temperature on a given day (°C), and  $T_{mel}$  is the basic snowmelt temperature (°C).

After obtained the snow remaining snow storage in the HRU, SWAT takes an areal depletion curve to considerate the unequable distribution in the subbasin. It is expressed as follows

$$SNO_{cov} = \frac{SNO_{day}}{SNO_{100}} * \left[ \frac{SNO_{day}}{SNO_{100}} + \exp \left( cov_1 - cov_2 * \frac{SNO_{day}}{SNO_{100}} \right) \right]^{-1} \quad (2-5)$$

where  $SNO_{cov}$  is the fraction of HRU area covered by snow,  $SNO_{day}$  is the water content of snow pack on a given day (mm H<sub>2</sub>O),  $SNO_{100}$  is the threshold depth of snow at 100% coverage (mm H<sub>2</sub>O),  $cov_1$  and  $cov_2$  are coefficients that define the shape of the curve, that determined by using to known point: 95% coverage at 95%  $SNO_{100}$  and 50% coverage at a user specified fraction of  $SNO_{100}$ .

### Evapotranspiration

There are three methods incorporated into SWAT to estimate the PET: the Penman-Monteith method (Allen, 1986; Allen et al., 1989), the Priestley-Taylor method (Priestley and Taylor, 1972) and Hargreaves method (Hargreaves et al., 1985). After the PET has been calculated, the water intercepted by the plant canopy will evaporate at first, if this kind of evaporation cannot satisfy the requirement of maximum amount of the evapotranspiration, then the sublimation and evaporation from the soil will be occurred, so the actual evapotranspiration include four sources in SWAT model: canopy interception evaporation, snow sublimation, water evaporation from river and ponding

and soil evaporation/transpiration.

### 2.3.2 MIKE SHE

MIKE SHE is a deterministic, dynamic, physically based and fully distributed hydrological model that describes hydrological processes through partial differential equations of mass, energy and momentum conservation. The hydrological process can be separated into five parts: interception/evapotranspiration, overland flow, channel flow, unsaturated zone and saturated zone (DHI, 2007). In the horizontal direction, the catchment terrain is described by the number of square grids with the elevation and geo-information to clearly present the spatial distributed relationship. In the vertical direction within each grid square, the vertical variations in the soil columns, aquifer structure and hydrogeological characteristics are described in a number of horizontal layers with variable depths at each grid square.

#### Runoff

After the water falls on the ground surface, the infiltration will be calculated depends on the soil physical attributes and the groundwater conditions in that all of the parameters have a clear physical meaning. When water enters the soil of the unsaturated zone, The One-dimensional Richards equation and Gravity flow equation can be used to solve the pressure head in the unsaturated zone (Hughes and Liu, 2008), which is converted to the soil moisture content according to the soil moisture retention curve. Some portion of the soil water in the unsaturated zone is removed by plant uptake or evaporation, and the rest will percolate to the saturation zone, the lateral flow in the soil is ignored in MIKE SHE model.

For the water infiltrated into the saturated zone, the spatial and temporal variations of the dependent variables are described by the three-dimensional Darcy equation that is solved by an iterative implicit finite difference technique. In addition, a dynamic coupling is set between MIKE SHE and MIKE 11 (Thompson et al., 2004) in which data are exchanged between the two modules after each computational time step and node to represent the dynamic interaction between the aquifers and stream channels. The channels are considered as lines running between model grid squares, and the river-aquifer exchange is calculated from both sides of the river based on vertical head gradients. When the soil moisture is saturated, and the head pressure of the aquifer water is higher than the surface, the aquifer water also will flow to surface and exchange with

the overland flow. Hence, the base flow of river only contains the contribution water from the saturated zone.

### **Snowmelt**

The snow-melting process within the watershed was simulated with the snowmelt module of MIKE SHE, which uses the simple degree-day method:

$$SNO_{mel} = b_{mel} * (T - T_{mel}) \quad (2 - 6)$$

In this module, only the average air temperature was taken into account, moreover, the values of the degree-day melt  $b_{mel}$  factor and threshold melting temperature  $T_{mel}$  do not change in the temporal scale.

### **Evapotranspiration**

In MIKE SHE model, the input data Reference Evapotranspiration control the maximum amount of the actual evapotranspiration, the calculation of the actual evapotranspiration is based on empirically derived equations that follow the work of Kristensen and Jensen (1975). In this model, the actual evapotranspiration and the actual soil moisture status in the root zone is calculated from the potential evaporation rate, along with maximum root depth and leaf area index for the plants. In addition, a Two-Layer UZ/ET (DHI, 2007) model has been integrated into MIKE SHE, The Two-Layer UZ/ET model divides the unsaturated zone into a root zone, from which ET can occur and a zone below the root zone, where ET does not occur. The Two-Layer Water Balance Method is an alternative to the more complex unsaturated flow process coupled to the Kristensen and Jensen module for describing actual evapotranspiration and the amount of water that recharges the saturated zone. In MIKE SHE model, the actual evapotranspiration can be divided five classes: canopy interception evaporation, snow sublimation, water evaporation from river and ponding, soil evaporation, and transpiration.

## **2.4 Methodology**

### **2.4.1 Modeling**

The catchment boundary and river network were obtained based on the DEM in SWAT model, and then employed in MIKE SHE model. The catchment was divided into 25 sub-basins and 98 HRUs in the SWAT model and grids with the resolution of  $2 \text{ km} \times 2 \text{ km}$  in MIKE SHE model. The dataset recorded by Tashkurgan station were used to drive

SWAT and MIKE SHE, additionally, the output PET calculated based on the Penman-Monteith method in SWAT were taken as the input reference evapotranspiration of MIKE SHE.

On a catchment scale, topography is the main influence on the meteorology. Generally, according to the topography factors such as elevation, gradient, slope aspect and location (longitude and latitude), most spatial variances of precipitation can be understood (Basist et al., 1994). Among thesectors, elevation is the most primary one (Daly et al., 1994; Konrad et al., 1996; Goovaerts, 1999; 2000). In the Yarkant River basin, the elevation extremely changes, and the precipitation and temperature observed at Tashkurgan station were interpolated based on their lapse rates.

In the SWAT model, the catchment was divided into ten elevation bands, and the average elevation and area proportion of all the sub-basins in each elevation band were calculated through ArcGIS, after which the daily precipitation and maximum and minimum temperatures in each elevation band were interpolated on the basis of the precipitation lapse rate (PLAPS) and temperature lapse rate (TLAPS). In the MIKE SHE model, the catchment was divided into ten regions according the elevation of each grid at 700-meter intervals, all the grids in a region share the same precipitation and temperature time series, which uses the same *PLAPS* and *TLAPS* values as those in SWAT. The intercepted equations are formulized as:

$$R_{band} = R_{day} + (EL_{band} - EL_{gauge}) * \frac{plaps}{days * 100} \quad R_{day} > 0.01 \quad (2-7)$$

$$T_{max,min,av/band} = T_{max,min,av/day} + (EL_{band} - EL_{gauge}) * \frac{tlaps}{1000} \quad (2-8)$$

where  $R_{band}$  and  $T_{max,min,av/band}$  are the precipitation (mm H<sub>2</sub>O) and maximum, minimum, and average daily temperatures (°C) in the elevation band, respectively;  $R_{day}$  and  $T_{max,min,av/day}$  are the precipitation (mm H<sub>2</sub>O) and maximum, minimum, and average daily temperatures (°C) at the gauged station;  $EL_{band}$  is the mean elevation in the elevation band (m);  $EL_{gauge}$  is the elevation at the gauged station (m); *plaps* and *tlaps* are the precipitation (mm H<sub>2</sub>O/km) and temperature (°C/km) lapse rates, respectively; *days* is the average number of precipitation days in the sub-basin per year; and 1000 is a factor required to convert metres to kilometres.

Because of scarce and insufficient meteorological station, *plaps* and *tlaps* cannot be directly decided based on the stationary records. More useful information from the previous meteorological studies in this region was concluded. Therefore, according to the meteorological factors' change follow the elevation (given in Section 1.2.2) and the

records of the around meteorological stations (Shown in Table 1-2). The *plaps* and *tlaps* were calculated and listed the Table 2-1.

**Table 2-1 The PCG and TCG at different altitude groups of Yarkant River basin**

Altitude group (m)	<3000	3000~5000	5000~7000	>7000
PLAPS (mm/km/year)	0.0	70.0	100.0	70.0
TLASP (°C/km)	-6.5	-6.8	-7.0	-6.8

## 2.4.2 Calibration

The simulated period was parted warm-up period 2000-2002, calibration period 2003-2007 and verification period 2008-2009. In physically based hydrological model, the parameters normally have their special physical meanings, they should, in principle, be assessable from catchment data. In practice, determination of model parameters in each calculated unit is not possible due to scaling problems as well as experimental constraints. Thus, the distributed, physically based models also need calibration. The manual calibration of complex models is difficult to be carried out in a credible and consistent manner due to a number of parameters as well as parameter sensitivity and uncertainty (Gupta et al., 2003). The auto-calibration modules, SWAT-CUP of SWAT and Auto Calibration Tool (ACT) in MIKE SHE package, have been used to calibrate parameters to improve the calibration efficiency. Sequential Uncertainty Fitting (SUFI-2) (Abbaspour et al., 2004) and Shuffled Complex Evolution approach (SCE) (Vrugt et al., 2003) were used in SWAT-CUP and ACT. The simulated daily discharge was calibrated by the objective function according the observation record at Kaqun station. Four statistical coefficients were used to determine the model performances: Nash-Sutcliffe efficiency coefficient (Nash et al., 1970) *NSE*, Pearson correlation coefficient *R* and root-mean-square error *RMSE*. Their formulations are written as:

$$NSE = 1 - \frac{\sum_{i=1}^n (Q_{obs,i} - Q_{sim,i})^2}{\sum_{i=1}^n (Q_{obs,i} - \bar{Q}_{sim,i})^2} \quad (2-9)$$

$$R = \frac{\sum_{i=1}^n (Q_{obs,i} - \bar{Q}_{obs,i})(Q_{sim,i} - \bar{Q}_{sim,i})}{\sqrt{\sum_{i=1}^n (Q_{obs,i} - \bar{Q}_{obs,i})^2} \sqrt{\sum_{i=1}^n (Q_{sim,i} - \bar{Q}_{sim,i})^2}} \quad (2-10)$$

$$RMSE = \sqrt{\frac{\sum_{i=1}^n (Q_{sim,i} - Q_{obs,i})^2}{n}} \quad (2-11)$$

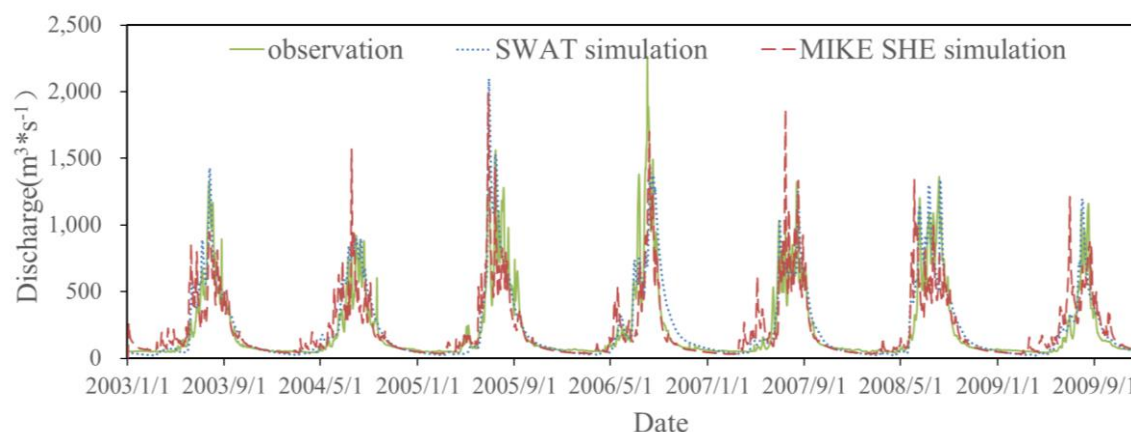
where  $Q_{obs,i}$  and  $Q_{sim,i}$  are the measured and simulated discharges at *i*th day ( $m^3/s$ ),

respectively;  $\bar{Q}_{obs}$  and  $\bar{Q}_{sim}$  are the average measured and simulated discharges in the simulation period ( $\text{m}^3/\text{s}$ ), respectively; and  $n$  is the value of the time steps.

## 2.5 Result and discussion

### 2.5.1 Simulation results

Figure 2.1 present the fitted curve of the simulation and the observation discharges at the Kaqun Station during 2003~2009 on the daily scale and month scale, respectively. The discharge hydrography curves both from the SWAT and MIKE SHE well matched with the observations from the October to next March. However, some fictional fluctuations were found in the early period of flood peak from April to May in the MIKE SHE model. During the peak season June to September, two simulations caught the overall trend of rising and recession of flood. In general, at the Kaqun station, the simulated discharge hydrography reflected the temporal characters of stream flow, the relative errors of the average annual volume of water resources were 8.2% and 0.1% in SWAT and MIKE SHE, respectively. The relative errors in June to September presented as 9.6% and -7.2% in SWAT and MIKE SHE, but higher values were obtained in April and May with 10.6% and 70% in SWAT and MIKE SHE.



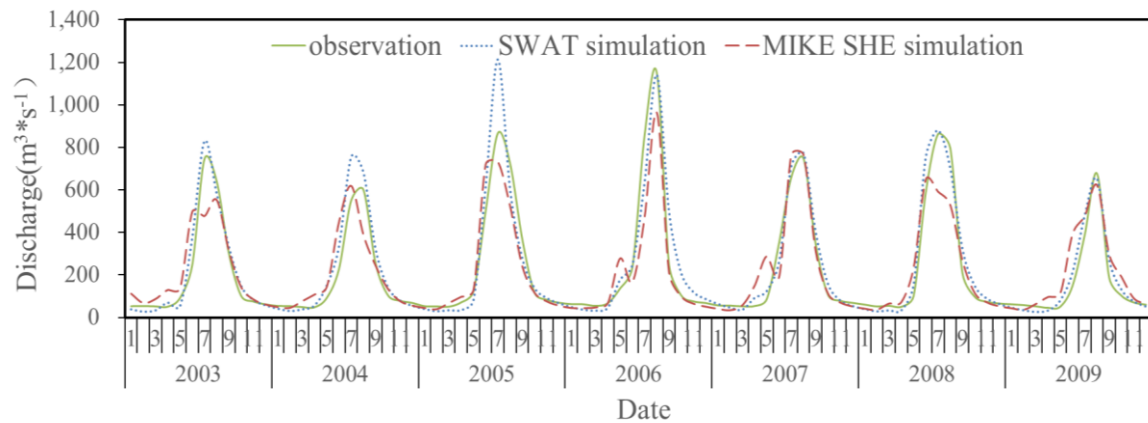


**Figure 2.1** The observed and simulated discharges at Kaqun station during 2003~2009 in the daily scale (upper one) and monthly scale (under one)

According to the evaluation criteria of calibration and verification (listed in Table 2-2), both the applications of two models in Yarkant River basin obtained acceptable performances, and the SWAT was a little better than the MIKE SHE. Obviously, the monthly simulation is better than the daily simulation. However, the criteria of evaluation coefficients are not the overall referential measurements to evaluate the accuracy of both the magnitude and timing of the simulation flows (Beven, 2001; Vázquez and Feyen, 2007), but the response of a hydrological model to the natural hydrological process should be analysed through the variation of different hydrologic elements.

Table 2-3 provides the quantification results of the average annual values of the different hydrologic elements from the SWAT and MIKE SHE models. From Table 2-3, it seems that there are some notable differences regarding the runoff contributed to stream, snow storage and evapotranspiration between SWAT and MIKE SHE. Because of the different structures and arithmetic, different constitutions and distributions would occur, it would be worth to exam the differences in more detailed view regarding the different structures and arithmetic.

**Table 2-2** Statistical coefficients of the SWAT and MIKE SHE performances on daily and monthly scale

		Daily			Monthly		
		<i>NSE</i>	<i>R</i> <sup>2</sup>	<i>RMSE</i>	<i>NSE</i>	<i>R</i> <sup>2</sup>	<i>RMSE</i>
SWAT	Calibration	0.76	0.77	151.61	0.91	0.92	82.94
	Verification	0.75	0.81	125.12	0.88	0.91	57.72
MIKE SHE	Calibration	0.71	0.80	159.91	0.90	0.91	107.12
	Verification	0.67	0.76	182.50	0.86	0.90	104.80



**Table 2-3 The average annual values of the water components from SWAT and MIKE SHE in Yarkant River basin in 2003-2009**

Element (mm)	SWAT	MIKE SHE
Precipitation	304.3	309.6
Snowfall	237.7	231.1
Snowmelt	145.6	152.8
Snow storage	60.6	46.6
Surface runoff	77.9	115.6
Lateral flow	66.5	-
Base flow	16.3	31.1
Snow sublimation	31.4	31.7
Canopy interception	13.72	15.6
River/pound water evaporation	27.38	37.1
Soil evaporation /Transpiration	18.2	29.8

### 2.5.2 Runoff

As shown in Figure 1.1, both in the SWAT and MIKE SHE, channel flow was derived from surface runoff and ground runoff, but the constitutions of ground runoff are quite distinct in two models. In the SWAT, the average annual ground water contribution was 82.6 mm which was the sum of the aquifer (base flow with value of 16.3 mm) and soil water (lateral flow with value of 66.5 mm). While, the ground water contribution in the MIKE SHE is only from the aquifer (base flow) with average annual volume of 31.1 mm. The constitution and distribution of stream runoff in daily scale is presented in Figure 2.2 below.

Previous studies reported that the rapid lateral flow in soil profile provides a dominant contribution to the storm flow in headwater catchments (Kienzler and Naef, 2008; Verseveld et al., 2009; Swarowsky et al., 2012). Additionally, Fan et al. (2014) used the isotope to study the constitution of the Tizinafu River, which is located in the same region as that of the Yarkant River. Their result demonstrate that the greatest portions of ice-snowmelt water will recharge the aquifer in the area located under 2500 m, but in the high mountain area, the greatest portions of ice-snowmelt water will infiltrate into the soil and contribute to the stream as lateral flow. This feature is described reasonably in SWAT model with subsurface runoff contribution rate of 41.4%, what is anymore, in SWAT, base flow present an obvious seasonality, and little contribution to stream from the November to the following March (Figure 2.2).

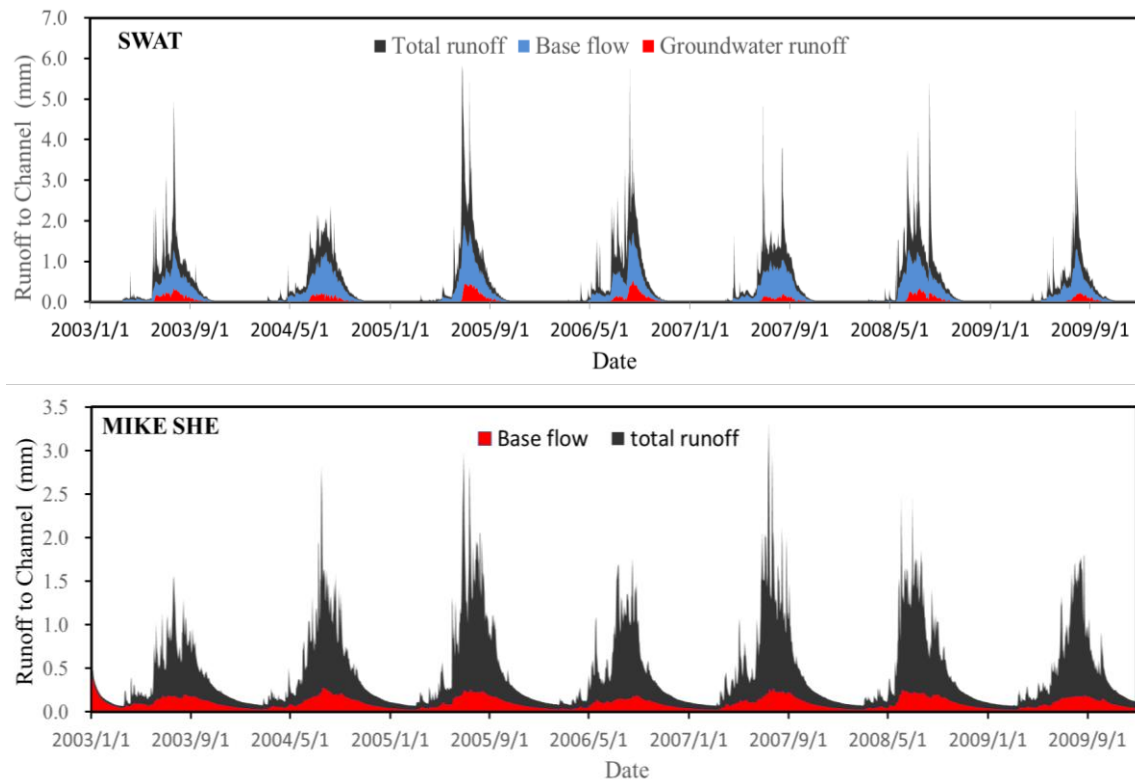


**Figure 2.2 The daily constitution of the simulation runoff from SWAT and MIKE SHE in Yarkant River basin**

In MIKE SHE, Richards and Gravity flow equation only take vertical flow into account in unsaturated zone, but when soil moisture is saturated, and head pressure of aquifer water is higher than surface, the infiltrated soil water could flow back to surface, and this part accounted for 39.4% of total stream runoff in this simulation (close to the subsurface lateral flow of 41.4% in SWAT). As well as the appropriate soil water recharge to aquifer, MIKE SHE got a persistent and steady contribution to stream in the low water period as base flow (Figure 2.2). The proportion of 21.3% agreed very well with the result of 23% from Fan et al. (2013), which was obtained through a multiple base flow separate approach.

### 2.5.3 Snow

#### Temporal distribution of snowmelt

The simulated daily snowmelt in Yarkant River basin from 2003 to 2009 is presented in Figure 2.3. The temporal distribution of the snowmelt is more concentrated in SWAT, and the amount of snowmelt from June to September constitutes 76.8% of the annual snowmelt. The period of snowmelt is longer and the temporal distribution is more dispersive in MIKE SHE, and the amount of snowmelt from June to September

constitutes 58.43%. Compared with the SWAT model, more snowmelt were taken place in the early period of flood reason, this finding can explain why more discharges were given during April to May in MIKE SHE model. What's more, the different algorithms of the snowmelt in the two models can explain the different temporal distribution of snowmelt.

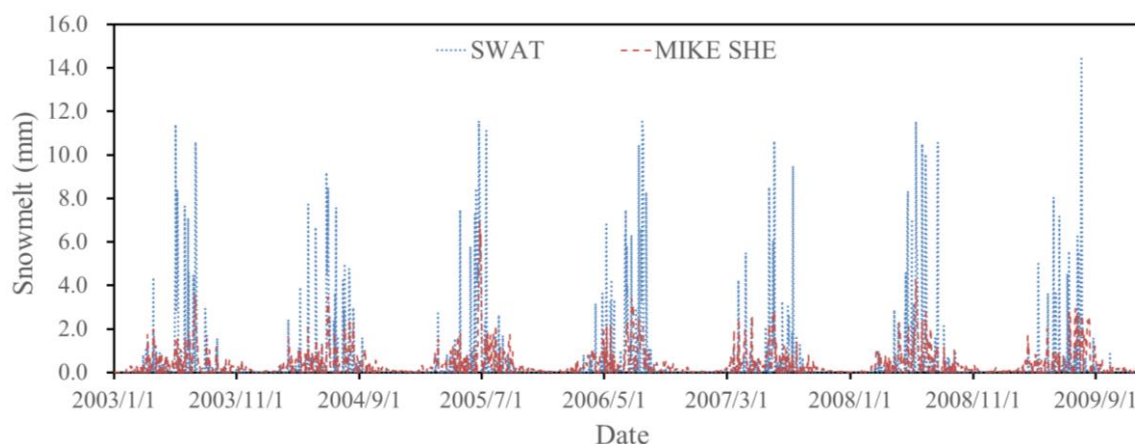


**Figure 2.3 The simulated daily snowmelt from SWAT and MIKE SHE in the Yarkant River basin**

In the SWAT model, the accumulated temperature what can reflect the status of solar radiation that significantly affects the snowmelt (Koivusalo, 2001) has been taken into account. However, in the MIKE SHE model, the amount of snowmelt lies on the average air temperature, and the change in the snowmelt closely follows the change in air temperature; accordingly, there is more snowmelt small peaking in MIKE SHE. What's more, because of the seasonal variation of the melt factor in the SWAT model, the more snowmelt that occurs in summer, the higher melt factor; this is possibly another cause for the more concentrated distribution in the SWAT model.

Temperature is primary and reliable in the degree-day approach: if the status of solar radiation and the snow pack-air temperature (Lang, 1968; Zuzel et al., 1975) and the seasonal variation of the melt factor (Hock, 2003) are considered, the simulation process would be more flexible for catching natural realities rather than only considering the air temperature. Consequently, the temporal distribution of the snowmelt in the SWAT model matches better with the runoff characteristics of Yarkant River basin, in which the greatest proportion of the water source derives from the melting snow and glaciers, and the amount of runoff from June to September accounts for 80% of the total annual runoff (Chen et al., 2006; 2010).

### Spatial distribution of snow storage

Elevation is one of central factor that significantly affects the mountain hydrological processes (Zhang et al., 2012), because there are large differences of the snow storage in the different elevation bands. The information of the elevation bands divided in Yarkant River is provided in Table 2-4. Because the areas of Band 9 in MIKE SHE and Band 10 in SWAT are very small, the proportion is approximately zero. Only the bands from 1 to 8 were chosen to compare the average depth of the annual snow storage, it has been illustrated in Figure 2.4.

**Table 2-4 The elevation ranges and area ratios of the elevation bands in Yarkant River basin parted in SWAT and MIKE SHE model**

Elevation bands	Elevation range	Area percentage	
		SWAT	MIKE SHE
Band 1	1450~2200	3.38%	3.95%
Band 2	2200~2900	6.04%	6.32%
Band 3	2900~3600	11.54%	12.18%
Band 4	3600~4300	17.32%	16.49%
Band 5	4300~5000	27.17%	26.03%
Band 6	5000~5700	28.64%	29.02%
Band 7	5700~6400	5.64%	5.71%
Band 8	6400~7100	0.25%	0.29%
Band 9	7100~7800	0.02%	0.00%
Band 10	7800~8611	0.00%	0.01%

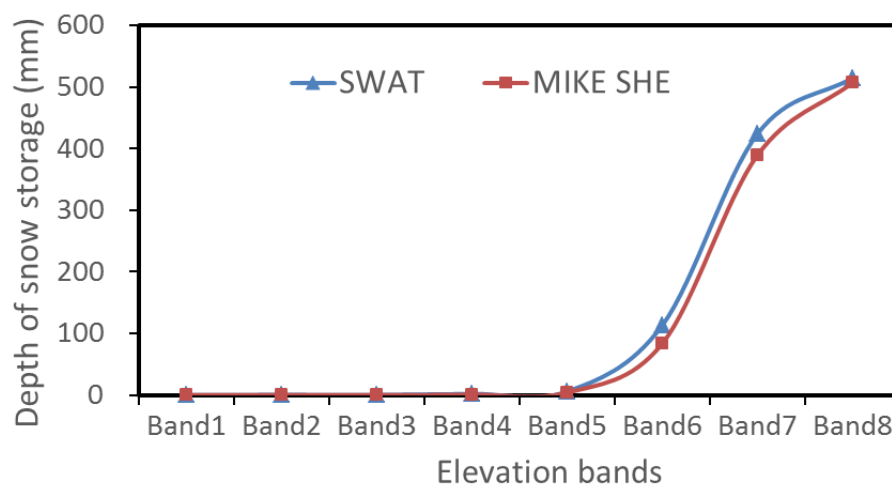


**Figure 2.4 The snow storage in the different elevation bands from SWAT and MIKE SHE in Yarkant River basin in 2003-2009**

From Figure 2.4, it is apparent that in the region from 1450 m to 7100 m, the simulated annual snow storage is consistent in different elevation bands between SWAT and

MIKE SHE. Increasing storage occurs in the high mountain where the elevation is greater than 5000 m, and the increasing amount is prominent with the higher elevation. The distribution is rough because the elevation bands cannot illustrate the status of snow storage; hence that, the fine distribution based on the model's resolution is presented in Figure 2.5. In the first column, the results are from SWAT and are distributed as a sub-basin; in the second column, the results are from MIKE SHE, and the average values of the grids under each sub-basin have been calculated and distributed as sub-basin; and in the third column, the results are from MIKE SHE and are displayed in grid view.

As shown in Figure 2.5, the two models have a similar tendency for spatial change during the different seasons: at the end of March, all most catchment is covered by snow, snowmelt first occurs around the outlet in April, the snow melt extends to the mountain region approximately 4500 m from July to September, and a new increasing storage appears after October. But in the region in which the elevation is greater than 5500 m, the snow cover shows a continuously increasing trend throughout the entire year. Furthermore, comparing the first and second column, the similar average depth of the snow storage in the same district has been illustrated through year. Between the first and third column, the spatial distribution of MIKE SHE is much more distinct than that of SWAT, and the differences in the snow storage depth between the grids in MIKE SHE are much more obvious than in the sub-basins in SWAT.

For the differences of snowpack, the effect of model structure cannot be detached. In the SWAT model, the HRU is the smallest calculated unit, but spatial relation exists in the sub-basins; therefore, an aerial depletion curve was introduced when considering the unequal distribution in the sub-basin. Based on the cognition of SWAT, the factors such as drifting, shading and topography that influence snow coverage vary annually, through which the areal coverage of snow can be corrected with the amount of snow in the sub-basin. The aerial depletion curve makes the spatial distribution more uniform. As a fully distributed model, in MIKE SHE model, each grid can reflect the actual spatial change of the snow storage in that place, consequently, the spatial distribution is more distinct.

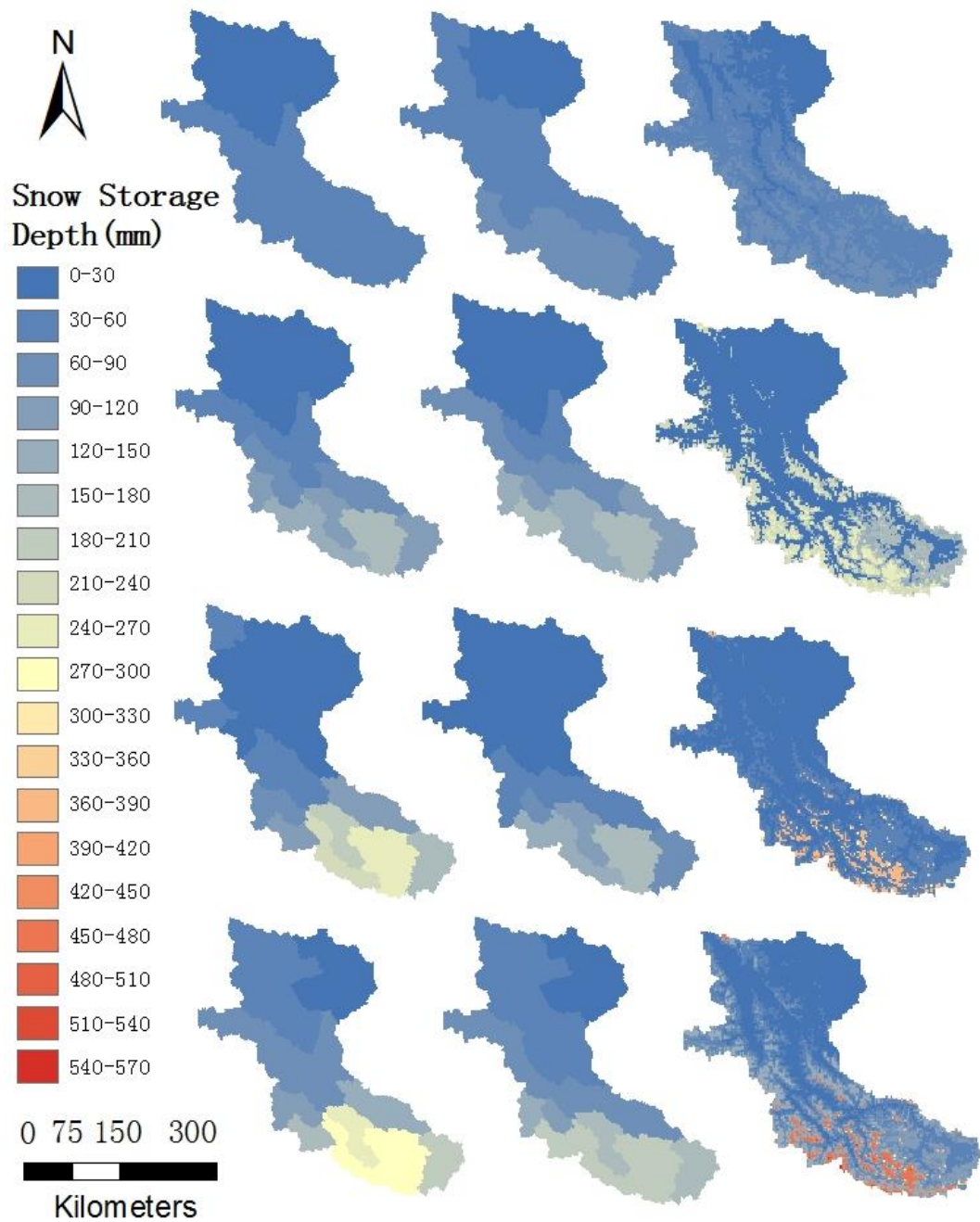


**Figure 2.5 Simulated snowpack of SWAT (1<sup>st</sup> column), MIKE SHE in sub-basin(2<sup>nd</sup> column) and MIKE SHE (3<sup>rd</sup> column) in Yarkant River basin on 31<sup>st</sup> Mar. (1<sup>st</sup> row), 30<sup>th</sup> Jun. (2<sup>nd</sup> row), 30<sup>th</sup> Sep. (3<sup>rd</sup> row) and 31<sup>st</sup> Dec. (4<sup>th</sup> row) 2003**

### **Remotely sensed crossing-verification**

In consideration of the importance of snow in the Yarkant River basin, the remotely sensing snow coverage data MODIS 10A2 (Table 1-3) was taken as a kind of crossing-verified data to test the MIKE SHE's output. The recognition accuracy rate of MODIS 10A2 to the snow covered area reached 88% in the north Xinjiang region (Huang et al, 2008). Since the poor recognition to the thin snowpack (Huang et al, 2008),

the grid in the MIKE SHE model which the snow covered depth were more than 50 mm was defined as snow coverage, otherwise, it should be defined as no snow coverage. Their crossing-verification figure was illustrated as Figure 2.6.

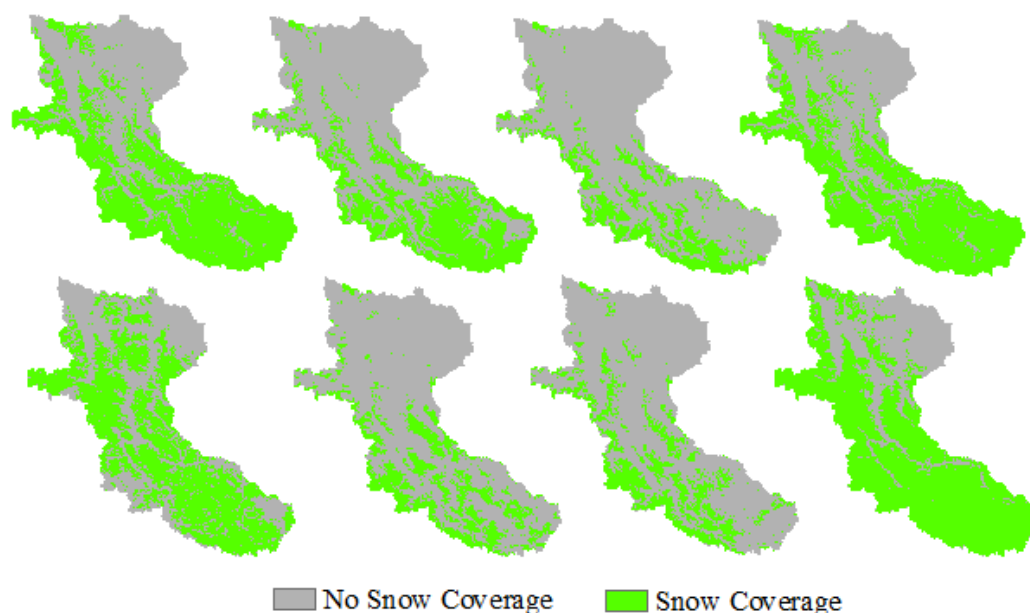


**Figure 2.6** Remotely sensed snow coverage (1<sup>st</sup> row), simulated of MIKE SHE (2<sup>nd</sup> row) in Yarkant River basin on 31<sup>st</sup> Mar. (1<sup>st</sup> column), 30<sup>th</sup> Jun. (2<sup>nd</sup> column), 30<sup>th</sup> Sep. (3<sup>rd</sup> column) and 31<sup>st</sup> Dec. (4<sup>th</sup> column) 2003

Relative to the remote sensing data, MIKE SHE's output in snow coverage presented the relative errors of -3.1%, 43%, -12.9% and -11.6% on the four different timings. The snowpack around 5000 m region mostly was melted in June and August, this is late correspond to remote sensing monitoring; can caused the high errors at end of June. Generally, the similarly overall tendencies both in temporal or spatial changes were found in remote sensing data and MIKE SHE's output. This crossing-verification indirectly resulted in the accuracy of MIKE SHE's simulation.

#### 2.5.4 Evapotranspiration

In this study, Penman-Monteith approach was selected to estimate the PET in SWAT model. Basin on Table 2-2, the differences of  $ET_a$  between SWAT and MIKE SHE were greatly reflected on river/pound water evaporation and soil evaporation/transpiration, while the other values are similar. Subsequently, the annual  $ET_a$  in MIKE SHE was 23.5 mm more than that in SWAT. For the difference in river/pound water evaporation, it is possible that the spatial relationship between calculated units is one cause. As shown in

Figure 1.1, in SWAT, HRUs are controlled by water balance independently, the surface runoff would directly contribute to the stream without the over land flow concentration. But the grids in MIKE SHE are linked by hydrodynamic relation, and the flood detention area is considered in the over land flow calculation, what the result is that larger area of water surface in MIKE SHE model may cause more water evaporation.

The soil evaporation in SWAT is limited by soil moisture content. When the water content of a soil layer is below field capacity, the evaporative demand will be reduced according to the following equations.

$$E'_{\text{soil}} = E_{\text{soil}} * \exp \left[ \frac{2.5 * (SW - FC)}{FC - WP} \right] \text{ when } SW \leq FC \quad (2 - 12)$$

$$E'_{\text{soil}} = E_{\text{soil}} \text{ when } SW > FC \quad (2 - 13)$$

Where  $E'_{\text{soil}}$  is the evaporative demand for soil layer adjusted for actual water content (mm);  $E_{\text{soil}}$  is the evaporative demand (mm); SW is the actual soil water content; FC and WP are the soil water content at field capacity and wilting point respectively. In addition to limiting the amount of water removed by evaporation in dry conditions, SWAT also defined a maximum value of soil evaporation that is 80% of the plant available water on a given day, and calculated as the total water content of the soil layer minus the water content of the soil layer at wilting point, this setting is also available under the bare land. At finally, the actual soil evaporation  $E''_{\text{soil}}$  can be expressed as equation11 in below.

$$E''_{\text{soil}} = \min(E'_{\text{soil}}, 0.8 * (SW - WP)) \quad (2 - 14)$$

However, in the MIKE SHE model, soil evaporation is restricted to the leaf area index, root depth and upper node in the unsaturated zone and all of the water in the soil will be used to meet the soil evaporation. Even the initial water content in the soil can compensate for the insufficient soil evaporation demand. Therefore, there could be more soil evaporation in the MIKE SHE model.



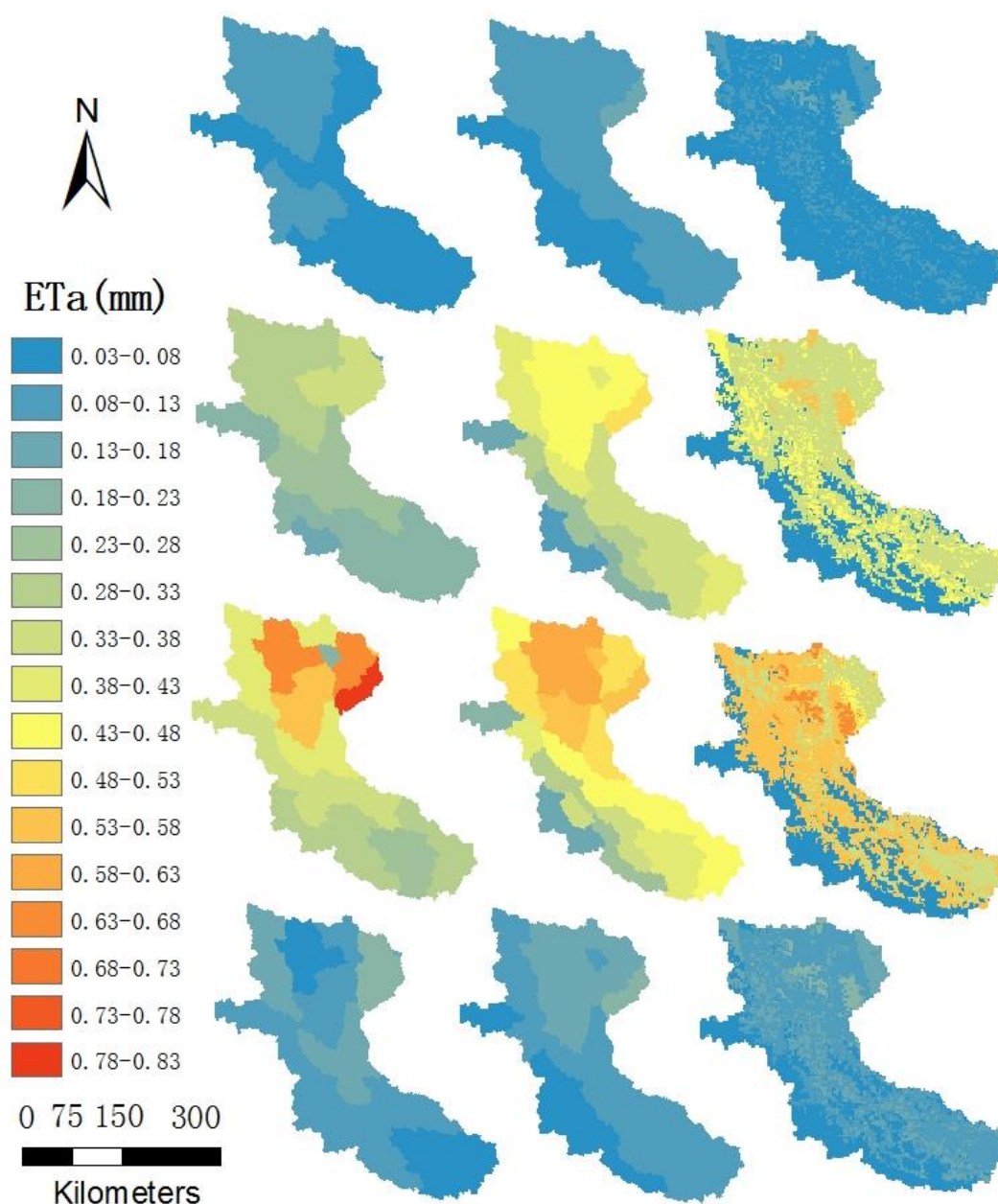


**Figure 2.7** The daily average evapotranspiration of SWAT (1<sup>st</sup> column), MIKE SHE in sub-basin(2<sup>nd</sup> column) and MIKE SHE (3<sup>rd</sup> column) in Yarkant River from Jan.~Mar. (first line), Apr.~Jun. (second line), Jul.~Sep. (third line), and Oct.~Dec (forth line) 2003

From the aspect of spatial distribution based on Figure 2.7, this relationship can be seen: in addition to the effect of temperature, the land use has significantly affected the spatial distribution of evapotranspiration. Comparing the first and second rows under the same resolution, the tendency of the spatial change is similar in the different seasons between the SWAT and MIKE SHE models: the evapotranspiration around the outlet of the catchment is much higher than that of the mountain area because of the temperature change in low and high mountain region. The difference is much more obvious in the

summer season. However, relative to the spatial resolution of MIKE SHE from the first and third rows, the semi-distributed SWAT model cannot support the specific information about the spatial distribution.

Combined with two models' simulation in evapotranspiration, some understanding can be obtained. In Yarkant River basin, water body evaporation was the primary way, and since the large area of snow cover, the sublimation was the second evaporation way. With the temperature change and plant growth, about 45% of annual evapotranspiration was happened during July to September. In the spatial distribution, the volume of evaporation in the region covered by evergreen needle-leaved tree was the highest with the approximate value of 290 mm per year, and the plant transpiration was the dominant way. Following is the region covered by closed open herbaceous with the annual value of 160 mm. The lowest region is the permanent snow coverage, and the annual volume was about 40 mm.

## **2.6 Summary and Conclusions**

Based on the statistic evaluation indices of discharges calibration on Kaqun station, both SWAT and MIKE SHE got acceptable performances in Yarkant River basin. Because there is no more observations can be used to calibrate models, it would be reasonable to cautiously draw the conclusions for model responses to hydrological processes. Therefore, the differences of multiple hydrologic components from two models were intercompared based on modules' structures and algorithms, the main consequences include the following aspects.

The phenomenon that most of ice-snowmelt water will infiltrate into the soil and contribute to the stream as subsurface runoff have been described by SWAT, with a contribution proportions of 41.4%. While, MIKE SHE generated a more reasonable base flow with a contribution of 21.3% also ignoring the soil lateral flow. SWAT obtained a better snowmelt process corresponding to the character of the river flow, but cannot distinctly reflect the spatial features of snowpack that could be detailedly achieved by MIKE SHE. The less  $ET_a$  in SWAT has been mainly caused by less water surface area and restrictive setup of soil evaporation function. In comparison, MIKE SHE also provided more information regarding the evapotranspiration being closely related to land use.

From the careful quantifying and reasoning mentioned above, the application of the SWAT and MIKE SHE models in Yarkant River basin can agree with natural

observations in some aspects but not in the entire cycle processes. However, combined the outputs from two models, SWAT complements the subsurface lateral flow to MIKE SHE which had a better groundwater simulation in this mountainous region; MIKE SHE can supplement the spatial distribution of snowpack and  $ET_a$  for SWAT's output. Therefore, some statements of the hydrological processes can be given as : 1) there were steady groundwater can contribute to the stream as base flow, taking account of 21% approximately; and the lateral interflow was the important contribution for the stream flow, take account of 40% approximately. 2) June to September was the concentrated snowmelt period with the proportion more than 70%; the region above 5000 m was mostly the permanent snow coverage. 3) water evaporation and sublimation were the primary evaporation ways, most evaporation dissipation was taken placed in the regions covered well vegetation and concentrated on July to September.

Without the multiple calibrations, a single model hardly clarifies the whole hydrological processes in the alpine catchment. Based on the joint application of multiple models, not only an improved understanding of hydrological processes can be obtained, but also the interpretations of variations between two models stated how the structure and algorithm impact on hydrological processes and provided an inspiring reference to hydrological processes study in other catchments with unique features. In future study on arid and scarcely gauged alpine basin, the joint application of multiple hydrological models and combined results could be an effective way to control the uncertainties from modules' structure and algorithm, and improving understanding of hydrological processes.

## References

- Abbaspour, K. C., Johnson, C. and Van, G. (2004). Estimating uncertain flow and transport parameters using a sequential uncertainty fitting procedure. *Vadose Zone Journal*. 3(4): 1340-1352.
- Allen, R. G. (1986). A Penman for all seasons. *Journal of Irrigation and Drainage Engineering*. 112(4): 348-368.
- Allen, R. G., Jensen, M. E., Wright, J. L. (1989). Operational estimates of reference evapotranspiration. *Agronomy Journal*. 81(4): 650-662.
- Barthel, R., Reichenau, T. G., Krimly, T., Dabbert, S., Schneider, K., Mauser, W. (2012). Integrated Modeling of Global Change Impacts on Agriculture and Groundwater Resources. *Water Resources Management*. 26(7): 1929-1951. Doi: 10.1007/s11269-012-0001-9.
- Basist, A., Bell, G. D., Meentemeyer, V. (1994). Statistical relationships between topography and precipitation patterns. *Journal of climate*, 7(9): 1305-1315.

- Beven, K., Freer, J. (2001). Equifinality, data assimilation, and uncertainty estimation in mechanistic modeling of complex environmental systems using the GLUE methodology. *Journal of Hydrology*. 249: 11-29.
- Boorman, D. B., Sefton, C. E. M. (1997). Recognizing the uncertainty in the quantification of the effects of climate change on hydrologic response. *Climatic Change* 35: 415-434.
- Chen, Y., Takeuchi, K., Xu, C., Chen, Y., and Xu, Z. (2006). Regional climate change and its effects on river runoff in the Tarim Basin, China. *Hydrological processes*. 20(10): 2207-2216. doi: 10.1002/hyp.6200.
- Chen, Y., Xu, C., Chen, Y., Li, W., and Liu, J. (2010). Response of glacial-lake outburst floods to climate change in the Yarkant River basin on northern slope of Karakoram Mountains, China. *Quaternary International*. 226(1-2): 75-81. doi: 10.1016/j.quaint.2010.01.003.
- Daly, C., Neilson, R. P., Phillips, D. L. (1994). A statistical topographic model for mapping climatological precipitation over mountainous terrains. *Journal of Applied Meteorology*, 33(2): 140-158.
- DHI, (2007). MIKE SHE user manual volime2: Reference Guide. DHI water & Environment.
- El-Nasr, A. A., Arnold, J. G., Feyen, J., Berlamont, J. (2005). Modeling the hydrology of a catchment using a distributed and a semi-distributed model. *Hydrological processes*. 19(3): 573-587. dio: 10.1002/hyp.5610.
- Fan, Y., Chen, Y., Liu, Y., Li, W. (2013). Variation of baseflows in the headstreams of the Tarim River Basin during 1960–2007. *Journal of Hydrology*. 487: 98-108. doi: 10.1016/j.jhydrol.2013.02.037.
- Fan, Y., Chen, Y., Li, X., Li, W., Li, Q. (2014). Characteristics of water isotopes and ice-snowmelt quantification in the Tizinafu River, north Kunlun Mountains, Central Asia. *Quaternary International*. doi: 10.1016/j.quaint.2014.05.020.
- Ferrant, S., Oehler, F., Durand, P., Ruiz, L., Salmon, M. J., Justes, E., Dugast, P., Probst, A., Probst, J. L., Sanchez, P., José, M. (2011). Understanding nitrogen transfer dynamics in a small agricultural catchment: Comparison of a distributed (TNT2) and a semi distributed (SWAT) modeling approaches. *Journal of Hydrology*. 406(1): 1-15. 10.1016/j.jhydrol.2011.05.026.
- Gan, T. Y., Dlamini, E. M., Biftu, G. F. (1997). Effects of model complexity and structure, data quality, and objective unctions on hydrological modeling. *Journal of Hydrology*. 192: 81-103.
- Gao, X., Zhang, S. Q., Ye, B. S., Jiao, C. J. (2010). Glacier Runoff Change in the Upper Stream of Yarkant River and Its Impact on River Runoff during 1961~2006. *Journal of Glaciology and Geocryology* 32(3): 445-453.
- Golmohammadi, G., Prasher, S., Madani, A., Rudra, R. (2014). Evaluating Three Hydrologic Distributed Watershed Models: MIKE-SHE, APEX, SWAT. *Hydrology*. 1(1): 20-39. dio: 10.3390/hydrology1010020.
- Goovaerts, P. (1999). Using elevation to aid the geostatistical mapping of rainfall erosivity. *Catena*, 34: 227-242.

- Goovaerts, P. (2000). Geostatistical approaches for incorporating elevation into spatial interpolation of rainfall. *Journal of Hydrology*, 228: 113-119.
- Gupta, H. V., Sorooshian, S., Hogue, T. S., Boyle, D. P. (2003). Advances in automatic calibration of watershed models. *Water Sciences and Application* 6: 9-28. doi: 10.1029/WS006p0009.
- Huang, X. D., Zhang, X. T., Li, X. (2008). Accuracy Analysis for MODIS snow products of MOD10A1 and MOD10A2 in Northern Xinjiang Area. *Journal of Glaciology and Geocryology*. 29(5): 722-729.
- Hargreaves, G. L., Hargreaves, G. H., Riley, J. P. (1985). Agricultural benefits for Senegal River basin. *Journal of Irrigation and Drainage Engineering-ASCE*. 111(2): 113-124.
- Hock, R. (2003). Temperature index melt modeling in mountain areas. *Journal of Hydrology*. 282(1-4): 104-115, doi: 10.1016/s0022-1694(03)00257-9.
- Hughes, J. D. and Liu, J. (2008). MIKE SHE: Software for Integrated Surface Water/Ground Water Modeling, *Ground Water* 46(6): 797-802. doi:10.1111/j.1745-6584.2008.00500.x.
- Kienzler, P. M. and Naef, F. (2008). Subsurface storm flow formation at different hillslopes and implications for the old water paradox. *Hydrological processes*. 22(1): 104-116. doi: 10.1002/hyp.6687.
- Knorad, C. E. (1996). Relationships between precipitation event typeset and topography in the Southern Blue Ridge Mountainous of the Southeastern USA. *International Journal of Climatology*, 21(4): 455-466.
- Koivusalo, H., Heikinheimo, M., Karvonen, T. (2001). Test of a simple two-layer parameterisation to simulate the energy balance and temperature of a snow pack. *Theoretical and Applied Climatology*. 70: 65-79.
- Kristensen, K. J. and Jensen, S. E. (1975). A model for estimating actual evapotranspiration from potential evapotranspiration. *Nordic Hydrology*. 6(3): 170-188.
- Lang, H. (1968). Relations between glacier runoff and meteorological factor observed on and outside the glacier. *IAHSPubl*.
- Loukas, A., Mylopoulos, N., Vasiliades, L. (2007). A modeling system for the evaluation of water resources management strategies in Thessaly, Greece. *Water Resources Management*. 21: 1673-1702. doi: 10.1007/s11269-006-9120-5.
- Liu, T., Willems, P., Pan, X. L., Bao, A. M., Chen X., Veroustraete, F., Dong, Q. H. (2011). Climate change impact on water resource extremes in a headwater region of the Tarim basin in China. *Hydrology and Earth System Sciences*. 8: 6593-6637. doi: 10.5194/hessd-8-6593-2011.
- Maurer, E. P., Brekke, L. D., Pruitt, T. (2010). Contrasting Lumped and Distributed Hydrological models for Estimating Climate Change Impacts on California Watersheds1. *Journal of American Water Resources Association*. 46(5): 1024-1035. doi: 10.1111/j.1752-1688.2010.00473.x.
- Najafi, M. R., Moradkhani, H., Jung, I. W. (2011). Assessing the uncertainties of hydrological model

- selection in climate change impact studies. *Hydrological processes*. 25(18): 2814-2826. doi: 10.1002/hyp.8043.
- Nasr, A., Bruen, M., Jordan, P., Moles, R., Kiely, G., Byrne, P. (2007). A comparison of SWAT, HSPF and SHETRAN/GOPC for modeling phosphorus export from three catchments in Ireland. *Water Research* 41(5): 1065-1073. doi: 10.1016/j.watres.2006.11.026.
- Neitsch, S. L., Arnold, J. G., Kiniry, J. R., Williams, J. R. (2011). *Soil and Water Assessment Tool Theoretical Documentation, Version 2009*, Soil and Water Research Laboratory, USA.
- Nash, J. E., Sutcliffe, J. V. (1970). River flow forecasting through conceptual models part I — a discussion of principles. *Journal of Hydrology*. 10: 282-290.
- Priestley, C. and Taylor, R. (1972). On the assessment of surface heat flux and evaporation using large-scale parameters. *Month Weather Review*. 100(2): 81-92.
- Rahman, K., Maringanti, C., Beniston, M., Widmer, F., Abbaspour, K., Lehmann, A. (2012). Streamflow Modeling in a Highly Managed Mountainous Glacier Watershed Using SWAT: The Upper Rhone River Watershed Case in Switzerland. *Water Resources Management*. 27(2): 323-339. doi: 10.1007/s11269-012-0188-9.
- Shi, P., Chen, C., Srinivasan, R., Zhang, X., Cai, T., Fang, X., Qu, S., Chen, X., Li, Q. (2011). Evaluating the SWAT Model for Hydrological modeling in the Xixian Watershed and a Comparison with the XAJ Model. *Water Resources Management*. 25(10): 2595-2612. doi: 10.1007/s11269-011-9828-8.
- Smith, M. B., Koren, V., Zhang, Z. (2012). Results of the DMIP 2 Oklahoma experiments. *Journal of Hydrology*. 418: 17-48
- Smith, M. B., Koren, V., Zhang, Z. (2013). The distributed model intercomparison project—Phase 2: Experiment design and summary results of the western basin experiments. *Journal of Hydrology*. 507: 300-329.
- Swarowsky, A., Dahlgren, R. A., O'Geen, A. T. (2012). Linking Subsurface Lateral Flowpath Activity with Streamflow Characteristics in a Semiarid Headwater Catchment. *Soil Science Society of Amercian Journal*. 76(2): 532. doi: 10.2136/sssaj2011.0061.
- Thompson, J. R., Sørensen, H. R., Gavin, H., Refsgaard, A. (2004). Application of the coupled MIKE SHE/MIKE 11 modeling system to a lowland wet grassland in southeast England. *Journal of Hydrology*. 293: 151-179. doi: 10.1016/j.jhydrol.2004.01.017.
- Vansteenkiste, T., Tavakoli, M., Ntegeka, V., Willems, P., Smedt, F., Batelaan, O. (2013). Climate change impact on river flows and catchment hydrology: a comparison of two spatially distributed models. *Hydrological processes*. 27(25): 3649-3662. doi: 10.1002/hyp.9480.
- Vázquez, R. F. and Feyen, J. (2007). Assessment of the effects of DEM gridding on the predictions of basin runoff using MIKE SHE and a modeling resolution of 600m. *Journal of Hydrology*. 334(1-2): 73-87. doi: 10.1016/j.jhydrol.2006.10.001.
- Verseveld, W. J., McDonnell, J. J., Lajtha, K. (2009). The role of hillslope hydrology in controlling

- nutrient loss. *Journal of Hydrology*. 367(3-4): 177-187. doi: 10.1016/j.jhydrol.2008.11.002.
- Vrugt, J. A., Gupta, H. V., Bouten, W., Sorooshian, S. (2003). A Shuffled Complex Evolution Metropolis algorithm for optimization and uncertainty assessment of hydrological model parameters. *Water Resources Research*. 39(8): 1-14. doi: 10.1029/2002wr001642.
- Wood, A. D. (2004). Hydrologic implications of dynamical and statistical approaches to downscaling climate model outputs. *Climatic Change*. 62: 189-216
- Xu, C. (1999). From GCMs to river flow a review of downscaling techniques and hydrological modeling approaches. *Process in Physical Geography*. 23(2): 229-249.
- Zhang, S., Gao, X., Zhang, X., Hagemann, S. (2012). Projection of glacier runoff in Yarkant River basin and Beida River basin, Western China. *Hydrological processes*. 26(18): 2773-2781. doi: 10.1002/hyp.8373.
- Zuzel, J. F., Cox, L. M. (1975). Relative importance of meteorological variables in snowmelt. *Water Resources Research*. 11(1): 174-177





# CHAPTER 3

## **The responses of hydrological processes to the different input data**

---

*Modified from: Liu, J., Liu, T., Bao, A. M., De. Maeyer, P., Alishir, K., Chen, X. (2016).  
Response of hydrological processes to input data in high alpine catchment—an  
assessment of Yarkant River basin in China. Water. 181(8):1-5. Dio: 10.3390/w8050181.*

## ABSTRACT

Most attentions have been paid to flow in studies on the hydrological model's input data; however, the point discharge data hardly interpret the deviations of the spatial input data in the distributed hydrological model. To study the effect of the different input data sources on hydrological processes in the catchment scale, eight MIKE SHE model programmes driven by the station-based data (SBD) and remote sensing data (RSD) were implemented. The significant influences of the input variables to water components were examined by an analysis of variance (ANOVA) model and catchment hydrology responses have been quantified through different water components. Results suggested that, compared to the SBD, the RSD precipitation resulted in greater differences in snow storage in the different elevation bands and that the RSD temperature led to more snowpack areas with a thinner depth; these changes in snowpack provided a positive interpretation of the distinctions of precipitation and temperature between RSD and SBD. For the potential evapotranspiration (PET), the larger RSD value caused less plant transpiration because of the adjusted parameters to satisfy the outflow. On the catchment scale, the spatiotemporal distribution of the responding sensitive water component (which can be defined by the ANOVA model) indicated a rational approach to assess the impact of the input data on the hydrological processes.

**Key words:** input data; hydrological processes; statistic hypothesis test; spatiotemporal distribution; Yarkant River; MIKE SHE

### 3.1 Introduction

Model simulation is a principal approach for studying hydrological processes on a catchment scale; however, the accuracy of the modelling results has been dwarfed owing to the uncertainties of the model, which are derived from the model parameters, input data and model structures (Beven et al, 1992). Most studies (Jasper et al, 2003; Misgana et al, 2005; Zhang et al., 2009; Jin et al., 2010) have analyzed the uncertainty of the parameters by different methods and the calibration focused on the model's parameters has implied the contributions from other sources of uncertainty (Ajami et al., 2006). However, it is unreasonable to detect uncertainty sources through the parameters assessment because of the highly non-linear relations among the hydrologic cycle. Ajami (Ajami et al., 2007) confirmed the importance of the input data and model structure to the model output by using the Integrated Bayesian Uncertainties Estimator (IBUNE), which considered all three of the uncertainty sources. Kavetski (Kavetski et al., 2006)

demonstrated a multitude of distinctions in the predicted hydrographs and calibrated parameters based on the Bayesian total error analysis, with or without consideration of the input uncertainty of the precipitation data. Similar conclusions were also drawn by Xu (Xu et al., 2006) by investigating the performance of the precipitation errors on seasonal and spatial distribution in a conceptual model. In addition to the precipitation data, Thompson's (Thompson et al., 2014) research revealed that the PET-related uncertainty existed in high and low discharge. Furthermore, a number of works illustrated that the uncertainties of the input data may profoundly impact the predicted water resources (Abbaspour et al., 2009; Bastola et al., 2011), river runoff (Chien et al., 2013; Xu et al., 2013) and extreme flow events (Dobler et al., 2012; Zhang et al., 2014). However, few attentions have been paid to the effect of the different input data on the whole hydrologic cycle process in a catchment scale.

In a mountain catchment with scarce gauges, the uncertainties of the input data are amplified owing to the lack of observed data (Blazkova et al., 2002). With the development of satellite technology, RSD affords abundant information to drive, calibrate and validate hydrological models (Stisen et al., 2008), especially, the RSD enriched the data resources in understanding the hydrological processes of the high-cold alpine catchment (Chen et al., 2014). Some applications of RSD in the hydrological model (even on semi-arid/arid watersheds) have attained a promising performance (Liu et al., 2012; Sun et al., 2012; Deus et al., 2013). However, most of the precious studies focused on the performance assessment of the RSD application only based on the calibrated output, but not the whole process.

RSD also supplies a wealth of new observation types, which can be applied to assess the model uncertainty (Van, 2011). According to the examination of McMichael et al. (2006), the uncertainty of the predictions among seven leaf area index (LAI) scenarios is less than 10% in the MIKE SHE simulation. Sun et al. (2012) demonstrated that the contributed uncertainties derived from RSD are smaller compared with those of the model parameters. However, Knoche et al. (2014) argued that the high-resolution land surface temperature (LST) data did not yield a positive result, and that the simulated hydrographs cannot explain the differences of the input data. Owing to the limitations of the satellite data in terms of the physical sensors, space–time coverage and spatial resolution (Prigent, 2010), the application of raw RSD has been threatened and has resulted in some controversial results. In addition, these analyses based on the simulated discharges cannot appropriately reveal the characteristics of the spatial impact from RSD.

This paper intends to characterize the influences of the different input data sources based on the variation of a distributed simulation output. Eight MIKE SHE model programmes (forced by SBD and RSD) are calibrated separately so as to obtain the most optimal performance. The significant impact of the input data on different water components is determined via an ANOVA model. Then, the effect of the different input data on the hydrological processes are studied through the distribution of the sensitive water components.

### **3.2 Study area**

The Yarkant River basin (shown as Figure 1.2) was chosen in this study. More detailed information can be seen in Section 1.2.

### **3.3 Forcing data**

The employed data sets (including the SBD and RSD) have been introduced in section 1.3.1 and section 1.3.2. Their processing methods are mentioned below.

#### **3.3.1 Station data**

The station meteorological data of Tashkurgan were interpolated based on the Equation 2-6 and 2-7. The same interpolations of precipitation and temperature were used in SWAT and MIKE SHE. When the PET calculated by SWAT on the sub-basin scale based on the Penman-Monteith equation, it was used in MIKE SHE as the input reference evapotranspiration.

#### **3.3.2 TRMM**

The remotely sensed precipitation data 3B42 version 6 with a spatial resolution of  $0.25^\circ$  was chosen. Although the TRMM V6 data had been calibrated on a global scale by using rain gauge stations (Huffman et al., 2007) and played an accelerative role as input data in the hydrological modeling research (Collischonn et al., 2008; Li et al., 2012), in such a mountainous region as the Yarkant River basin with arid climate conditions, extreme topography and few rain gauges, the accuracy is still unfavorable, especially on a daily temporal scale (Ji et al., 2013).

According to the recorded data from 2000 to 2009 at the Tashkurgan, Shache and Pishan meteorological stations, an examination was applied to diagnose whether the TRMM

satellite detected the correct precipitation events (Equations 3-1 and 3-2). In this examination,  $TRMM_{dec}$  is defined as the total number of days on which the precipitation events were detected by TRMM but not recorded by SBD on the same date,  $SBD_{dec}$  is defined as the total number of days with precipitation events occurring in SBD but not in TRMM on the same date,  $TRSB_{dec}$  is defined as the total number of days on which precipitation events were detected by both TRMM and SBD. In addition,  $D_r$  and  $D_w$  are considered as the probability of the correct and incorrect precipitation events detected by TRMM and calculated for the satellite grids the stations are on. Their calculations can be written as:

$$D_r = \frac{TRSB_{dec}}{TRSB_{dec} + SBD_{dec}} \quad (3-1)$$

$$D_w = \frac{TRMM_{dec}}{TRMM_{dec} + TRSB_{dec}} \quad (3-2)$$

The evaluation results are listed in Table 3-1; for the three stations, the  $D_w$  values are much larger than  $D_r$ , this indicated many precipitation events detected by TRMM were redundant. In the deep analysis, the different intensity classes of precipitation were estimated by the same approach, the results suggested that the high values of  $D_w$  mainly correspond with the low-intensity precipitation events (<0.3 mm) with a high probability for incorrect precipitation events ( $D_{w\_0.3}$ ) (Table 3-1).

**Table 3-1. Comparison between the raw and corrected TRMM precipitation**

Station	$D_r$	$D_w$	$D_{w\_0.3}$	$R_{raw}$	$R_{cor}$
Tashkurgan	0.54	0.75	0.95	0.11	0.45
Shache	0.21	0.87	0.96	0.67	0.77
Pishan	0.15	0.88	0.99	0.36	0.67

As concluded from Table 3-1, the direct application of the raw TRMM data in the Yarkant River basin for model simulation is inappropriate. Therefore, a correction is executed based on the local intensity scaling (LOCI) approach (Schmidli et al., 2006), which can correct the wet-day frequencies and intensities and effectively improve the raw data with too many drizzle days. First, a wet-day threshold  $P_{thres}$  was determined from the raw TRMM data to ensure that the threshold exceedance matched the SBD, this value was set as 0.3 because the TRMM detected too many redundant rainy days with amount of precipitation less than 0.3 mm (Table 3-1), and then a scaling factor  $s_m$  was calculated and used to ascertain that the mean of the corrected precipitation was equal to the observed precipitation, the equations are written as:

$$s_m = \frac{\mu(P_{SBD,m} | P_{SBD,m} > 0)}{\mu(P_{TRMM.raw,m} | P_{TRMM.raw,m} > P_{thres})} \quad (3-3)$$

$$P_{TRMM.cor,m} = \begin{cases} 0, & \text{if } P_{TRMM.raw,m} < P_{thres} \\ P_{TRMM.raw,m} \times s_m, & \text{otherwise} \end{cases} \quad (3-4)$$

Where  $P_{SBD,m}$  and  $P_{TRMM.raw,m}$  are the SBD and raw TRMM precipitation in the  $m^{th}$  month, and  $P_{TRMM.cor,m}$  is the corrected TRMM precipitation in the  $m^{th}$  month.  $\mu(\cdot)$  represents the expectation operator (e.g.,  $\mu(P_{TRMM.raw,m})$  is the mean value of the raw TRMM precipitation at a given month  $m$ ).

After correction, the quality of the raw TRMM data improved largely; comparing with the raw TRMM, the corrected TRMM was much closer to the SBD in the aspect of the mean annual precipitation. In addition, the monthly correlation coefficient (SBD and raw TRMM  $R_{raw}$ , SBD and corrected TRMM  $R_{cor}$ ) also got a remarkable improvement (Table 3-1). Eventually, this correction approach can be spread to the whole basin based on the ordinary Kriging method with a circular model interpolated  $s_m$  using ArcGIS and providing the revised TRMM data.

### 3.3.4 LST

Regarding the MOD11C1, daily LST data with a spatial resolution of  $0.05^\circ$  was used. The Version 4.1 was chosen because of its better presentation in semi-arid and arid regions (Hulley et al., 2009). The daily air mean temperature data are needed as an input by MIKE SHE; previous research affirmed that there is a good linear regression relation between LST and air temperature (Vogt et al., 1997; Cristóbal et al., 2008). Because of the missing LST data in the the Shache station, the data at the Tashkurgan and Pishan stations were diagrammatized to verify this relation (Figure 3.1).

The mean values of the regression coefficients at the Tashkurgan and Pishan stations were utilized in a simple transform equation in the Yarkant River basin, based on the Equation 3-5, the daily mean air temperature for the MIKE SHE model was acquired.

$$T_{air} = 0.7592 * LST - 5.565 \quad (3-5)$$

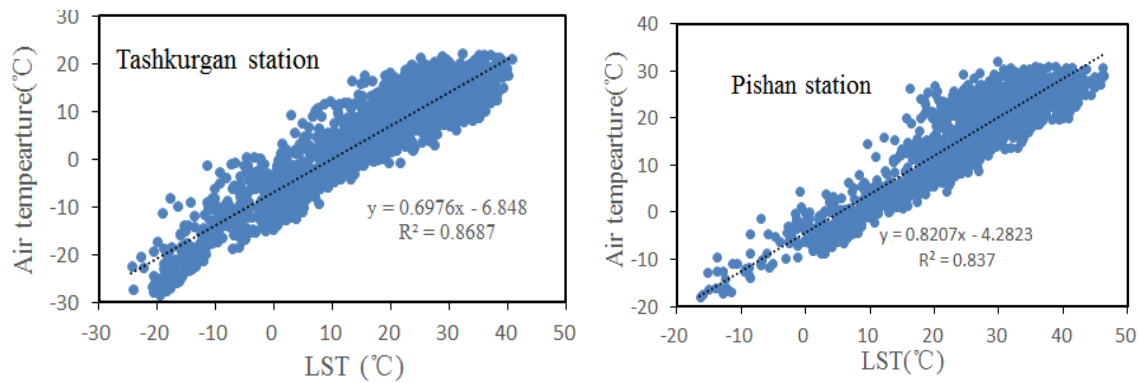


**Figure 3.1 Regression relation between the daily air temperature and LST at the Tashkurgan and Pishan station in 2000~2009**

### 3.3.4. PET

The remotely sensed PET were introduced in section 1.3.2 and directly used in the MIKE SHE model as the input reference evapotranspiration data.

## 3.4. Methodology

### 3.4.1 Model programmes

Because of the strong spatial heterogeneity with the extreme topographical conditions and well coupling with the RSD, the fully distributed hydrological model MIKE SHE was employed in this study to catch the detailed spatial variation. The detailed introductions about MIKE SHE can be found in section 2.3.2. In MIKE SHE, all input and output data can achieve the same spatial resolution as set in the model, in this way, the spatial features and distinctions of the inputs and outputs can be well embodied.

**Table 3-2 Eight models in this research based on the different input data**

Data source			Model
Rainfall	Temperature	Evapotranspiration	Abbreviation
station	station	station	STA
TRMM	station	station	TRMM
station	LST	station	LST
station	station	GPET	GPET
TRMM	LST	station	TRLS
TRMM	station	GPET	TRGP
station	LST	GPET	LSGP
TRMM	LST	GPET	RSD

In this study, the MIKE SHE model set up in Chapter 2 was taken as a benchmark and

three types of RSD (precipitation, temperature and PET) and their combinations were applied individually to replace the SBD. Finally, eight models were utilized based on the different input data (Table 3-2). The entire simulated period is uniform from 2000 to 2009, including the warm-up period of 2000-2002, calibration period of 2003-2007 and verification period of 2008-2009.

### 3.4.2 Calibration

In order to obtain an optimal performance for each model, the same calibration procedures have been executed separately. The Auto Calibration Tool based on the global optimization algorithm Shuffled Complex Evolution (SCE), which is a part of the MIKE SHE package was chosen for calibration. The main significant parameters of snowmelt, including the degree-day factor (DDF) and threshold melting temperature (TMT), land surface flow including Manning values (MAN), interflow including horizontal (HHC) and vertical hydraulic conductivity (VHC), evapotranspiration including LAI and root depth (RD), were chosen for calibration. In the calibration, the standard deviation (STD) was chosen as a statistic type of output measure and the weighted sum of STD was taken as an objective function. Additionally, the same three statistical coefficients given in section 2.4.1 were used as the judged criteria of the performances.

### 3.4.3 Hypothesis test

The natural processes of hydrologic cycles constitute a complex system with highly nonlinear relations between the “affected” and the “caused”. To evaluate the effect of the input data uncertainty on the hydrological process, it is necessary to define the sensitivity of the water components to the different input data. In this study, a statistical hypothesis test based on the ANOVA model, which is useful in comparing three or more groups for statistical significance, has been chosen to test the significant effect of the input data on water components.

Three types of input data (precipitation, temperature and PET) were taken as effect factors  $A$ ,  $B$  and  $C$ , they were investigated at  $a$ ,  $b$  and  $c$  levels, respectively and  $a=b=c=2$  (SBD and RSD two levels); when  $A$  is at  $i$  level ( $i=1,2$ ),  $B$  is at  $j$  level ( $j=1,2$ ),  $C$  is at  $k$  level ( $k=1,2$ ), the resulting water component can be denoted by  $u_{i,j,k}$ . The ANOVA model (Michael et al., 2005) for three factors with fixed effects can be identified as:

$$y_{ijkm} = u \dots + \alpha_i + \beta_j + \gamma_k + (\alpha\beta)_{ij} + (\alpha\gamma)_{ik} + (\beta\gamma)_{jk} + (\alpha\beta\gamma)_{ijk} + \varepsilon_{ijkm} \quad (3-6)$$



Where  $y_{ijkm}$  is the observation for the  $m^{\text{th}}$  case or trial for the treatment consisting of  $i^{\text{th}}$  level of  $A$ , the  $j^{\text{th}}$  level of  $B$ , and the  $k^{\text{th}}$  level of  $C$ ;  $u \dots$  is the grand mean of all dependent variables;  $\alpha_i$ ,  $\beta_j$  and  $\gamma_k$  are the main effects of factors  $A$ ,  $B$  and  $C$ ;  $(\alpha\beta)_{ij}$ ,  $(\alpha\gamma)_{ik}$  and  $(\beta\gamma)_{jk}$  are the main effects of the two-factor interaction;  $(\alpha\beta\gamma)_{ijk}$  is the main effect of the three-factor interaction;  $\varepsilon_{ijkm}$  is the independent random error that follows a normally distributed  $N(0, \delta^2)$ .

Based on the equation 3-6, the  $y_{ijkm}$  in different levels of each factor and their sum of squares can be written as equation 3-7.

$$SSTO = SSA + SSB + SSC + SSAB + SSAC + SSBC + SSABC + SSE \quad (3-7)$$

The mean square is equal to the sum of squares divided by the corresponding degree of freedom, and it can be given as follows:

$$\begin{aligned} MSSA &= \frac{SSA}{a-1}, & MSSB &= \frac{SSB}{b-1}, & MSSC &= \frac{SSC}{c-1} \\ MSSAB &= \frac{SSAB}{(a-1)(b-1)}, & MSSAC &= \frac{SSAC}{(a-1)(c-1)}, & MSSBC &= \frac{SSBC}{(b-1)(c-1)} \\ MSSABC &= \frac{SSABC}{(a-1)(b-1)(c-1)}, & MSSE &= \frac{SSE}{abc(n-1)} \end{aligned}$$

Finally, when factor  $A$  is tested, we assume that the null hypothesis  $H_0$ , which means that the influence of the factor on the result is not significant, could be acceptable. Thus,  $\alpha_1 = \alpha_2 = 0$ ; in this case,  $F_A = MSSA/MSSE$  is  $F_{[a-1, (n-1)abc]}$  distributed, and the probability  $p = P(F_{[a-1, (n-1)abc]} > F_A)$  can be calculated. When the calculated p-value is larger than the significance level ( $\alpha$ ), set as 0.05 in this study, suggesting that the assumption is correct, the null hypothesis  $H_0$  will be accepted; otherwise, the alternative hypothesis  $H_a$  should be accepted. Other hypotheses could be tested in the same way. The prerequisite for the hypothesis, the calculation of the appropriate test statistic's F-value and the percentile of the F distribution, are charted in Table 3-3.

**Table 3-3 The formulation of the test's statistics and percentile of the F distribution of the main effects of three factors and their interaction**

Test statistics	Percentile of F distribution
$F_A = MSA/MSSE$	$F[a-1, (n-1)abc]$
$F_B = MSB/MSSE$	$F[b-1, (n-1)abc]$
$F_C = MSC/MSSE$	$F[c-1, (n-1)abc]$
$F_{A*B} = MSAB/MSSE$	$F[(a-1)(b-1), (n-1)abc]$
$F_{A*C} = MSAC/MSSE$	$F[(a-1)(c-1), (n-1)abc]$
$F_{B*C} = MSBC/MSSE$	$F[(b-1)(c-1), (n-1)abc]$
$F_{A*B*C} = MSABC/MSSE$	$F[(a-1)(b-1)(c-1), (n-1)abc]$

### 3.5 Results and discussion

#### 3.5.1. Simulated discharges

After separate calibration, the final values of the chosen parameters were obtained. Among the eight models, MAN ranged from 25 to 60 regarding different land use, while, for the different soil types, HHC and VHC represented a scope of 0.0003 to 0.001 and 0.0035 to 0.01. MAN, HHC and VHC showed insignificant changes between the different models for the same land use or soil type. The calibrated values of other parameters are listed in Table 3-4. When the temperature was replaced, the parameters of snow (DDF and TMT) were adjusted drastically; when PET was replaced, remarkable changes of parameters occurred in evapotranspiration (LAI and RD). In the other causes, the variations were insignificant. Because of the periodic growth, LAI and RD of herbs are distinct in aspect of temporal variations (Fabio et al., 2008).

**Table 3-4 The final values of the calibration parameters in different models**

Models	STA	TRMM	LST	GPET	TRLS	TRGP	LSGP	RSD
F(mm/day/°C)	2.01	2.03	1.25	1.98	1.25	2.00	1.23	1.25
TMT(°C)	-0.98	-1.00	-0.56	-1.01	-0.57	-1.02	-0.56	-0.55
LAI_NLT*	3.81	3.82	3.78	2.65	3.82	2.64	2.63	2.66
RD_NLT(mm)*	4500	4500	4500	4000	4500	4000	4000	4000

\*LAI\_NLT and RD\_NLT are the LAI and RD of the evergreen needle-leaved tree

The TRMM, LST and GPET models were chosen to compare with the STA illustrated in Figure 3.2. In the TRMM model, the discharges in the early flood season from April to May were overestimated, more fictional fluctuations were simulated. Because the LOCI approach only corrects the magnitude and probability of the TRMM but not the frequency distribution, this might be a potential reason for the less desirable performances in the TRMM application. Additionally, similar but more moderate phenomena were found in the LST model but few differences were determined between the GPET and STA model.

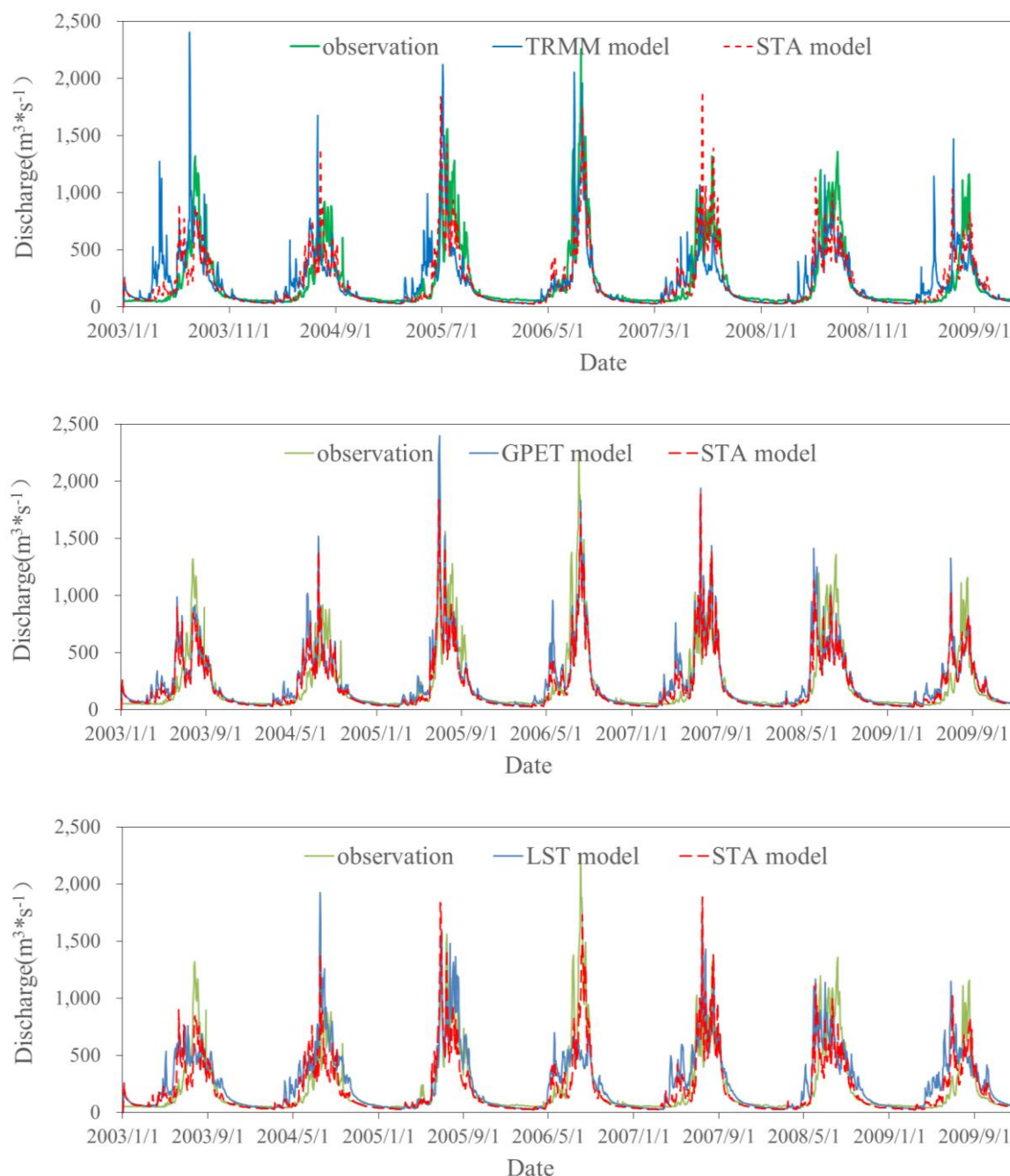


**Figure 3.2** The comparisons of daily discharge at Kaqun station between the TRMM (upper one), LST (middle one), GPET (under one) simulations and the STA simulation, observation

Based on the multiple evaluation coefficients (Table 3-5) in the verification period, the performances of most model programmes were acceptable; the NSC of the models was higher than 0.5 and all  $R^2$  values exceeded 0.6. The STA model expressed the best result with the highest NSC and  $R^2$  values and the smallest RMSE, which suggested that the interpolation of the meteorological data based on the lapse with the elevation was feasible. In general, the application of the corrected RSD in the Yarkant River basin was acceptable, though without improvement.

**Table 3-5 Statistical coefficients of the performance of different models**

Model	STA	TRMM	LST	GPET	TRLS	TRGP	LSGP	RSD
NSC	0.70	0.52	0.53	0.64	0.55	0.51	0.56	0.50
R <sup>2</sup>	0.80	0.62	0.67	0.73	0.71	0.63	0.70	0.60
RMSE	172.10	207.15	204.49	183.52	197.35	222.81	204.11	214.66

The boxplot of the mean monthly simulated discharge (Figure 3.3) at the outlet station derived from the eight models indicates significant differences from April to September. The large differences suggested that: even for the simulated discharge at the outlet station, which are aimed by the auto-calibration scheme, the deviations of eight programmes surely exist and are dominantly illustrated on the peak flow, which was recharged by mixed precipitation and snow melting water. However, the station discharges hardly explain the hydrological processes in a catchment scale. If the input data are only evaluated based on the simulated runoff, this evaluation will affect the other water balance components negatively. Alternatively, the variability of the distributed output is more valuable. Accordingly, the distributed water components would support a superior way to comprehend the effect of the input data uncertainty on the simulation of hydrological processes.

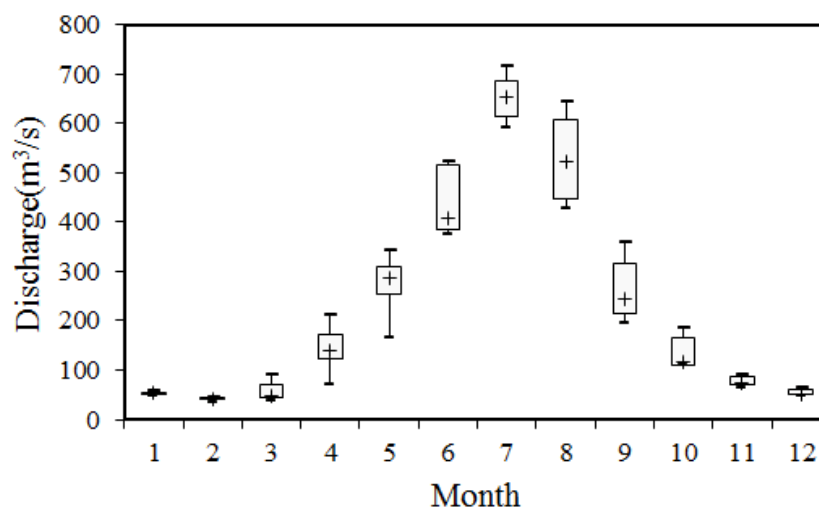


**Figure 3.3** Boxplot of the mean monthly discharges at the outlet station derived from eight model programmes in 2003–2009

### 3.5.2 Sensitivities of water components

In this study, the hypothesis tests aimed at differentiating the water components based on their mean annual values and each group test dataset was first adopted by the normal distribution and variance homogeneity test. In view of the different actual evapotranspiration ( $ET_a$ ) sources in the MIKE SHE model,  $ET_a$  were divided into: snow

sublimation (SNOWS), canopy interception (CI), river and pond water evaporation (WE), soil evaporation (SOILE) and plant transpiration (PT). These five  $ET_a$  sources together with the overland flow (OLF), base flow (BF) and snow storage (SS) were employed for the hypothesis test; the results of probability  $p$  values are provided in Table 3-6.

**Table 3-6 The probability  $p$  values of the hypothesis  $H_0$  test**

Groups	A	B	C	A*B	A*C	B*C	A*B*C
OLF	0.000	0.221	0.691	0.040	0.714	0.399	0.336
BF	0.003	0.436	0.008	0.087	0.619	0.450	0.553
SS	0.003	0.000	0.945	0.001	0.828	0.415	0.430
SNOWS	0.271	0.000	0.224	0.789	0.546	0.120	0.282
CI	0.000	0.000	0.000	0.007	0.089	0.028	0.431
WE	0.000	0.000	0.000	0.937	0.085	0.072	0.573
SOILE	0.138	0.238	0.000	0.747	0.241	0.739	0.932
PT	0.541	0.535	0.000	0.751	0.637	0.809	0.905

Table 3-6 indicates that the factor  $A$  precipitation had a very significant influence on most of the hydrologic components, except SNOWS, SOILE and PT; the factor  $B$  temperature takes/has a crucial role in the snow, PI and WE process and all evapotranspiration sources - except SNOWS - were strongly sensitive to the factor  $C$  PET. Through the statistical hypothesis test, the sensitivities of the water components to the different data types have been illustrated intuitively and the distributed output SS can be specified to analyze the deviations of precipitation and temperature from RSD and SBD. PT was employed in the PET deviation analysis.

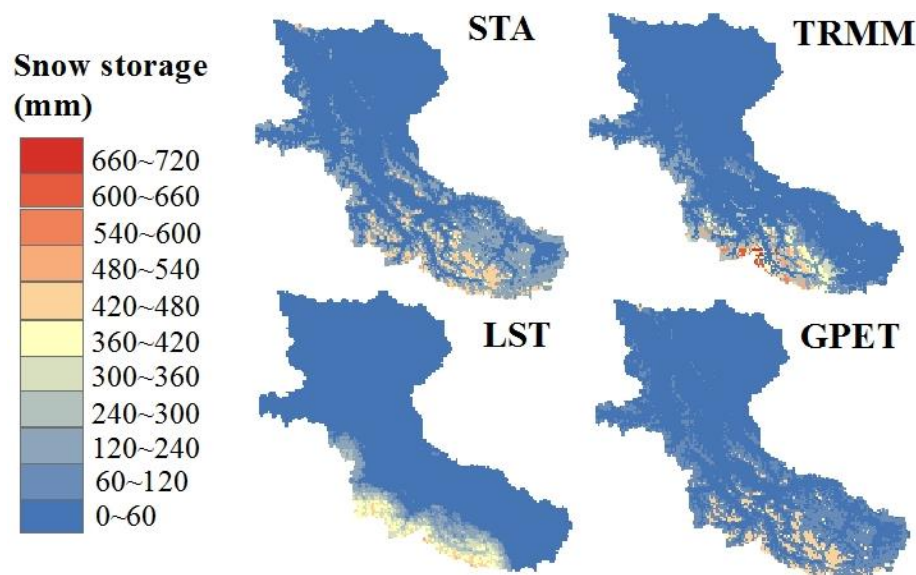
### 3.5.3 Response of the hydrological processes

#### Snow storage

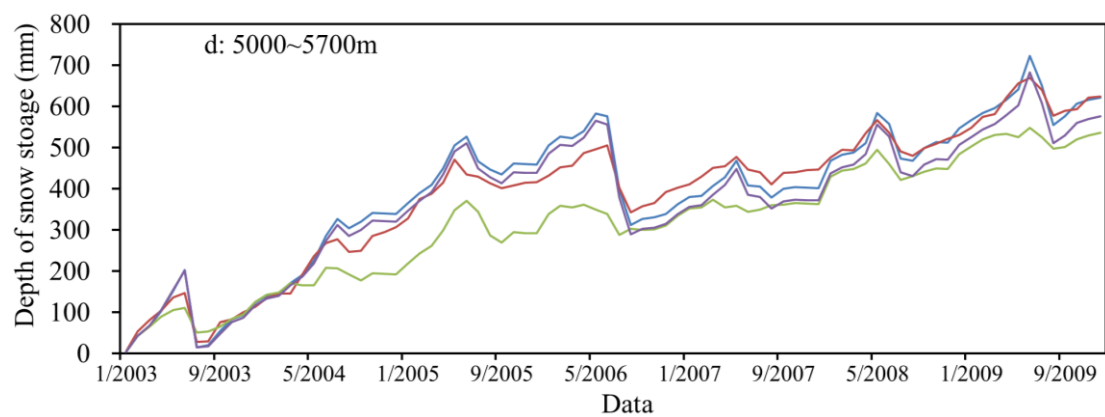
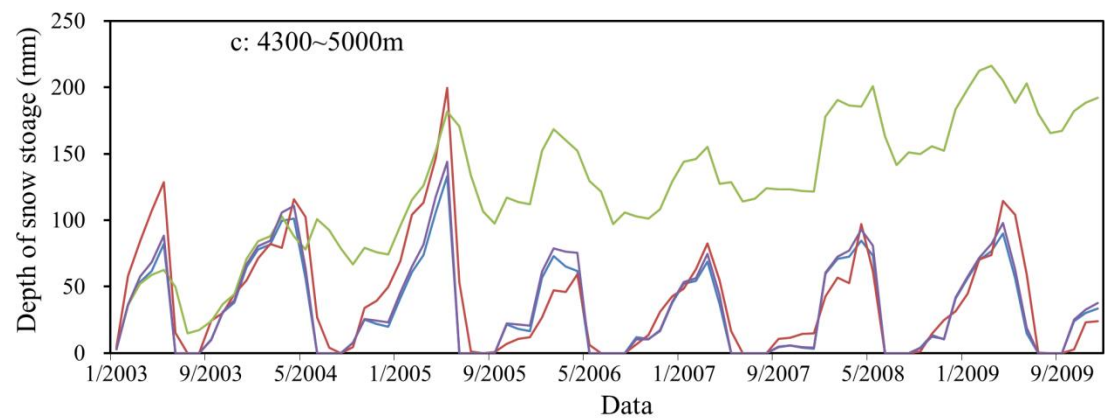
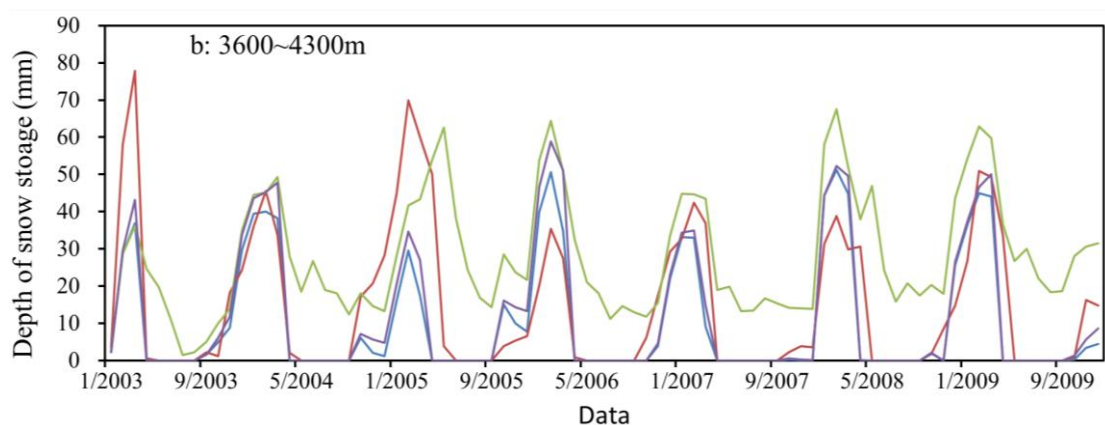
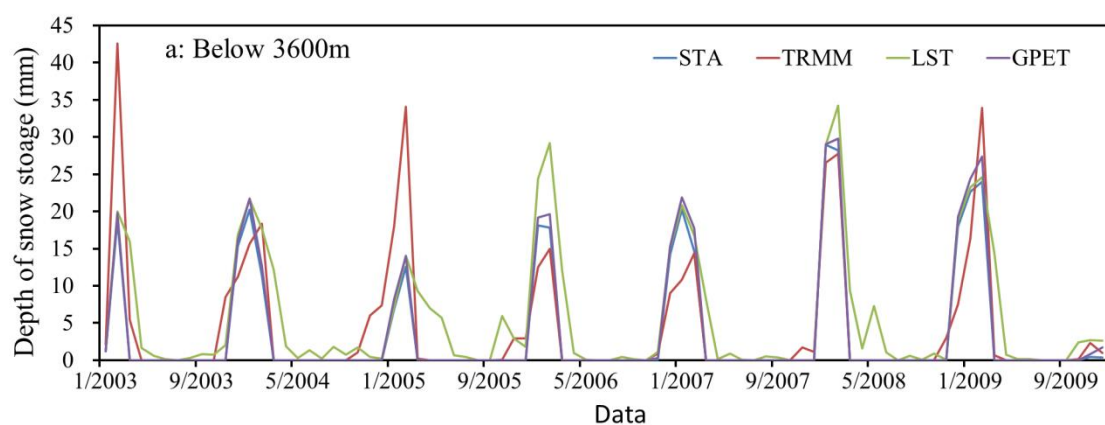
Figure 3.4 illustrates the spatial distribution of the simulated mean annual snow storage depth from the STA, TRMM, LST and GPET models. When the significant impact factors, precipitation and temperature of snow storage (Table 3-6) were replaced by RSD in the TRMM and LST models, the spatial distribution of the snowpack underwent a huge change. In addition, the temporal distribution in the different elevation bands (Figure 3.5) also represented the significant variation among STA, TRMM and LST.

Firstly, compared with the STA model, the TRMM model resulted in significant variations of mean annual snow storage depth with change proportions of -9.4% and

12.3% in the 5000–5700 m and the higher 6400 m zones, respectively. These differences may be interpreted by the distribution of SBD and TRMM precipitation (Figure 3.6). Despite, two dataset calculated similar average annual precipitation values with 309.86 mm and 323.14 mm, the TRMM data resulted in a more reasonable spatial distributed characteristic by a more reasonable isopluvial zone, which reflects the influencing factors distance and elevation. For the interpolated station data, the spatial distribution was relatively piecemeal. Compared with the average annual values of interpolated station data in the different elevation bands, the TRMM precipitation was 12% larger in the higher 6400 m zone. While in the 5000–5700 m district, the underestimation of the TRMM precipitation was remarkable with the percentage of 18%. These deviations matched well the changes in snow storage. In the region with an elevation lower than 5000 m, since there is no permanent snowpack, the differences between the SBD and TRMM precipitation are not reflected in snow storage.



**Figure 3.4** Spatial distribution of the simulated mean annual snow storage by the STA, TRMM, LST and GPET model in the Yarkant River basin during 2003–2009.





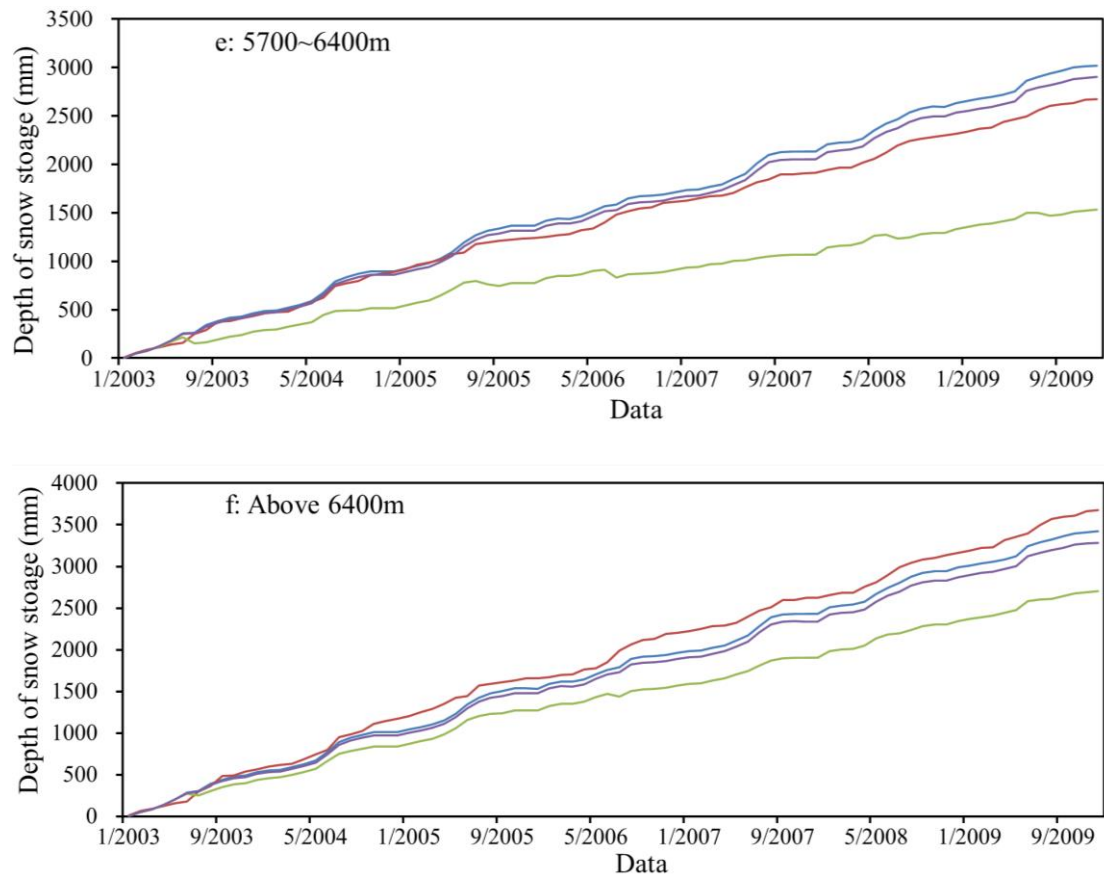


**Figure 3.5** The temporal distribution of snow storage in the different elevation bands.

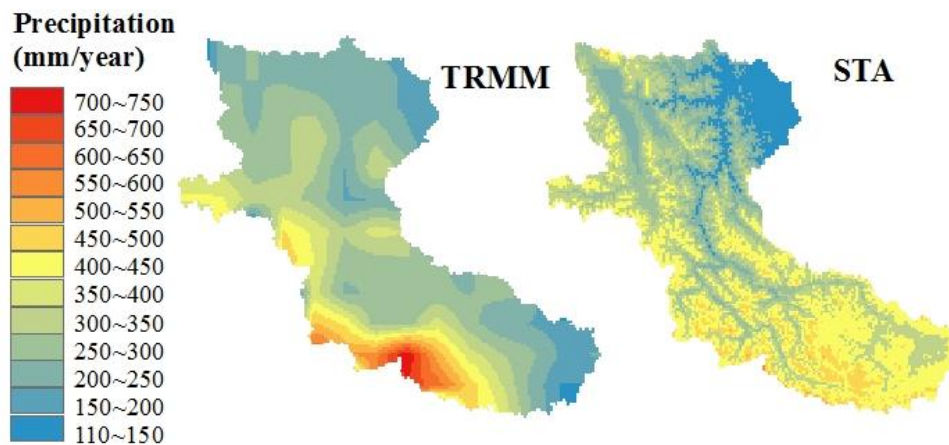


**Figure 3.6** Spatial distribution of the mean annual precipitation for TRMM and SBD in the Yarkant River basin during 2003~2009

Another noteworthy change in Figure 3.4 was the snow coverage area in the STA and LST model. The annual snow covered area with different depth bigger than 0 mm, 5 mm, 10 mm, 15 mm in the STA and LST model was listed in Table 3-7. Compared to the STA model, LST obtained the total covered area increased by 17.1%, however, the snow



covered area with a depth exceeding 5 mm greatly decreased. These values suggest that there are more snow covered areas with a very thin depth (smaller than 5 mm in the LST model). These changes could be caused by the distinctive distribution of temperature datasets between SBD and LST (Figure 3.7). For SBD, a piecemeal spatial distribution similar to the precipitation was observed. The variation tendency in the spatial distribution did not show remarkable differences. Compared to SBD in the district with an elevation lower than 3600 m, the LST data were lower by 3.2°C. While in the 5000–5700 m elevation band, the LST data were higher by 1.1°C than SBD. In the 3600–5000 m region, there was little distinction between the datasets.

**Table 3-7 The snow covered area with a bigger depth than in STA and LST**

Model	0 mm (km <sup>2</sup> )	5 mm (km <sup>2</sup> )	10 mm (km <sup>2</sup> )	15 mm (km <sup>2</sup> )
STA	30856	16228	15956	15936
LST	36136	10204	8620	8448
Errors	17.1%	-37.1%	-46.0%	-47.0%

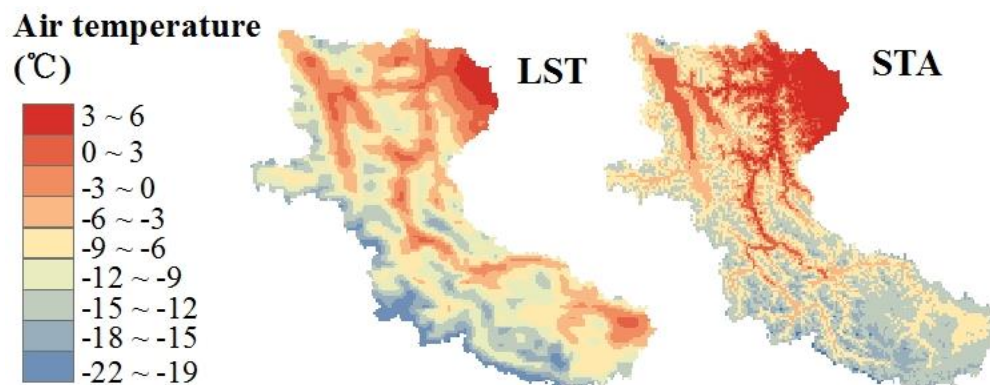


**Figure 3.7 Spatial distribution of the mean annual temperature between the station and TRMM data in the Yarkant River basin in 2003~2009.**

The detailed characteristics can be found based on Figure 3.5, in the 3600~5000 m region, the temperature from the two datasets were similar. Nevertheless, attributed to the smaller DDF and higher TMT in the LST model (Table 3-4), the snowmelt speed decreased and the permanent snowpack appeared; even in the 4300~5000 m region, the snow storage exhibited an uptrend. Finally, the LST model simulated a 52.2% increase in snow storage compared with the STA model in this region. However, the depth of the snowpack with an average of 4.2 mm at 3600~4300 m was very thin; this is why we detected the augmented  $SS_0$  in the LST model. In the higher 5000 m region where the dominant snowpack was located, the calculated higher air temperature in the LST model took a leading role and

caused a reduction of the annual snowpack by 41.2%. Another point of Figure 3.5 is the continuous increase of snow storage in the region with the elevation higher than 5700 m, a dominant reason is that: In this region there is hardly snowmelt because of the very low temperature; the snowdrift and snow slide become the primary movement methods. Unfortunately, these movements have not been included in MIKE SHE yet, so this snow storage generally increased as the accumulation of snowfall.

### Plant transpiration

No matter from Figure 3.4 and Figure 3.5, there is little or no variation between the STA and GPET since the PET cannot significantly influence the evapotranspiration (Table 3-6). The sensitive water component plant transpiration (Table 3-6) was taken as an example to analyse the effect of PET and the significant deviations between the STA and GPET model (Figure 3.8). Based on the Kristensen and Jensen's method, which integrated the evapotranspiration simulated by MIKE SHE, the transpiration was closely related to the parameters' density of the crop green material (such as LAI and RD), which was derived from the land use data. Thus, according to the different land use types, the average annual transpirations of the four models are listed in Table 3-8. Based on the results, two profound changes could be noted: in the evergreen needle-leaved trees and closed-open herbaceous regions, the plant transpiration from the GPET model was smaller, with rates of 33.4% and 35.6%, than those of the STA model. These results could be ascribed to the smaller LAI and RD (Table 3-4) values in the GPET model adjusted to satisfy the water balance.

**Table 3-8 The amount of the mean annual transpiration for different land use types from four models in 2003~2009a**

Land use type	STA(mm)	TRMM(mm)	LST(mm)	GPET(mm)
Evergreen Needle-leaved Tree	62.30	65.26	59.44	41.53
Closed-open Herbaceous	15.27	15.15	14.08	9.81
Sparse Herbaceous	4.09	3.94	3.98	2.50
Closed-open Shrub	8.16	13.07	7.62	6.79
Bare Areas	3.48	3.27	3.51	2.28
Water, Snow and Glacier	0.36	0.35	0.41	0.39

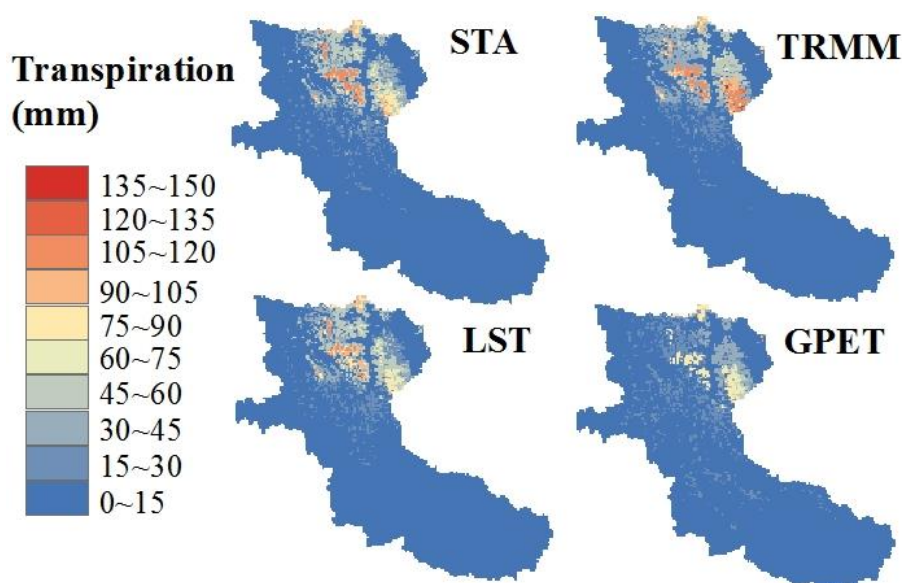


**Figure 3.8** The spatial distribution of the simulated mean annual transpiration of the STA, TRMM, LST and GPET model in the Yarkant River basin during 2003~2009.

Because of the low resolution of the GPET data ( $1^\circ$ ), the spatial distribution feature was not very evident; only the monthly temporal distribution of two datasets of PET are compared in Figure 3.9. The mean annual PET in the Yarkant River basin was 256.5 mm and 309.2 mm in two datasets, respectively. The higher PET in the GPET model was mostly detected from May to August with an increasing rate of 34.78%. Based on the calculation of MIKE SHE in the GPET model, the larger input PET values cause more evapotranspiration dissipation and a weaker simulated performance. In order to decrease the evapotranspiration, the transpiration was reduced through adjusting LAI and RD which were chosen as calibration parameters to a smaller value (Table 3-4).

In addition, compared with STA, the reduction percentage of transpiration from GPET in different seasons in evergreen needle-leaved trees zones was insignificant. Owing to the seasonal variation of LAI and RD of the closed–open herbaceous, peak values appear in summer, the change was also mainly represented from May to August with a reduced proportion of 54.3% compared with 23.1% during the other months. Although the different  $ET_a$  sources are calculated based on different parameters, all of these  $ET_a$  sources are sensitive to PET and can yield a clearer statement regarding the uncertainty of the input PET.

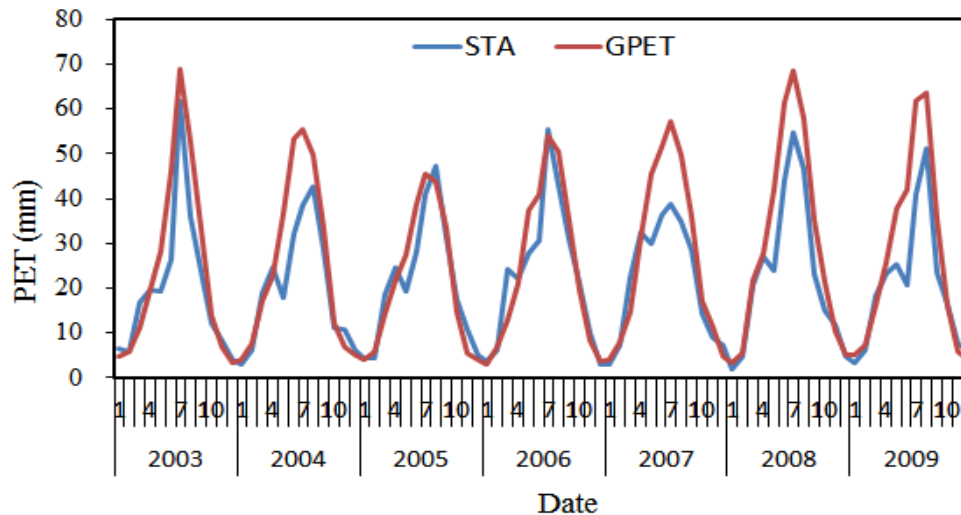


**Figure 3.9** The temporal distribution of the mean monthly PET from SBD and RSD in the whole Yarkant River basin during 2003~2009.

### 3.6 Conclusions

In the high and scarce gauges' alpine watershed of the Yarkant River basin, the application MIKE SHE model driven by dissimilar data sources demonstrated reasonable results and the simulated discharge barely explained the deviations of the input data reflecting on the peak of flow hydrography at the outlet station.

An ANOVA model indicated that precipitation, temperature and PET had a significant influence on different water components in hydrological processes on the basis of the ANOVA model, the sensitive component snow storage was chosen to analyse the effect of uncertainty in precipitation and temperature, including the plant transpiration for PET.

The application of TRMM made the differentiation of snow storage distribution more evident; it was stockpiled in the higher-altitude region. Corresponding to the overestimation of 12% in the higher 6400 m and underestimation of 18% at 5000~5700 m in the TRMM precipitation, the TRMM model resulted in a coherent change of 12.3% and -9.4% in snow storage compared with the STA model.

The application of LST caused a more extensive everlasting snow-covered area with a thinner depth. Because of the relatively smaller DDF and higher TMT, the LST model simulation obtained a larger snow storage area with a rate of 52.2% and a lower snow line in the 3600~5000 m region compared with STA. In the 5000~5700 m region, the overestimation of temperature intensified the snowmelt and caused a reduction of snow storage with a rate of 41.2%.

The GPET application resulted in less plant transpiration, especially in the area of high vegetation coverage. Compared with the STA model, owing to the larger GPET value, the GPET model had to reduce the plant transpiration by adjusting the calibrated parameters RD and LAI to satisfy the water balance. The reductions primarily occurred in the lush vegetation region of evergreen needle-leaved trees and closed–open herbaceous areas with proportions of 33.4% and 35.6%, respectively.

The different input data sources had a significant impact on the hydrological process; these are hardly explained by the discharge hydrography. By examining the significant impact factors of the water components, the uncertainties of one certain type of input data can be determined by the spatiotemporal distribution of the responding water components. Furthermore, the proposed method in this study can be used to analyze the changes in the hydrological processes and the distributed patterns of water components caused by the different input data. In the hydrologic cycle process, one type of input data would have a significant effect on several water components. In this study, each water component was analyzed based on certain input data. The hydrology characteristics are quite different in various watersheds; consequently, the more prominent components should be used for intercomparison to define the uncertainty of the input data in the whole process.

## References

- Abbaspour, K. C., M. Faramarzi, S. S. (2009). Ghasemi and H. Yang: Assessing the impact of climate change on water resources in Iran. *Water Resources Research*. DOI: 10.1029/2008wr007615.
- Ajami, N. K.; Duan, Q.; Gao, X.; Soroosh, S. (2006). Multimodel combination techniques for analysis of hydrologic simulations Application to distributed model intercomparison project results. *Journal of Hydrometeorology*. 4: 755-768.
- Ajami, N. K.; Duan Q.; Sorooshian S. (2007) An integrated hydrologic Bayesian multimodel combination framework: Confronting input, parameter, and model structural uncertainty in hydrologic prediction. *Water Resources Research*. 43: 1-10. DOI: 10.1029/2005wr004745
- Bastola, S., Murphy, C. and Sweeney, J. (2011). The role of hydrological modeling uncertainties in climate change impact assessments of Irish river catchments. *Advances in Water Resources*. 34, 562-576, DOI: 10.1016/j.advwatres.2011.01.008.
- Beven, K.; Binley, A. (1992). The future of distributed models: model calibration and uncertainty prediction. *Hydrological processes*. 6: 279-298.
- Blazkova, S.; Beven, K. (2002). Flood frequency estimation by continuous simulation for a catchment treated as ungauged (with uncertainty). *Water Resources Research*. 38: 1411-1414. DOI: 10.1029/2001wr000500

- Chen, R. S.; Kang, E. S.; Ding, Y. J. (2014). Some knowledge on the parameters of China's alpine hydrology. *Advances in Water Science*. 25(3): 307-317.
- Chien, H.; Yeh, P. J.; Knouft, J. H. (2013). Modeling the potential impacts of climate change on streamflow in agricultural watersheds of the Midwestern United States. *Journal of Hydrology*. 491: 73-88. DOI: 10.1016/j.jhydrol.2013.03.026
- Collischonn, B.; Collischonn, W.; Tucci, C. E. (2008). Daily hydrological modeling in the Amazon basin using TRMM rainfall estimates. *Journal of Hydrology*. 360: 207-216. DOI: 10.1016/j.jhydrol.2008.07.032
- Cristóbal, J.; Ninyerola M.; Pons, X. (2008). Modeling air temperature through a combination of remote sensing and GIS data. *Journal of Geophysical Research*. 113. DOI: 10.1029/2007jd009318
- Deus, D.; Gloaguen, R.; Krause, P. (2013). Water Balance Modeling in a Semi-Arid Environment with Limited in situ Data Using Remote Sensing in Lake Manyara, East African Rift, Tanzania. *Remote Sens-basel*. 5: 1651-1680. DOI: 10.3390/rs5041651
- Dobler, C.; Bürger, G.; Stötter, J. (2012) Assessment of climate change impacts on flood hazard potential in the Alpine Lech watershed. *Journal of Hydrology*. 460: 29-39. DOI: 10.1016/j.jhydrol.2012.06.02
- Fabio, F.; Christian, R.; Tobias, J.; Gabriel, A. and Stefan, W. (2008). Alpine Grassland Phenology as Seen in AVHRR, VEGETATION, and MODIS NDVI Time Series – a Comparison with in Situ Measurement. *Sensors*. 8: 2833-2853.
- Huffman, G. J.; Adler, R. F.; Bolvin, D. T.; Gu, G.; Nelkin, E. J.; Bowman, K. P.; Hong, Y.; Stocker, E. F.; Wolff, D. B. (2007). The TRMM multisatellite precipitation analysis (TMPA): Quasi-global, multiyear, combined-sensor precipitation estimates at fine scales. *Journal of Hydrometeorology*. 8: 38-55. DOI: 10.1175/jhm560.1
- Hulley, G. C.; Hook, S. J. (2009). Intercomparison of versions 4, 4.1 and 5 of the MODIS Land Surface Temperature and Emissivity products and validation with laboratory measurements of sand samples from the Namib desert, Namibia. *Remote Sensing Environment*. 113: 1313-1318. DOI: 10.1016/j.rse.2009.02.018
- Kavetski, D.; Kuczera, G.; Franks, S. W. (2006). Bayesian analysis of input uncertainty in hydrological modeling: 2. Application. *Water Resources Research*. 42. DOI: 10.1029/2005wr004376
- Knoche, M.; Fischer, C.; Pohl, E.; Krause, P.; Merz, R. (2014). Combined uncertainty of hydrological model complexity and satellite-based forcing data evaluated in two data-scarce semi-arid catchments in Ethiopia. *Journal of Hydrology*. 519: 2049-2066. DOI: 10.1016/j.jhydrol.2014.10.003
- Jasper, A. V.; Hoshin, V. G.; Willem, B. and Soroosh, S. (2003). A Shuffled Complex Evolution Metropolis algorithm for optimization and uncertainty assessment of hydrological model parameters. *Water Resources Research*. 39: 1-16. DOI: 10.1029/2002wr001642

- Ji, X.; Luo Y. (2013). Quality Assessment of the TRMM Precipitation Data in Mid Tianshan Mountains. *Arid Land Geography*. 36: 253-262.
- Jin, X. L.; Xu, C. Y.; Zhang, Q.; Singh, V. P. (2010). Parameter and modeling uncertainty simulated by GLUE and a formal Bayesian method for a conceptual hydrological model. *Journal of Hydrology*. 383: 147-155. DOI: 10.1016/j.jhydrol.2009.12.028
- Liu, T.; Willems, P.; Feng, X. W.; Li, Q.; Huang, Y.; Bao, A. M.; Chen, X.; Veroustraete, F.; Dong, Q. H. (2012). On the usefulness of remote sensing input data for spatially distributed hydrological modeling: case of the Tarim River basin in China. *Hydrological processes*. 26: 335-344. DOI: 10.1002/hyp.8129
- Li, X. H.; Zhang, Q.; Xu, C. Y. (2012). Suitability of the TRMM satellite rainfalls in driving a distributed hydrological model for water balance computations in Xinjiang catchment, Poyang lake basin. *Journal of Hydrology*. 426: 28-38. DOI: 10.1016/j.jhydrol.2012.01.013
- Michael, H. K.; Christopher, J. N.; John, N.; William, L. (2005). *Applied Linear Statistical Models*, in: McGraw-Hill Education, 2 Penn Plaza, New York, USA.
- McMichael, C. E.; Hope, A. S.; Loaiciga, H. A. Distributed hydrological modeling in California semi-arid shrublands: MIKE SHE model calibration and uncertainty estimation. *J. Hydro*. 2006, 317, 307-324. DOI: 10.1016/j.jhydrol.2005.05.023
- Misgana, K. M.; John, W. N. (2005). Sensitivity and uncertainty analysis coupled with automatic calibration for a distributed watershed model. *Journal of Hydrology*. 306: 127-145. DOI: 10.1016/j.jhydrol.2004.09.005
- Prigent, C. (2010). Precipitation retrieval from space: An overview. *Comptes Rendus Geoscience*. 342: 380-389. DOI: 10.1016/j.crte.2010.01.004
- Schmidli, J.; Frei, C.; Vidale, P. L. (2006). Downscaling from GCM precipitation: a benchmark for dynamical and statistical downscaling methods. *International Journal of Climatology*. 26: 679-689. DOI: 10.1002/joc.1287
- Stisen, S.; Jensen, K. H.; Sandholt, I.; Grimes, D. I. (2008). A remote sensing driven distributed hydrological model of the Senegal River basin. *Journal of Hydrology*. 354: 131-148. DOI: 10.1016/j.jhydrol.2008.03.006
- Sun, W.; Ishidaira, H.; Bastola, S. (2012). Calibration of hydrological models in ungauged basins based on satellite radar altimetry observations of river water level. *Hydrological processes*. 26: 3524-3537. DOI: 10.1002/hyp.8429
- Thompson, J. R.; Green, A. J.; Kingston, D. G. (2014) Potential evapotranspiration-related uncertainty in climate change impacts on river flow: An assessment for the Mekong River basin. *Journal of Hydrology*. 510: 259-279. DOI: 10.1016/j.jhydrol.2013.12.010
- Van, D. A. Model-data fusion: using observations to understand and reduce uncertainty in hydrological models. 19th International Congress on Modeling and Simulation (Modsim2011), Perth, Australia, 12 to 16 Dec. 2011, Chan, F.; Marinova, D. and Anderssen, R. S. Modeling and

Simulation Society of Australia and New Zealand.

- Vogt, J. V.; Viau, A. A.; Paquet, F. (1997). Mapping regional air temperature fields using satellite-derived surface skin temperatures. *International Journal of Climatology*. 17: 1559-1579. DOI: 10.1002/(sici)1097-0088(19971130)17:14<1559::aid-joc211>3.0.co;2-5
- Xu, C. Y.; Tunemar, L.; Chen, Y. D.; Singh, V. P. (2006). Evaluation of seasonal and spatial variations of lumped water balance model sensitivity to precipitation data errors. *Journal of Hydrology*. 324: 80-93. DOI: 10.1016/j.jhydrol.2005.09.019
- Xu, Y. P.; Zhang, X.; Ran, Q.; Tian, Y. (2013). Impact of climate change on hydrology of upper reaches of Qiantang River Basin, East China. *Journal of Hydrology*. 483: 51-60. DOI: 10.1016/j.jhydrol.2013.01.004
- Zhang, X. S.; Raghavan, S.; David, B. (2009). Calibration and uncertainty analysis of the SWAT model using Genetic Algorithm and Bayesian Model Averaging. *Journal of Hydrology*. 374: 307-317. DOI: 10.1016/j.jhydrol.2009.06.023
- Zhang, X.; Xu, Y. P.; Fu, G. (2014). Uncertainties in SWAT extreme flow simulation under climate change. *Journal of Hydrology*. 515: 205-222. DOI: 10.1016/j.jhydrol.2014.04.064



# CHAPTER 4

## **The effects of climate change on the hydrological processes**

---

*Modified from: Liu, J., Luo, M., Liu, T., Bao, A. M., De. Maeyer, P., Chen, X. (2016). Local climate change and responses of hydrological processes in an arid alpine catchment in Karakoram. Submitted paper.*

## ABSTRACT

Climate change and the impacts on hydrological processes in Karakoram region are highly important to the available water resources in downstream oases. In this study, a modified quantile perturbation method (QPM) which is improved by considering the frequency changes in different precipitation intensity ranges, and Delta method were used to extract signals of change in precipitation and temperature, respectively. Using a historical period (1986-2005) for reference, an average ensemble of 18 available Global Circulation Models (GCMs) indicated that the annual precipitation will increase by 2.9-4.4% in Representative Concentration Pathway 4.5 (RCP4.5) and by 2.8-7.9% in RCP8.5 in different future periods (2020-2039, 2040-2059, 2060-2079 and 2080-2099) due to an increased intensity of extreme precipitation events in - winter. Compared with historical period, the average ensemble also indicated that temperature in future periods will rises by 0.31-0.38 °C/10a in RCP4.5 and by 0.34-0.58 °C/10a in RCP8.5. Through coupling with a well-calibrated MIKE SHE model, the simulations suggested that, under the climate change scenarios, increasing evaporation dissipation would lead to decreasing snow storage in the higher altitude mountain region and likewise with regard to available water in the downstream region. The alterations of snow strong are quite different in elevation bands, the permanent snowpack area below 5600 m would completely vanished in 2060-2079, and the snow storage in 5600-6400 m would be reduced dramatically, however, there is little or no changes in the above 6400 m region. Warming could cause a stronger spring and early summer stream runoff and a reduced late summer flow due to the snowmelt change in temporal distribution. Furthermore, both the frequency and the intensity of the flood would be enhanced. All the changes of hydrological processes are stronger under RCP8.5 than those under RCP4.5. In Karakoram region, the transformations among different forms of water resources alter the distributions of hydrologic components under future climate scenarios, and more researches are needed about the transient water resources system and the worsening of flood threats in the study area.

**Keywords:** climate change; hydrological processes; snow; streamflow; MIKE SHE modelling; Karakoram

### 4.1 Introduction

Nearly all regions in the world have experienced the influences of climate change on

water resources (IPCC, 2013). Hydrologic systems in arid/semi-arid regions are particularly sensitive to climate changes (Chen et al., 2006; Guo et al., 2015), as are highly glaciated regions (Claudia et al., 2012; Huss et al., 2008). Regarding retreating glaciers caused by the warming temperature, a stronger spring and early summer river runoff and a reduced late summer flow have been observed in the most highly glaciated watersheds (Barontini et al., 2009; Bavay et al., 2013; Jeelani et al., 2012; Liu et al., 2009). However, the effects differ substantially from region to region, Su et al. (2016) indicated the earlier and stronger spring runoff may help the irrigation water of Indus Basin in the spring growing seasons. Immerzeel et al. (2010) suggested the effects in the Brahmaputra basins seem likely to face the severer water availability and flood security owing to the high dependence on the irrigated agriculture and the large population but the effect may be positive in Yellow River since the low dependence on melting water and increased upstream precipitation. In addition to stream runoff, evaporation has received some study, and significant increasing trends in response to climate change have been reported (Calanca et al., 2006; Thompson et al., 2014). Moreover, the strong influences on groundwater system in the large-scale agricultural catchment also have been ascertained (Roosmalen et al., 2009). These studies separately focused on one or more water components of hydrological processes under climate change but little attention was paid to the redistribution of water resources in hydrological processes from a water balance perspective.

The snowpack and glaciers in mountainous areas play the role of a “water tower” in Central Asia. Along the north slope of Karakoram, the Yarkant River basin is the dominant catchment. In this catchment, approximately 70% of the stream runoff is derived from meltwater (Chen et al., 2010). In the previous studies of the Yarkant River basin, most studies focused on the past climate change (Chen et al., 2010; Xu et al., 2011; Xu et al., 2013; Zhang et al., 2009) and observed the aggravating changes in snowpack melt and stream runoff. For the effect of future climate change, Zhang et al. (2012) employed a Delta method to extract the variable signals of precipitation and temperature, the responses of stream flow to different climate scenarios were studied, and found that there will be a small increase of stream flow both in May and October. However, the Delta method is not able to capture changes in precipitation extreme (Onyutha et al., 2016) and if the processing methods of GCMs include severe uncertainties or methodological errors, these processed data would cause further bias when used in hydrologic simulations.

Teng et al (2012) suggested that one certain GCM coupling 5 hydrological models, the

deviations of the simulated results were about 7%, however, one certain hydrological model coupling 15 different GCMs, the deviations increased to 28%-35%. Several downscaling methods were compared in Ghosh's (2012) study and the results indicated that most uncertainties were derived from GCMs and authors suggested that the average ensemble of GCMs could be a better choice. Quintana et al (2010) applied the dynamical downscaling, statistical downscaling and bias correction to deal with the GCM data and found that the uncertainties caused by the processing methods would be enlarged in the hydrology simulation. Thus, firstly, the local climate change in the Yarkant River basin must be clarified based on an appropriate method and then understand the response of hydrological processes.

Change in precipitation is surely complex and crucial among hydrometeorology factors. In the past several decades, a clear enhancement in heavy precipitation has been investigated in many regions (Min et al., 2011) and this meteorological process could change the frequency or intensity of extreme hydrologic events (Eric et al., 2014). Previously, some studies (Liu et al., 2011; Ntegeka et al., 2014; Taye et al., 2011; Willems and Vrac, 2011) extracted the change signals of precipitation frequency and intensity based on the quantile perturbation method (QPM) to obtain a reasonable temporal distribution of future precipitation. The perturbation approach is one of common methods to obtain the differences between current and future climate (Lettenmaier et al. 1999; Middelkoop et al., 2001), and the quantile-based perturbation approach that considers the intensity perturbation on the different quantiles is available for extreme precipitation events (Onyutha et al., 2016). Based on the perturbation approach, the QPM was developed by Ntegeka et al (2008), and both the changes in intensify and frequency of rainy days were taken into account separately. In these studies, according to the overall change in frequency, new random precipitation events were generated based on a historical observation sorting. Through comparing the new average value with the scenario data series, several times of random generation sets were reselected to ensure a total amount of change. Although random generation can accelerate the processing procedure, it may also add uncertainties to the newly generated data series because of the randomly added or subtracted precipitation events.

The objectives of this paper are investigating the local climate change and the effects on the hydrological processes in the Yarkant River basin of Karakoram region. In the scenarios of the Representative Concentration Pathways 4.5 and 8.5 (RCP4.5 and RCP8.5), 21-member GCM's average variable signals of precipitation and temperature were extracted in the meteorological station. Referring to the observed data, the future

meteorological data can be obtained and used to drive a well-calibrated MIKE SHE model. On the basis of simulated outputs, the changes of different water components in the hydrological processes are tested. In this process, two points are characterized, i) A modified QPM improved by considering the frequency changes in the different precipitation intensity ranges. Through this approach, the uncertainties caused by randomly adding or subtracting precipitation events can be decreased when new data series are generated. ii) Quantifying the response of hydrological processes from a water balance perspective in a catchment scale. In this way, not only the stream runoff but also the redistribution of water resources and change in different forms of water resources can be clarified.

## 4.2 Study area and data

The Yarkant River basin (shown as Figure 1.2) was chosen in this study. More detailed information can be found in Section 1.2.

And the climate change data including 21 GCM and their detailed information have been mentioned in 1.3.3.

## 4.3 Methodology

At present, there are two major approaches to using GCMs runs for assessment, which also represent two totally different logics: i) Dynamic downscaling by RCM model with one boundary forcing; and ii) statistic downscaling with idea of statistic accounting with large number of samples. Dynamic downscaling use one best GCM runs as boundary data to force the RCM model in order to get the detailed and spatial information all over study area. While, it means, the model setup, calibration and validation processes has massive work load (Solman and Nunez, 1999). Statistic downscaling has less work load and use the general trend of selected runs to represent the climate change trend. Moreover, the statistical method can be applied based the multiple GCMs, which is available to reduce the uncertainty of GCMs (Ghosh et al, 2010).

In this study, the statistical method is employed to extracted the change signals of the stationary data series in GCMs. Compared with HP, all change signals of precipitation and temperature in four FPs featured by each GCM were extracted statistically. Due to the uncertainty among GCMs, the average tendency of multiple GCMs was strongly suggested (Ghosh et al, 2012); therefore, the average ensemble of available GCMs was

employed. Based on the extracted change signals, the future precipitation and temperature in different periods were generated by a modified QPM and Delta method, and use to force a well-calibrated MIKE SHE model. Then the hydrological processes in future periods can be obtained through MIKE SHE's simulation. The modified QPM and the Delta method were used to analyse the data for each calendar month. The time series data of the GCMs' historical runs and scenario runs were extracted on the location of Tashkurgan station (Figure 1.2).

#### 4.3.1 Modified QPM for precipitation

For the precipitation time series, the frequency change and quantile perturbation should not be completely independent indexes; rather, their relationship should be determined. In the modified QPM, the specific locations of added or subtracted rainy events defined by frequency changes were determined in the rank time series of precipitation data. Eleven quantiles, with values of 0.01, 0.05, 0.1, 0.2, 0.3, 0.4, 0.5, 0.6, 0.7, 0.8 and 0.9, were selected to divide the rank time series into 12 segments in accordance with different grades of precipitation intensity. In each segment, the due number of rainy days can be calculated based on the quantile value and compared with the existing numbers of rainy days in this segment, and the added or subtracted numbers of rainy days can be decided.

A large deviation was noted among GCMs' precipitation (Baguis et al. 2010; Liu et al. 2011). Therefore, in order to obtain a more accurate average trend from the selected GCMs, based on the annual precipitation of 21 GCMs. The consistency check was implemented by Eq. (1), the outliers examined by Eq.(1) would be rejected by consistency check.

$$P \in \text{MEAN} \pm \text{STD} \quad (4 - 1)$$

Where  $P$  stands for the annual precipitation of each GCM and  $\text{MEAN}$  and  $\text{STD}$  are the average value and standard deviation of the 21 GCMs, respectively. According to the results of consistency examination, three GCMs (CanESM2, ACCESS1.3 and HadGEM2-ES) were deprecated. Based on the 18 remaining GCMs, the frequency change of rainy days when the daily precipitation exceeded 0.1 mm and the quantile perturbations at the quantiles  $i$  in each GCM were formulated as

$$f_{RD\_m} = \frac{FP\_RD_m}{HP\_RD_m} \quad (4 - 2)$$

$$f_{PI(i,m)} = \frac{FP\_PI_{(i,m)}}{HP\_PI_{(i,m)}} \quad (4-3)$$

where  $f_{RD,m}$  represents the monthly frequency change factor of rainy days in the  $m^{\text{th}}$  month;  $FP\_RD_m$  and  $HP\_RD_m$  are the number of rainy days in the  $m^{\text{th}}$  month of the FPs and HP, respectively;  $f_{PI(i,m)}$  is the precipitation intensity perturbation factor at the quantile  $i$  in the  $m^{\text{th}}$  month; and  $FP\_PI_{(i,m)}$  and  $HP\_PI_{(i,m)}$  are the precipitation intensities at the quantile  $i$  in the  $m^{\text{th}}$  month of the FPs and HP, respectively. The 18 GCMs' average ensemble is written as  $\overline{f_{RD,m}}$  and  $\overline{f_{PI(i,m)}}$

For each calendar month ( $m=1, 2, \dots, 11, 12$ ), the detailed steps are as follows:

1. Calculate the number of rainy days ( $OBS\_RD_m$ ) and quantiles of each precipitation event ( $OBS\_PI_{(i,m)}$ ) in the observed time series of HP;
2. Interpolate  $FP\_PI_{(i,m)}$  and  $HP\_PI_{(i,m)}$  in the GCMs, maintaining the same quantile  $i$  with  $OBS\_PI_{(i,m)}$  throughout the linear method, then calculate  $f_{PI(i,m)}$  based on Eq. (3) and  $\overline{f_{PI(i,m)}}$ ;
3. Obtain the future precipitation intensity at each quantile  $i$  ( $NOBS\_PI_{(i,m)}$ ), formulated as  $NOBS\_PI_{(i,m)} = OBS\_PI_{(i,m)} * \overline{f_{PI(i,m)}}$ ;
4. Obtain the number of future rainy days ( $NOBS\_RD_m$ ), formulated as  $NOBS\_RD_m = OBS\_RD_m * \overline{f_{RD,m}}$ ;
5. Count the existing number of rainy days ( $N_E$ ) for which quantile  $i$  is not more than 0.01 in step 3;
6. Calculate the due numbers of rainy days ( $N_D$ ) for which quantile  $i$  is not more than 0.01 based on the result in step 4, formulated as  $N_D = NOBS\_RD_m * 0.01$ . If  $N_D > N_E$ ,  $(N_D - N_E)$ , no rainy days should be replaced in step 3, and the precipitation of added rainy days is equal to average value of existing rainy days  $N_E$ . Perform the above subtraction and round the difference between  $N_D$  and  $N_E$  to the nearest integer;
7. Sequentially repeat steps 5 and 6 at the other quantiles (0.05, 0.1, 0.2, 0.3, 0.4, 0.5, 0.6, 0.7, 0.8 and 0.9) until the number of rainy days in step 3 is equal to  $NOBS\_RD_m$ .

In this modified QPM, the future precipitation time series only included the quantile perturbation signal initially obtained in step 3, then through the frequency change in each segment divided by quantiles, the lacking or redundant rainy days are defined (step 4 to step 6). Finally, adding or subtracting these rainy days with fixed values in accordance with the precipitation intensity in each segment, the rank time series of the future precipitation data are obtained.

### 4.3.2 Delta method for temperature

Regarding temperature, no frequency issue needs to be considered, so the Delta method (Gleick. 1986; Hay et al. 2000) was employed so as to extract the monthly change temperature signal. By calculating the mean monthly absolute difference between the HP and FPs in the GCMs, the change factor of temperature can be obtained. The future daily temperature is calculated as:

$$T_{NOBS(m,d)} = T_{OBS(m,d)} + (T_{FP(m)} - T_{HP(m)}) \quad (4 - 4)$$

where  $T_{NOBS(m,d)}$  is the future temperature of the FHs on the  $d^{\text{th}}$  day in the  $m^{\text{th}}$  month;  $T_{OBS(m,d)}$  is the observation temperature on the  $d^{\text{th}}$  day in the  $m^{\text{th}}$  month and  $T_{FP(m)}$  and  $T_{HP(m)}$  represent the average temperature of the GCMs in the  $m^{\text{th}}$  month of the FPs and HP, respectively.

### 4.3.3 Hydrological modeling

Due to the strong spatial heterogeneity in extreme topographical conditions and the good performances in hydrological processes, the fully distributed hydrological model MIKE SHE was employed in this study to catch the detailed spatial variation. The model's establishment and calibration can be found in chapter 2 and 3. Additionally, the performances of this well-calibrated model have been introduced. In this climate change study, the generated meteorological data in the future period were used to couple the MIKE SHE model.

## 4.4 Future climate change

### 4.4.1 Precipitation



### Changes in frequency

The mean monthly frequency changes of the different FPs with respect to HP determined by the GCMs are similar between RCP4.5 and RCP8.5 (Figure 3). In general, from September to the following March, the number of rainy days continuously declines in FPs; this declining trend is stronger in RCP8.5 than in RCP4.5. Nevertheless, the number of rainy days mostly increases in June and July and exhibits moderate change ratios. Regarding mean annual rainy days, 18 GCMs' average ensemble indicates little change, with factors of 1.00, 0.99, 0.98 and 0.97 in RCP4.5 and of 1.00, 0.99, 0.97 and 0.94 in RCP8.5. However, the uncertainties among the 18 GCMs present large ranges: 0.92-1.09, 0.88-1.11, 0.90-1.11 and 0.88-1.11 in RCP4.5 and 0.93-1.07, 0.89-1.15, 0.84-1.18 and 0.76-1.04 in RCP8.5, and the deviations among 18 GCMs in different periods mainly reflect on summer.

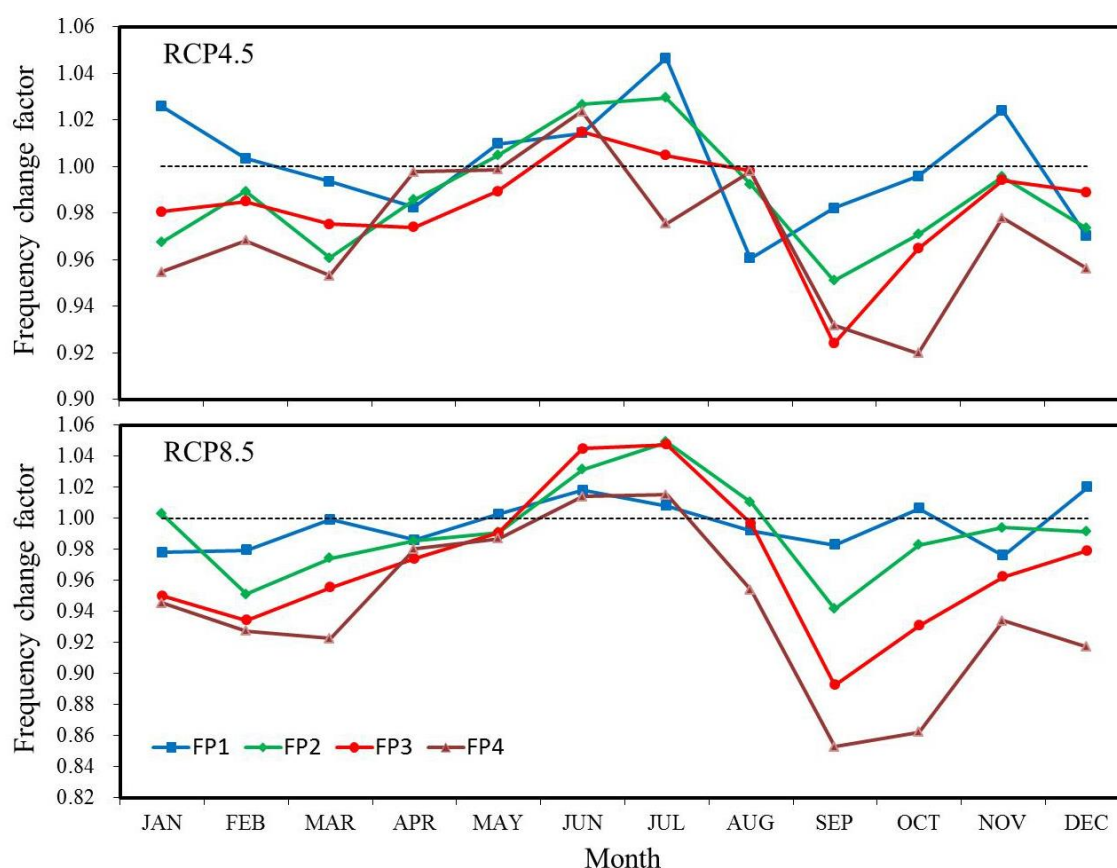


**Figure 4.1** The mean frequency changes of the rainy days in each month of future periods relative to those of the history period determined by the 18 GCMs

**Table 4-1 The average, maximum/minimum values of the annual rainy days change factors in future periods relative to those of the history period determined by the 18 GCMs**

		FP1	FP2	FP3	FP4
RCP4.5	Mean	1.00	0.99	0.98	0.97
	Maximum	1.09	1.11	1.11	1.11
	Minimum	0.92	0.88	0.90	0.88
RCP8.5	Mean	1.00	0.99	0.97	0.94
	Maximum	1.07	1.15	1.18	1.04
	Minimum	0.93	0.89	0.84	0.76

### Quantile perturbation

The precipitation data at the quantiles of 0.01, 0.05, 0.1, 0.2 and 0.5 were chosen to illustrate the mean monthly quantile perturbation of precipitation intensity in the different FPs relative to those in HP determined by the GCMs (Figure 4.2). Both in two scenarios, the rainfall intensity at the different quantiles will not drastically change in summer, however, significant variations occur in winter. The intensity of extreme precipitation (at the 0.01 quantile) in winter is the most significant and much stronger in RCP 8.5. Such as in January of PF4, the average increased proportion can be as high as 40% in RCP4.5 and 67% in RCP8.5 and the ranges represent -19%-221% in RCP4.5 and -15%-258% in RCP8.5. Compared to extreme precipitation, the other precipitation intensities show a slightly growing perturbation.

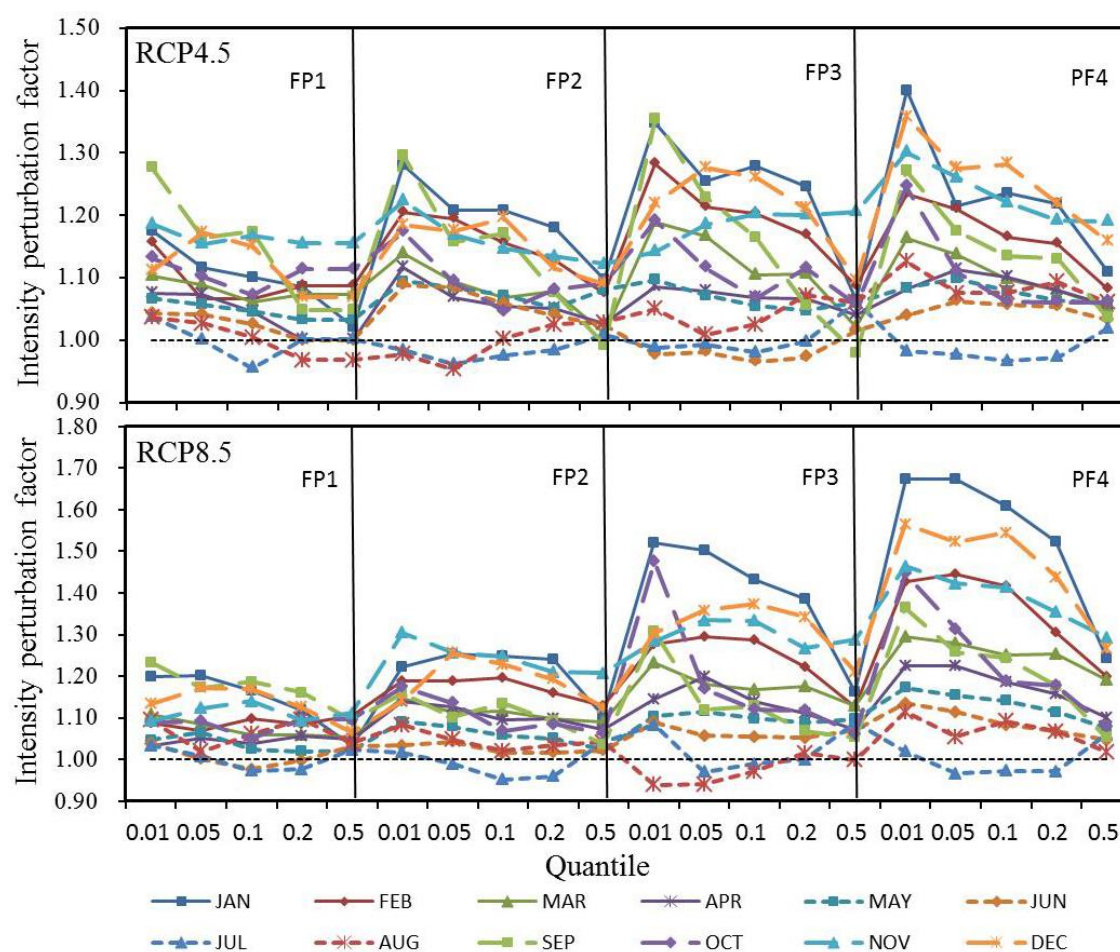


**Figure 4.2** The mean quantile perturbations of precipitation intensity in each month of future periods relative to those of the history period determined by the 18 GCMs

### Precipitation volume

After adding these average change signals to the observation using the modified QPM, new time series were obtained to describe the future situation. The monthly change rate of precipitation volume in FPs is provided in Figure 4.3. In two scenarios, owing to the trending-off effect of incremental rainy days and reduced precipitation intensity, the volumes of precipitation barely shift in summer. However, the stronger precipitation intensity is more than offset by declining rainy days; therefore, more abundant precipitation occurs in winter. Finally, compared with the HP, the annual precipitation in FPs demonstrates upward tendencies and is listed in Table 4-2. Based on the average ensemble of 18 GCMs, in the future, primarily because of heavier extreme precipitation in winter, the annual precipitation in the Yarkant River basin will exhibit a moderate increasing trend until 2100 in both scenarios but stronger in RCP8.5.

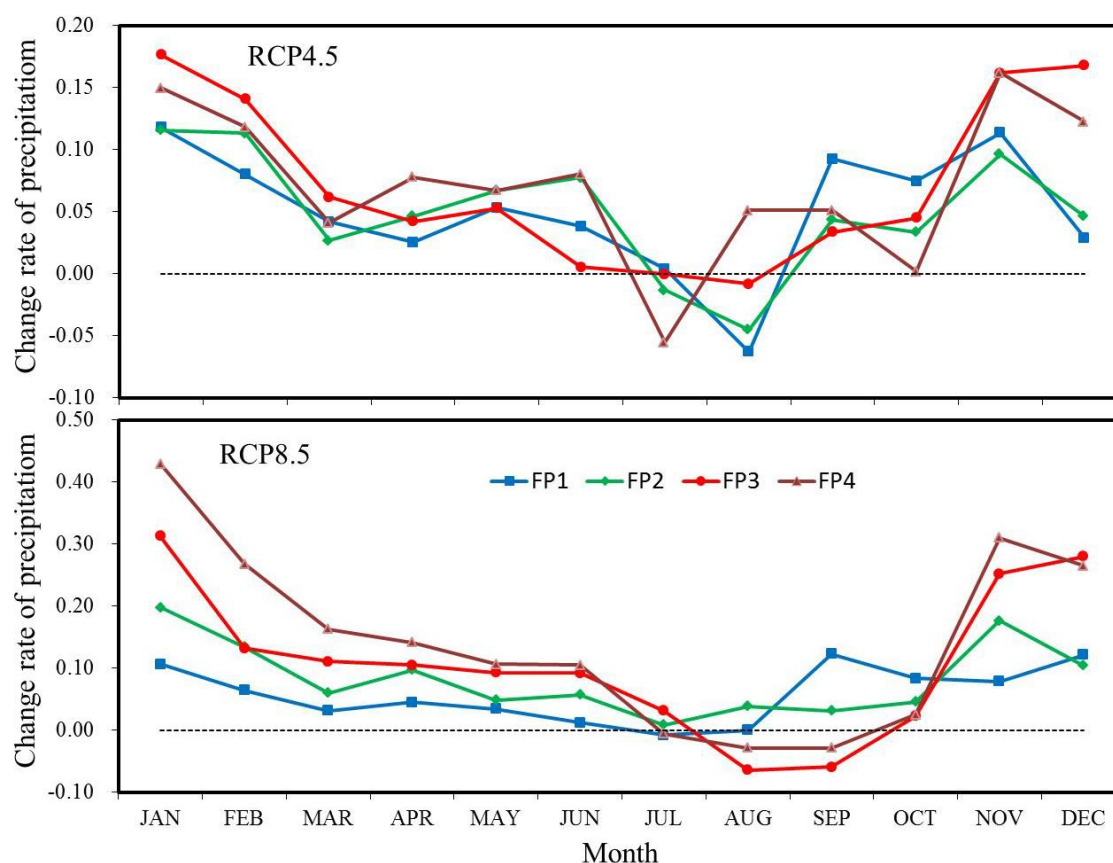


**Figure 4.3** The amount change rates of the generated future monthly precipitation with respect to those observed in the history period

**Table 4-2** The increased rates of annual precipitation in future periods relative to the history period

Scenario	FP1	FP2	FP3	FP4
RCP4.5	2.9%	3.6%	3.0%	4.4%
RCP8.5	2.8%	5.3%	6.3%	7.9%

#### 4.4.2 Temperature

The monthly absolute change in temperature in the FPs with respect to that of the HP is presented in Figure 4.4. Obviously, because of the different greenhouse gas emission scenarios, the warming will slow down at the end of this century in RCP4.5 but will keep a continuous rising tendency in RCP8.5. After 2060, the warming rate will moderately decrease and present the values from  $0.38^{\circ}\text{C}/10\text{a}$  at the beginning to  $0.31^{\circ}\text{C}/10\text{a}$  at the end of this century. The high emission of RCP8.5 causes an increase in warming rates from  $0.34^{\circ}\text{C}/10\text{a}$  at the beginning to  $0.59^{\circ}\text{C}/10\text{a}$  at the end of this century. The temperature changes are much larger than the precipitation in GCM.

Furthermore, in the FPs, the wide range of warming trends relative to HP among 18 GCMs (listed in Table 4-3) suggests that the large uncertainties among the different GCMs, it is really hard to choose one certain GCM in climate change, however, the average ensemble of most GCMs in CMIP 5 could be a better choice.

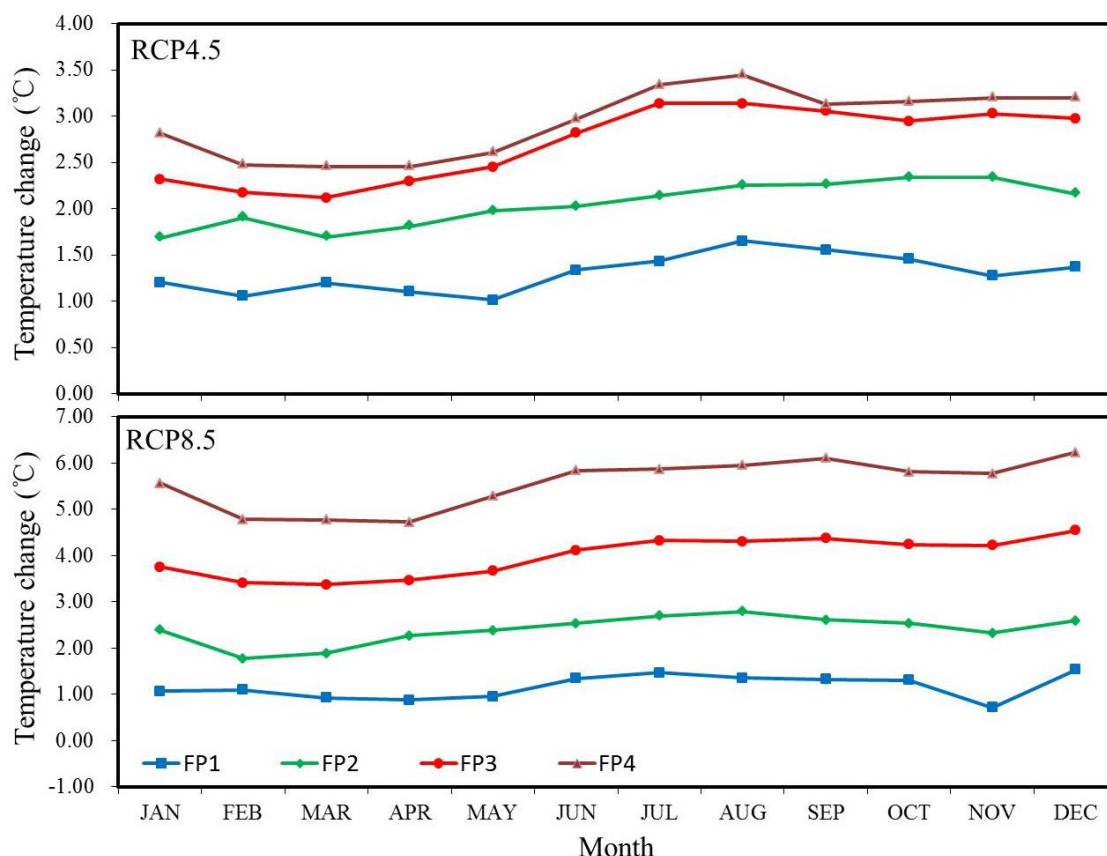


**Figure 4.4** The mean monthly changes in temperature of future periods compared to those of the history period determined by the 18 GCMs

**Table 4-3** The average, maximum/minimum values of the annual rainy days change factors in future periods relative to those of the history period determined by the 18 GCMs

Warming rate (°C/10a)		FP1	FP2	FP3	FP4
RCP4.5	Mean	0.38	0.38	0.36	0.31
	Maximum	0.20	0.18	0.13	0.17
	Minimum	0.61	0.71	0.82	0.75
RCP8.5	Mean	0.34	0.44	0.53	0.59
	Maximum	0.11	0.19	0.32	0.39
	Minimum	1.16	0.88	1.07	1.11

The Yarkant River basin is a high-altitude mountain catchment, and the cold air gathering effect of mountain in on popular topic in the physical geography study

(Michael et al. 2005; Baguis et al. 2010). Considering the elevation-dependent warming in the mountain region (Rangwala *et al.* 2012), one nearby meteorological station, Pishan station, which is located at 1 375 m, was used to investigate the elevation lapse rate (EPR) of the temperature in the GCMs. The average yearly temperature of the GCMs, both in RCP4.5 and RCP8.5- at Tashkurgan and Pishan station are listed in Table 4-4. Before 2060, the warming in the mountainous region is lower than the plain region with a value of 0.91°C, this differences will decrease to 0.75°C. During climate change, the different warming in the mountain and plain region will cause the EPR change, according to the Table 4-4, the quantified values of EPR change can be calculated. No matter in RCP4.5 or RCP8.5, warming differences between two stations are very close in different HPs, therefore, the EPR of the future temperature in the MIKE SHE model will decrease by 0.54 °C/km before 2060 and 0.44 °C/km after 2060.

**Table 4-4 The average yearly temperature determined the GCMs at Tashkurgan and Pishan station and the elevation lapse rates (EPR) were calculated based on these two stations.**

		HP	FP1	FP2	FP3	FP4
RCP4.5	Tashkurgan (°C)	-5.84	-4.53	-3.79	-3.13	-2.90
	Pishan (°C)	3.22	5.45	6.18	6.69	6.90
	Differences (°C)	/	-0.92	-0.91	-0.76	-0.74
	EPR change(°C/km)	-5.28	-5.82	-5.81	-5.73	-5.72
RCP8.5	Tashkurgan (°C)	-5.84	-4.68	-3.46	-1.84	-0.29
	Pishan (°C)	3.216	5.3	6.49	7.95	9.5
	Differences (°C)	/	-0.92	-0.90	-0.73	-0.74
	EPR change(°C/km)	-5.28	-5.82	-5.8	-5.71	-5.71

## 4.5 Effects on hydrological processes

### 4.5.1 Variation in water components

Based on the simulated results using the MIKE SHE model of the Yarkant River basin, the quantified water balance components at the catchment scale for each period are listed in Table 4-5. Because of the impact of climate change, all water components will be influenced correspondingly. Though the precipitation moderately changes in the future, the water resources in different forms would change strongly. With an increasing temperature, the stockpile (snow storage) would reduce persistently, at the end of this century, the snow storage will reduce 16.6 mm in RCP4.5 and 26.3 mm in RCP8.5 relative to 1986~2005. What is more, the dissipation (evapotranspiration) is more significant, the increase at the end of this century shows the values of 23.5 mm in

RCP4.5 and 47.3 mm in RCP8.5. Clearly, the variations in dissipation exceed those of the stockpile and supply and the diminishing snow storage in the mountain region and streamflow to the downstream region will be consumed by the increasing evapotranspiration and these changes are more dramatically in RCP8.5. In this way, the available water resources in the downstream oasis could decrease and face a more limited situation. The detailed variation of snow and streamflow would be analysed thoroughly.

**Table 4-5 The annual amounts of the water balance components in the Yarkant River basin during each period**

Water components		HP	FP1	FP2	FP3	FP4
RCP4.5	Precipitation (mm)	262.1	269.8	268.8	270.0	273.7
	Snow storage (mm)	36.9	31.8	25.5	20.7	20.3
	Stream runoff (mm)	110.2	107.5	108.5	107.7	106.3
	Evapotranspiration (mm)	108.6	118.3	123.7	128.7	132.1
RCP8.5	Precipitation (mm)	262.1	268.4	274.5	278.0	279.4
	Snow storage (mm)	36.9	34.6	23.9	18.1	10.6
	Stream runoff (mm)	110.2	106.1	112.1	107.8	103.6
	Evapotranspiration (mm)	108.6	119.9	129.5	143.1	155.9

## 4.5.2 Snow

### Snow/Precipitation

The snow/precipitation (S/P) means the proportion of snow to the total precipitation. Snow is an important water component of the hydrological processes in the alpine catchment. In the MIKE SHE model, a critical temperature is used to distinguish the different precipitation forms, snow or rain. Therefore, under the future climate change scenarios, the S/P would be very sensitive to warming. With the temperature increasing in the Yarkant River basin, more and more snowfall could translate to rainfall in FPs and it mostly occurs during May to September. However, the variations are very rare during November to next April in RCP4.5 and December to next February in RCP8.5 (shown in Figure 4.5). Comparing the FP3 and FP4, the S/P in each month is similar in RCP4.5 but reduces continually in RCP8.5, these represent the same change tendency in temperature in two scenarios. Though the total volume of precipitation will just vary a little, the forms will change sharply. Compared to the HP, the change ratios of S/P from June to September are presented as -4.6%, -13%, -24.5%, -25.6% in RCP4.5 and -2.2%, -16.1%, -38%, -54.7% in RCP8.5, however, these values in other months are only given



as -0.3%, -4.3%, -5.4%, -6.8% in RCP4.5 and -0.9%, -2.2%, -6.8%, -10.7% in RCP8.5. Thus, despite the warmer temperature, precipitation hardly tends to occur as rain and snow still are the primary precipitation form in winter.

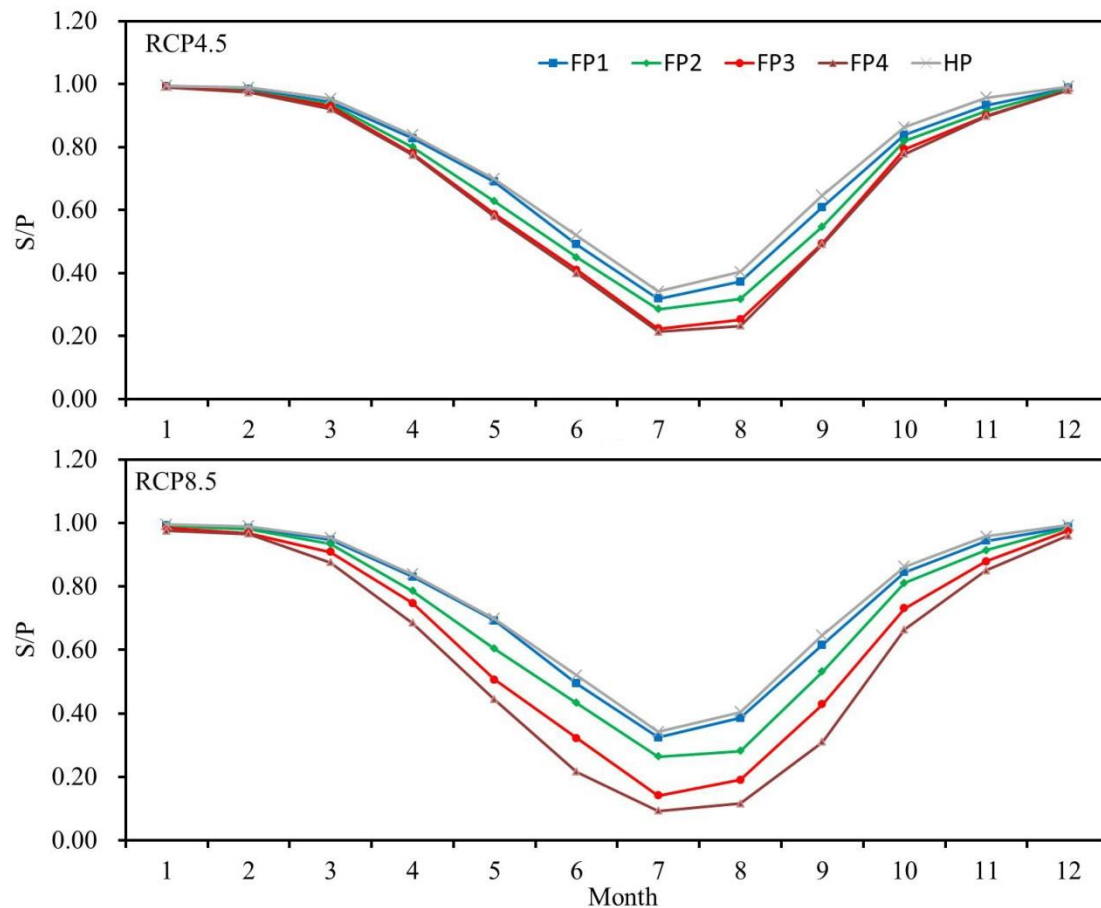


**Figure 4.5** The monthly values of S/P in different periods in the Yarkant River basin

## Snowmelt

With the rising temperature, not only the snowfall but also the snow storage and snowmelt could change greatly. In the scenario of RCP4.5, before 2060, May is a month for accumulating snowpack but after 2060, it becomes a month of snow dissipation (Figure 4.6). Moreover, the degradation trend will be stronger in July and weaker in August. These variations of snow storage change coincide with the snowmelt. The monthly distribution of snowmelt in FP1 is similar to HP but after 2040, snowmelt caused by a warming trend will exhibit an increased occurrence in the earlier period (April to May) (Figure 4.6). Therefore, the less snowpack melts in June, the peak in July becomes more spiculate. Together with the drastically decreased snowfall in summer,



the snowmelt in a later period (August to October) also represents the distinct reduction. This tendency will be more severe after 2060. The change in snowmelt is also reflected on the snow storage.

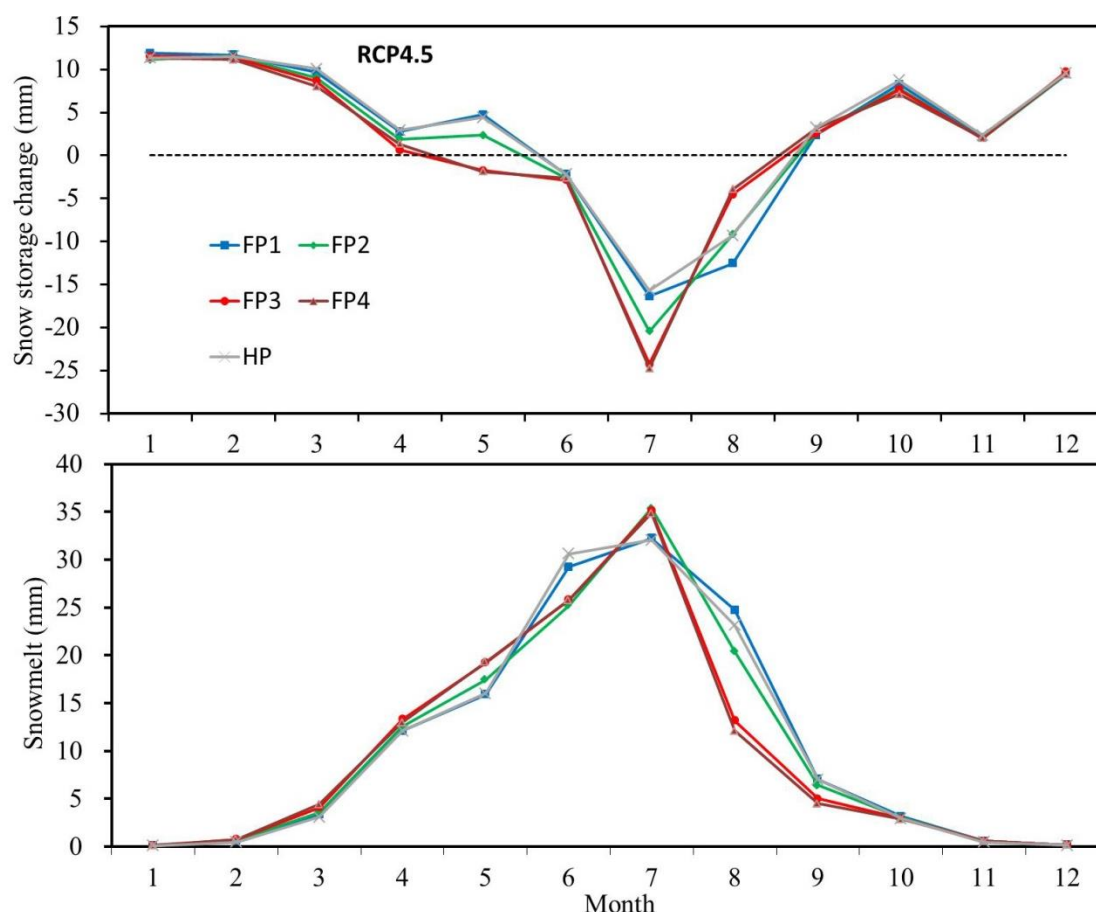


**Figure 4.6** The monthly volumes of snowpack change and snowmelt in each period in the Yarkant River basin in RCP4.5

This tendency will be more severe in the scenario of RCP8.5 (Figure 4.7). Similarly, the initial snowpack accumulation could become snowpack dissipation after 2060 in May. What is more, September is a month of snow dissipation before 2060, but after 2060 it becomes a snowpack balance. For the distribution of snowmelt, the peak will move forward to June from July after 2060. The significant increase in snowmelt could begin in March and last to June and a directly vast decrease will occur from July, due to the decreasing snowfall from May to September and the increasing snowmelt from March to May.

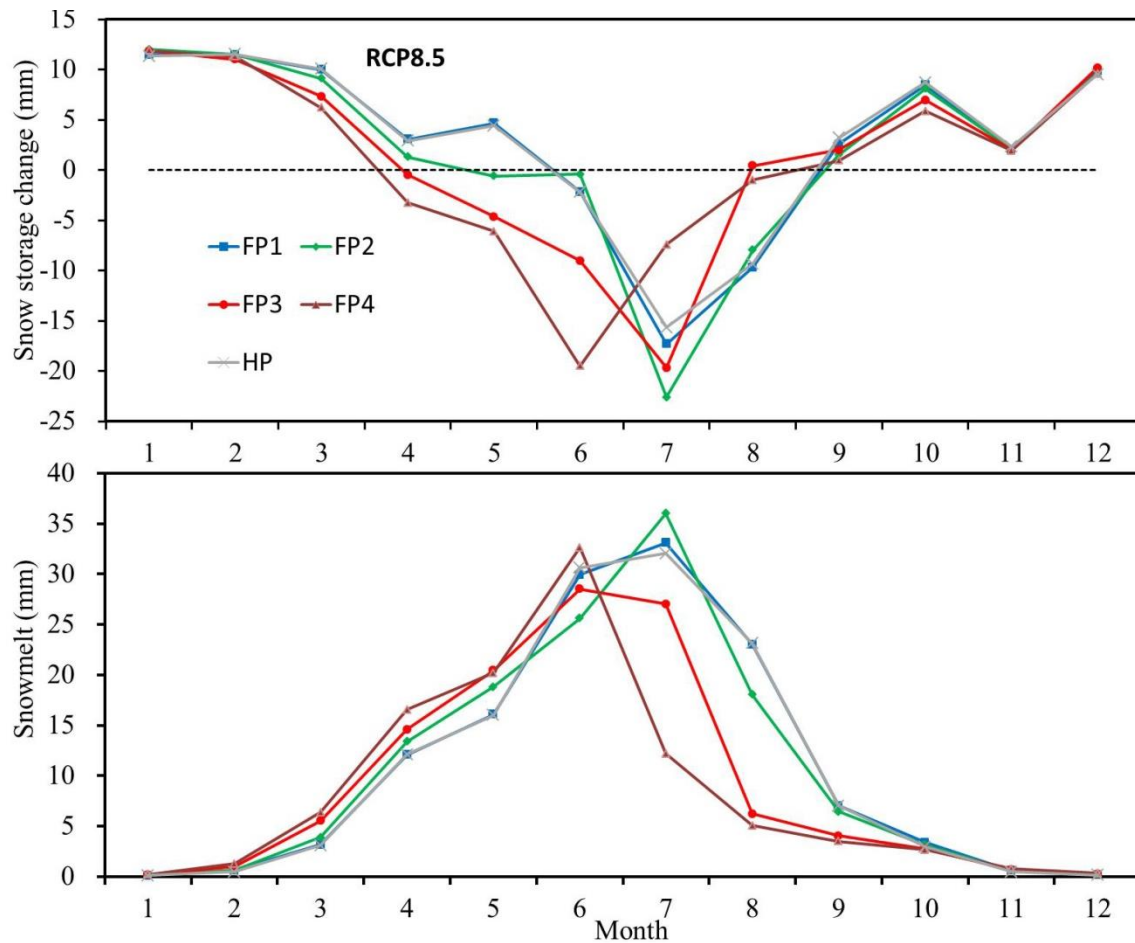


**Figure 4.7** The monthly volumes of snowpack change and snowmelt in each period in the Yarkant River basin in RCP8.5

### Snow storage

Based on Figure 4.6 and 4.7, no matter which different period or scenario, a new cycle of snowpack accumulation could begin in September and the snow storage in August is the minimum of the entire year and is defined as permanent snow storage in this study. In this way, snow storage at the end of August can simply be considered as permanent snow storage. Figure 4.8 provides the spatial distribution of snowpack on August 31<sup>st</sup> of each period's last year. Under two scenarios of RCP4.5 and RCP8.5, before 2060, most middle mountain regions could be covered by a thin snowpack and the permanent snow cover area accounted for 34.4% of the entire catchment. However, the covered area in the middle mountains will vanish during 2060-2079 and the permanent snow storage area could decrease by 82.3%, occupying only 5.95%.

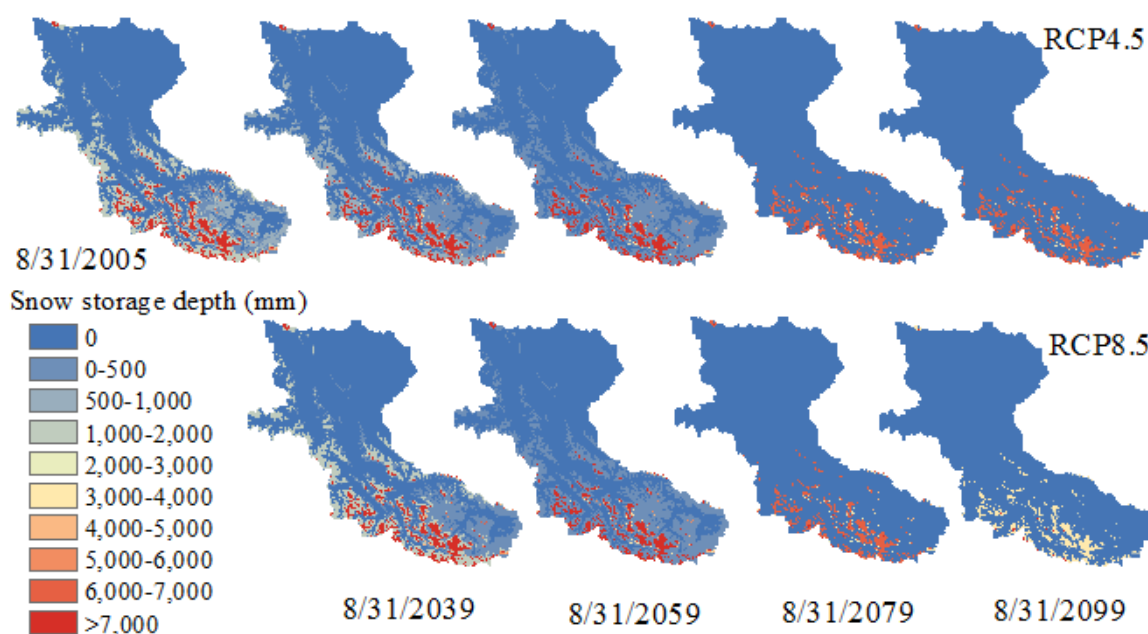


**Figure 4.8** The spatial distribution of the snowpack on August 31<sup>st</sup> of the last year in each period under RCP4.5 (first row) and RCP8.5 (second row)

In accordance with Figure 4.8, Figure 4.9 illustrates the distribution of permanent snow storage in the different elevation bands. By comparing the snow storage distribution in the elevation bands before and after 2060, the permanent snow storage region will be lifted by 600 m and the snow accumulation around 5000-5600 m will vanish completely in 2060-2079. Although the location of the permanent snow storage remains the same before 2060, compared with HP, the volumes of snow storage at 5000-5600 m in FP1 and FP2 will diminish significantly, with proportions of 33.2% and 72.1% in RCP4.5, 16.4% and 84.4% in RCP8.5. The shrinkages of snow storage in 5600-6400 are significantly different between RCP4.5 and RCP8.5, especially after 2060. The climate change scenario of RCP4.5 will decrease snow storage in 5600-6400 with the ratios of 3.6%, 8.8%, 17.3% and 19.4% in the FPs relative to HP. However, under RCP8.5, the effect become much acuter, most permanent snow storage will disappear at the end of the century and the proportion reduced by 0.2%, 8.6%, 27.2% and 61% in FPs. Different phenomena occurs in the extreme cold regions above 6400 m, where the average annual temperature was -19.5 °C in the HP, the small or absent change in permanent snow storage in two scenarios suggests that the rising temperature hardly affects the snow at this elevation because the increased temperature mostly remains lower than the snow's critical melting temperature.

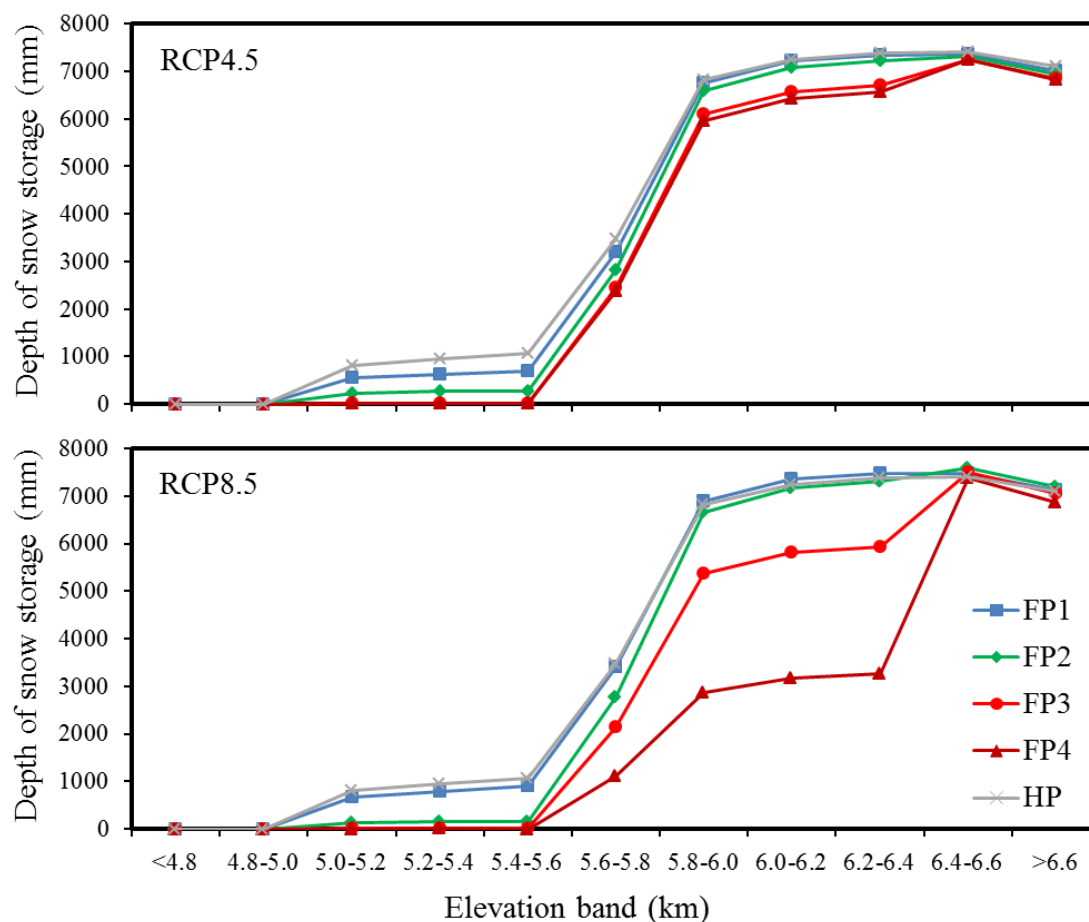


**Figure 4.9** The distribution of permanent snow storage in the different elevation bands on August, 31<sup>st</sup> of each period's last year

It is also noticeable that the climate change trend in the low-altitude regions should not simply be extended to high-altitude regions. If the elevation-dependent warming is not considered when processing the temperature using GCMs, the warming in high-altitude regions will be overestimated and results in a large deviation (e.g. the disappearance of permanent snow storage at 5000-5600 m will be earlier and completely vanish after 2040). The deviation will hinder an understanding of future changes in water resources.

### 4.5.3 Streamflow

At catchment outlet of Kaqun station, the streamflow in the FPs will change with ratios of -2.6%, -1.5%, -2.2%, -3.5% in RCP4.5 and -3.7%, 1.7%, -2.2%, -6.0% in RCP8.5 (Table 4-5), compared to the HP. In general, the runoff reflects a decreased tendency and suggests that less water resources will be available for the downstream region. Similar to the change in snowmelt, the streamflow rises in spring and early summer and drops in late summer (Figure 4.10). In FP1, the monthly streamflow at

Kaquun keeps a very similar distribution as in HP but the discharge in May and July began to rise because of more melting water in FP2. After 2060, other variations regarding the reductions in August and September need to be noted. In RCP8.5, the discharge in July will cut down because of more melting water in HP4 relative to HP3. All of these changes reflect a high correlation with snowmelt. From a temporal perspective, May to September will remain the flood season with contribution ratios of 80.5%, 81.5%, 82.4%, 82.8% in RCP4.5 and 80.6%, 82.3%, 83.6%, 83.1% in RCP8.5. This very moderate growth discharge in the flood season is mainly ascribed to stronger and more flood events and can be further explained by the following analysis.

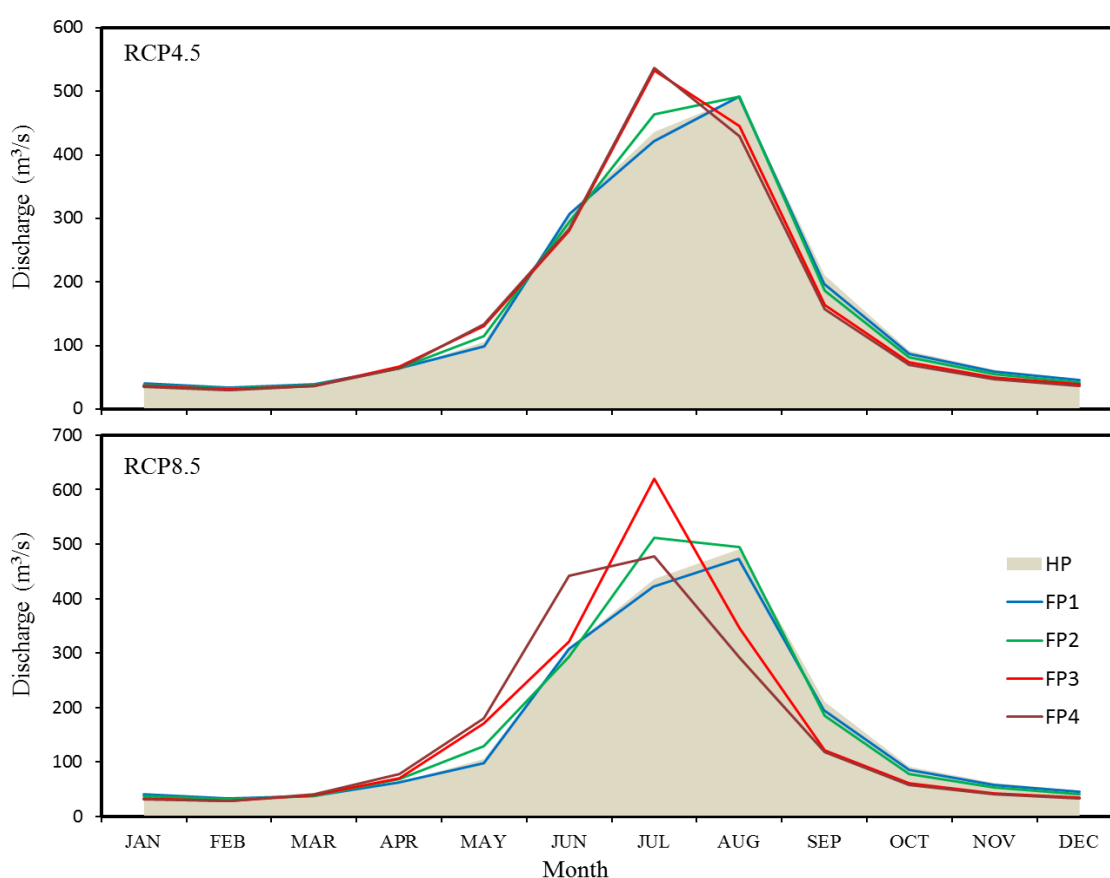


**Figure 4.10 Average monthly discharge in each period at Kaqun station**

Figure 4.11 illustrates the exceedance probability curves of the simulated discharge at Kaqun station for each period. For extreme flows with exceedance probabilities below 0.08, the average discharge will significantly increase with the ratios of 17.2%, 20.5%, 24.3%, 25.6% in the four FPs of RCP4.5 relative to the HP and these values represent 1.4%, 13.8%, 27%, 20.6% in RCP8.5. The normal flow with exceedance probabilities from 0.08 to 0.4 show moderate variations before 2060 and quantify the ratios of

1.6% and -4.3% in RCP4.5, -4.6% and -1.7% in RCP8.5. However, the variations became more drastic after 2060 and demonstrate values of -10.7% and -13.1% in RCP4.5 and -16.7% and -20.2%. Alternatively, the flows with exceedance probabilities above 0.4 will be correspondingly reduced by 8.6%, 13.4%, 16.4%, 18.3% in RCP4.5 and 6.4%, 14.1%, 25.1%, 27.0% in RCP 8.5.

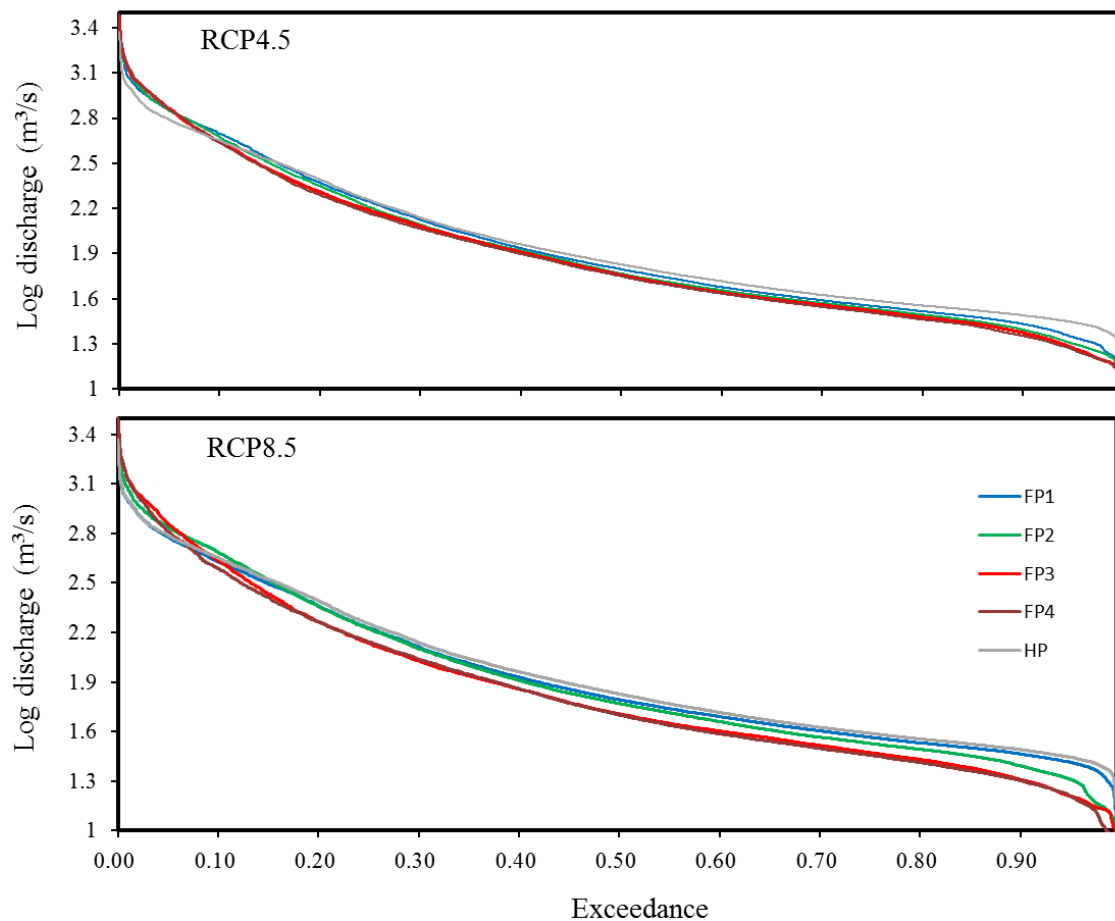


**Figure 4.11 Exceedance probabilities of the simulated discharge at Kaqun station in each period**

The variance of the flow probability indicates that the disequilibrium of the water resources will be more severe in the future; thus more water will be involved in flood events and less water will be available in the dry season, the phenomenon will be stronger in RCP8.5 than RCP4.5. One possible reason for these changes is that more snowfall will be replaced by rainfall, and snowmelt will move forward and more melt water concentrates in early summer. These variations accelerate the river conflux and increase the frequency and intensity of flooding. Considering a hypothesis, the events of daily discharge above  $1000 \text{ m}^3/\text{s}$  (with exceedance probabilities smaller than 0.01) are

taken as the flood, the occurrence frequencies are quantified in the HPs and represent values of 1.8%, 2.1%, 2.5%, 2.5% of RCP4.5 and 1.1%, 1.6%, 2.7%, 2.3% of RCP8.5. Additionally, the occurrence time moves earlier: from the middle of June in the HP to early June after 2020 and as early as late May after 2060, it could even happen in middle May in FP4 of RCP8.5. These changes indicated a more severe flood security and an unsteady distribution of water resources.

## 4.5 Conclusions

A 21-member average ensemble of GCMs under RCP4.5 and RCP8.5 was used to analyse the climate change impact in the Yarkant River basin in Karakoram. A modified QPM was employed in order to extract the change signals of precipitation in GCMs. In this modified QPM, according to the frequency variations in different quantile segments, the added and subtracted rainy days were assigned to a fixed range in the rank time series. The Delta method with elevation-dependent warming was applied to process the temperature change trends in GCMs. All the change signals of precipitation and temperature presented the notable uncertainties among the employed GCMs. Referring to the observed meteorological data in the baseline period, an average ensemble of change signals were used to generate the future meteorological data. Coupled with a well-calibrated MIKE SHE model, the responses of the hydrological processes to climate change were analysed from a water balance perspective.

In the Yarkant River basin, this century's precipitation growth in the FPs (mean ratios of 2.9%-4.4% in RCP4.5 and 2.8%-7.9% in RCP8.5) will be triggered primarily by the enhanced intensity of extreme precipitation in winter. In two scenarios, the slight increase in frequency and decrease in intensity at different quantiles result in little variation of the precipitation volume in summer. In winter, the stronger precipitation intensity is more than offset by declining rainy days and consequently, the precipitation in winter exhibits an increasing trend. Concerning temperature, the warming tendencies are obviously distinct between two scenarios, RCP4.5 shows the moderately mean ratio with 0.31/10a-0.38/10a in FPs, but RCP8.5 presents the ever-increasing values with 0.34/10a-0.59/10a. Furthermore, because warming is elevation dependent, the temperature in the low-altitude region increases more dramatically than in the high-altitude region and the EPR values indicate differences of 0.54 °C/km and 0.44 °C/km before and after 2060, respectively.

Under the influence of the local climate change, the spatiotemporal distribution of snow

will alter sharply and a large variation will develop between the different elevation bands. In each FP, snowfall will decrease significantly from June to September with proportions of 6.4%-28.9% in RCP4.5 and 3.4%-61.7% in RCP8.5 and the snowmelt from March to May will be enhanced; as a result, increasingly less snowpack is melting from August to October. For the permanent snow-covered region, the altitude will lift by 600 m during 2060-2079, and the covered area at 5000-5600 m will completely vanish. At 5600-6400 m, snow storage will diminish significantly (by 19.4% in RCP4.5 and 61% in RCP8.5) by the end of this century. However above 6400 m, because the increased temperature hardly exceeds the critical value for snowmelt, little or no change in snow storage occurs in this region.

The streamflow at the catchment outlet will exhibit a moderate descending trend and a more severe disequilibrium. Because of the more intense dissipation via evapotranspiration, the predicted discharge in HPs at Kaqun station will diminish at a ratio of 1.5%-3.5% in RCP4.5 and 2.2%-6% in RCP8.5. More importantly, the runoff distribution will be much more incongruous. As the snowmelt changes, streamflow will also increase from spring until early summer and decrease in late summer. Furthermore, earlier and stronger flood events will happen more frequently.

In the Yarkant River basin, the future climate change will strongly impact the hydrological processes and trigger a significant reform of water resources. The enhanced evapotranspiration will also result in more water consumption. The shrinking of the snow-covered area and snow storage volume will reduce the water storage in solid form in the high mountainous region. The declining streamflow at the mountain outlet will threaten the available water resources for agricultural downstream irrigation. Moreover, in the future flood period, a larger flood discharge and more frequent flood events will create greater challenges for flood security. These responses of hydrological processes indicate that the future climate change could strongly affect the water resources and thus a new strategy for irrigation agriculture in the downstream region is needed so as to adapt to the water variation supplied by the alpine catchment.

## References

- Baguis, P., Roulin, E., Willems, P. and Ntegeka, V. (2010): Climate change scenarios for precipitation and potential evapotranspiration over central Belgium. *Theoretical and Applied Climatology*, 99: 273-286. doi:10.1007/s00704-009-0146-5.
- Barontini S, Grossi, G., Kouwen, N., Naran, S., Scaroni, P. and Ranzi, R. (2009). Impacts of climate



- change scenarios on runoff regimes in the southern Alps. *Hydrology and Earth System Science*, 6, 3089-3141. doi:10.5194/hessd-6-3089-2009.
- Bavay, M., Grünewald, T. and Lehning, M. (2013). Response of snow cover and runoff to climate change in high Alpine catchments of Eastern Switzerland. *Advances in Water Resources*, 55, 4-16. doi:10.1016/j.advwatres.2012.12.009.
- Calanca, P., Roesch, A., Jasper, K. and Wild, M. (2006). Global Warming and the Summertime Evapotranspiration Regime of the Alpine Region. *Climatic Change*, 79, 65-78. doi:10.1007/s10584-006-9103-9.
- Chen, J., Brissette, F. P. and Leconte, R. (2011). Uncertainty of downscaling method in quantifying the impact of climate change on hydrology. *Journal of Hydrology*, 401, 190-202. doi:10.1016/j.jhydrol.2011.02.020.
- Chen, Y., Takeuchi, K., Xu, C., Chen, Y. and Xu, Z. (2006). Regional climate change and its effects on river runoff in the Tarim Basin, China. *Hydrological processes*, 20, 2207-2216. doi:10.1002/hyp.6200.
- Chen, Y., Xu, C., Chen, Y., Li, W. and Liu, J. (2010). Response of glacial-lake outburst floods to climate change in the Yarkant River basin on northern slope of Karakoram Mountains, China. *Quaternary International*, 226, 75-81. doi:10.1016/j.quaint.2010.01.003.
- Clarke, L., Edmonds, J., Jacoby, H., Pitcher, J., Reilly, J. and Richels, R. (2007). Scenarios of greenhouse gas emissions and atmospheric concentrations. Sub-report. In: *Of Synthesis and Assessment Product 2.1* by the U.S. Climate Change Science Program and the Subcommittee on Global Change Research. Department of Energy, Office of Biological & Environmental Research: Washington, D.C. USA, 2.1A.
- Claudia, S., Christoph, M., Wolfgang, S., Reinhold, S. and Swbastian, W. (2012). Downscaled GCM projections of winter and summer mass balance for Central European glaciers (2000-2100) from ensemble simulations with ECHAM5-MPIOM. *International Journal of Climatology*, 33: 1270-1279. doi:10.1002/JOC.3511.
- Eric, P. S. J., Alan, F. H., Clifford, F. M., Se-Yeun, L., Matt, S. and Richard, S. (2014). Estimates of Twenty-First-Century Flood Risk in the Pacific Northwest Based on Regional Climate Model Simulation. *Journal of Hydrometeorology*, 15: 1881-1899. doi: 10.1175/JHM-D-13-0137.1
- Gleick, P.H. (1986). Method for evaluating the regional hydrologic effects of global climate changes. *Journal of Hydrology*, 88:97-116. doi:10.1016/0022-1694(86)90199-x.
- Ghosh, S., and Katkar, S. (2012). Modeling Uncertainty Resulting from Multiple Downscaling Methods in Assessing Hydrologic Impacts of Climate Change. *Water Resources Management*, 26, 3559-3579, doi:10.1007/s11269-012-0090-5.
- Guo, L., and Li, L. (2015). Variation of the proportion of precipitation occurring as snow in the Tian Shan mountains, China. *International Journal of Climatology*, 35: 1379-1393. doi:10.1002/JOC.4063.

- Hay, L.E., Wilby, R. and Leavesley, G. H. (2000). A comparison of delta change and downscaled GCM scenarios for three mountainous basins in the United States. *Journal of American Water Resources Association*, 36: 387–397. doi:10.1111/j.1752-1688.2000.tb04276.x.
- Huss, M., Farinotti, D., Bauder, A. and Funk, M. (2008). Modeling runoff from highly glacierized alpine drainage basins in a changing climate. *Hydrological processes*, 22, 3888-3902. doi:10.1002/hyp.7055.
- Immerzeel, W. W., Beek, L. P. and Bierkens, M. F. (2010). Climate change will affect the Asian water towers. *Science*, 328: 1382-1384. doi:10.1126/science.1183188.
- IPCC, 2013. *Climate change 2013: The Physical Science Basis. Contribution of Working Group I to the Fifth Assessment Report of IPCC*. Cambridge University Press, Cambridge, United Kingdom and New York, USA.
- Jeelani, G., Feddema, J. J., Veen, C. J. and Stearns, L. (2012). Role of snow and glacier melt in controlling river hydrology in Liddar watershed (western Himalaya) under current and future climate. *Water Resources Research*, 48, 1-16. doi:10.1029/2011wr011590.
- Lettenmaier, D. P., Wood, A. W., Palmer, R. N., Wood, E. F., Stakhiv, E. Z. (1999). Water resources implications of global warming: A U.S regional perspective. *Climate change*, 43, 537-579.
- Liu, J., Liu, T., Bao, A., Maeyer, P. D., Kurban, A. and Chen, X. (2016). Response of hydrological processes to input data in high alpine catchment: an assessment of Yarkant River in China. *Water*, 8, doi:10.3390/w8050181.
- Liu, J., Liu, T., Bao, A., Maeyer, P. D., Feng, X. W., Miller, S. N. and Chen, X. (2016). Assessment of Different Modeling Studies on the Spatial Hydrological processes in an Arid Alpine Catchment. *Water Resources Management*, 30, 1757-1770. doi:10.1007/s11269-016-1249-2.
- Liu, T., Willems, P., Pan, X. L., Bao, A. M., Chen, X., Veroustraete, F. and Dong, Q. H. (2011). Climate change impact on water resource extremes in a headwater region of the Tarim basin in China. *Hydrology and Earth System Science*, 15, 3511-3527. doi:10.5194/hess-15-3511-2011.
- Liu, S. Y., Yong, Z., Song, Z. Y. and Yong, D. (2009). Estimation of glacier runoff and future trends in the Yangtze River source region, China. *Journal of Glaciology*, 55, 353-362. doi:10.3189/002214309788608778.
- Michael, H. K.; Christopher, J. N.; John, N.; William, L. (2005). *Applied Linear Statistical Models*, in: McGraw-Hill Education, 2 Penn Plaza, New York, USA.
- Middelkoop, H., Daamen, K., Gellens, D., Grabs, W., Kwadijk, J. C., Lang, H., Parment, B. A., Schadler, B., Schulla, J., Wilke, K. (2001). Impact of ClimateChange on the Hydrological Regime and Water Resources Management in the Rhine Basin. *Climatic Change*, 49, 105-128.
- Min, S.K., Zhang, X., Zwiers, F. W. and Hegerl, G. C. (2011). Human contribution to more-intense precipitation extreme. *Nature*, 470, 378-381. doi:10.1038/nature09763.
- Ntegeka, V., Baguis, P., Roulin, E. and Willems, P. (2014). Developing tailored climate change scenarios for hydrologic impact assessments. *Journal of Hydrology*, 508, 307-321.

- doi:10.1016/j.jhydrol.2013.11.001.
- Ntegeka, V., Willems, P., Baguis, P., Roulin, E. (2008). Climate change impact on hydrological extremes along rivers and urban drainage systems. Summary report Phase 1: Literature review and development of climate change scenarios: Belgian Science Policy - SSD Research Programme, CCI-HYDR project, Leuven/Brussels, Belgium.
- Onyutha, C., Tabari, H., Rutkowska, A., Nyeko-Ogiramoi, P. and Willems, P. (2016). Comparison of different statistical downscaling methods for climate change rainfall projections over the Lake Victoria basin considering CMIP3 and CMIP5. *Journal of Hydro-environment Research*, 12, 31-45. doi:10.1016/j.jher.2016.03.001.
- Quintana S., Ribes, P. A., Martin, E., Habets, F. and Boé, J. (2010). Comparison of three downscaling methods in simulating the impact of climate change on the hydrology of Mediterranean basins. *Journal of Hydrology*, 383, 111-124. doi:10.1016/j.jhydrol.2009.09.050.
- Rangwala, I., and Miller, J. R. (2012). Climate change in mountains: a review of elevation-dependent warming and its possible causes. *Climatic Change*, 114: 527-547. doi:10.1007/s10584-012-0419-3.
- Roosmalen, L. V., Sonnenborg, T. O., Jensen, K. H. (2009). Impact of climate and land use change on the hydrology of a large-scale agricultural catchment. *Water Resources Research*, 45, 150-164. Dio: 10.1029/2007WR006760.
- Solman, S., Nunez, M. (1999). Local estimates of global climate change: a statistical downscaling approach. *International Journal of Climatology* 19, 835–861.
- Su, F., Zhang, L., Ou, T., Chen, D., Yao, T., Tong, K. and Qi, Y. (2016). Hydrologic response to future climate changes for the major upstream river basins in the Tibetan Plateau. *Global Planet Change*, 136, 82-95. doi:10.1016/j.gloplacha.2015.10.012.
- Taye, M. T., Ntegeka, V., Ogiramoi, N. P. and Willems, P. (2011). Assessment of climate change impact on hydrologic extremes in two source regions of the Nile River Basin. *Hydrology and Earth System Science*, 15, 209-222. doi:10.5194/hess-15-209-2011.
- Teng, J., Vaze, J., Chiew, F. H. S. (2012) Estimating the Relative Uncertainties Sourced from GCMs and Hydrological models in Modeling Climate Change Impact on Runoff. *Journal of Hydrometeorology*, 13(1): 122-139.
- Thompson, J. R., Green, A. J. and Kingston, D. G. (2014). Potential evapotranspiration-related uncertainty in climate change impacts on river flow: An assessment for the Mekong River basin. *Journal of Hydrology*, 510, 259-279. doi:10.1016/j.jhydrol.2013.12.010.
- Willems, P., and Vrac, M. (2011). Statistical precipitation downscaling for small-scale hydrologic impact investigations of climate change. *Journal of Hydrology*, 402, 193-205. doi:10.1016/j.jhydrol.2011.02.030.
- Xu, C., Chen, Y., Chen, Y., Zhao, R. and Ding, H. (2013). Responses of surface runoff to climate change and human activities in the arid region of central Asia: a case study in the Tarim River

- basin, China. *Environment Management*, 51, 926-938. doi:10.1007/s00267-013-0018-8.
- Xu, H., Zhou, B. and Song, Y. (2011). Impacts of climate change on headstream runoff in the Tarim River Basin. *Hydrology. Research*, 42, 20-29. doi:10.2166/nh.2010.069.
- Zhang, Q., Xu, C. Y., Tao, H., Jiang T. and Chen, Y. D. (2009). Climate changes and their impacts on water resources in the arid regions: a case study of the Tarim River basin, China. *Stochastic Environment Research and Risk Assessment*, 24, 349-358. doi:10.1007/s00477-009-0324-0.
- Zhang, S., Gao, X., Zhang, X. and Hagemann, S. (2012). Projection of glacier runoff in Yarkant River basin and Beida River basin, Western China. *Hydrological processes*, 26, 2773-2781. doi:10.1002/hyp.8373.

# CHAPTER 5

## General discussion

---

*This chapter presents an overview of the research objectives and reviews the main answers to the research questions (Section 5.1). Then, critical reflections on the methodologies are summarized, including how to answer the research questions in a more effective way (Section 5.2). Eventually, recommendations for future work are proposed (Section 5.3).*

## 5.1 Summary and discussion of research questions

Water resources are essential for economic development and ecological stabilization in arid and semi-arid regions. In order to improve the utilization efficiency of limited water resources, many studies (Williams, 1999; Ma et al., 2005; Zhang et al., 2010) have been conducted over the past several decades and focused on the relations among environment, ecology, and climate change. Mountain hydrology plays a key role in the management of water resources in arid and semi-arid regions. Hydrologic feedbacks in mountainous regions dominate the availability of water resources, influence human activities, constitute ecological and environmental systems, and contribute to global and regional climate variability (Roger et al., 2006). A better understanding of hydrological processes could greatly help to systematically handle with water resource issues. However, because of the extreme topographic patterns, steep altitudinal gradients of meteorological variables, high seasonal variability of hydrologic components, low density and weak representativeness of gauging, and the complex water cycle, hydrological processes in study area are significantly different from those in lower-elevation regions and increase the modeling difficulties (Kang et al, 2007). The Yarkant River basin is a typical high alpine catchment in an arid region. Its water supply sustains the livelihood of more than 9 million people in the Tarim River basin. Since the previous studies of hydrological processes in the Yarkant River basin were still insufficient, the primary theme of this dissertation is to investigate the hydrological processes and their variation under climate change in the Yarkant River basin and support local water authorities to understand the local hydrological features.

From the general goal, four research questions were distilled.

***RQ1: How is the hydrological processes described in different hydrological models?***

***RQ2: How do remote sensing data perform in hydrological modeling?***

***RQ3: What are the responses of hydrologic components to different forcing data?***

***RQ4: What are the effects of climate change on the hydrological processes?***

The four research questions were rephrased and answered in Chapters 2-4. The corresponding research objectives of each question attempt to address the main challenges in understanding hydrological processes in alpine catchments. An overview of the research objectives, methods used and findings is given in Table 5-1. This table aids in understanding the links between the research objectives and the research questions, and how they are presented in each chapter.

### **RQ1: How is hydrological processes described in different hydrological models?**

Because of the limitations of the understanding and mathematical expression of natural hydrological processes, hydrological models cannot completely describe natural processes and are built in a simplified and conceptual way using different structures and algorithms (Moradkhani et al, 2008). Consequently, each model has its own unique characteristics and respective applications (Gayathri et al, 2015), and hydrological models have often produced uncertain results regarding the probable changes in spatial and temporal distributions of calibrated hydrologic components (Yang et al, 2000; Jiang et al, 2007; Barthel et al, 2012). Moreover, model descriptions of overall integrated processes are much more uncertain. To answer the question RQ1, the models SWAT and MIKE SHE were jointly applied for hydrological modeling in Chapter 2. The joint application is based on the cross-calibration of main hydrologic components, including runoff, snow and evapotranspiration. Afterward, the hydrological processes and the influences of model structure and algorithm were analyzed.

Firstly, we evaluated the discharge hydrography of SWAT and MIKE SHE simulations at the Kaqun station. After calibration the discharge hydrography curves were generally well matched with the observations and presented an accurate result of the calibrated output. However, huge differences were found in the constitution of stream runoff, snow distribution and evapotranspiration distribution. These differences in various models indicate that some biases may be caused in our understanding of these hydrological processes based one single simulation.

Regarding the contribution of stream runoff, several studies have identified that subsurface lateral flow is a dominant contributor to storm flow in headwater catchments (Swarowsky et al., 2012; Kienzler and Naef, 2008; Verseveld et al., 2009). Fan et al. (2014) used isotopes to study the constitution of the Tizinafu River (neighboring to the Yarkant River) and found that most melt water above 2500m would infiltrate into the soil and contribute to the stream as subsurface lateral flow. The SWAT model calculated that the subsurface lateral flow comprised 41.4% of the total flow. Because of the algorithm differences, the lateral flow in soil profiles was ignored by MIKE SHE model. The MIKE SHE model did not consider this phenomenon, but gave the steady and uninterrupted base flows in the Yarkant River. Fan et al (2013) used multiple base flow separation methods and determined that steady and uninterrupted base flows contributed 21.3% of the total flow. This ratio was much closer to the MIKE SHE simulation result of 23% and suggested the better base flow simulation in MIKE SHE model.

**Table 5-1 Overview of the contents of this dissertation**

Chapter	RQ	Objectives	Employed methods	Main findings
Chapter 2: Joint application of multiple models in hydrological processes study	RQ1	<ul style="list-style-type: none"> <li>- Investigate the performances of the SWAT and MIKE SHE in simulation of different hydrologic components;</li> <li>- State the hydrological processes in the Yarkant River basin</li> </ul>	<ul style="list-style-type: none"> <li>- Cross-validate the outputs and analyze the differences based on model structure and algorithm</li> <li>- Combine the simulations of multiple models</li> </ul>	<ul style="list-style-type: none"> <li>- SWAT and MIKE SHE can agree with natural processes in some aspects but not in all</li> <li>- A general hydrological process was given with the quantized hydrological components</li> </ul>
Chapter 3: The responses of hydrological processes to the different input data	RQ2 and RQ3	<ul style="list-style-type: none"> <li>- Check the application of RSD in modeling</li> <li>- State the responses of hydrological processes to different input data</li> </ul>	<ul style="list-style-type: none"> <li>- Accuracy checking and bias correction based on LOCI</li> <li>- ANOVA model to define the significant impact of input data to hydrologic outputs</li> <li>- Comparing the differences of the sensitive hydrological components</li> </ul>	<ul style="list-style-type: none"> <li>- TRMM overestimated low intensity precipitation events</li> <li>- Corrected RSD had acceptable simulation but without improvement</li> <li>- Differences between SBD and RSD clearly reflected in the corresponding sensitive water components</li> </ul>
Chapter 4: The effects of climate change on hydrological processes	RQ4	<ul style="list-style-type: none"> <li>- Understand future climate change in the Yarkant River basin</li> <li>- Describe the changes in the future hydrological processes</li> </ul>	<ul style="list-style-type: none"> <li>- Extract the change signal of precipitation and temperature and obtained future data based on modified QPM and Delta</li> <li>- Compiling the MIKE SHE model and analyze the simulated outputs</li> </ul>	<ul style="list-style-type: none"> <li>- Stronger extreme precipitation events caused a moderately increased volume</li> <li>- Great differences of warming between RCP4.5 and RCP8.5</li> <li>- Hydrological processes sharply change in future climate scenarios and trigger significant reforming of the water resource components.</li> </ul>



For the calculation of snowmelt, the degree-day approach takes temperature as the dominant factor, essentially as a simple expression of energy transport and conservation on the snowpack surface (Braithwaite, 1995; Krenke et al, 1996). Because of the less input data and parameters, degree-day approach has been widely applied in snow and glaciers melt (Hock, 2003). It has achieved similar performance to the energy-balance approach in many catchments and even better results in some sparsely gauged regions (WMO, 1986; Hock, 2005). The degree-day approach was used in both the SWAT and MIKE SHE models. However, more impact factors, including the accumulated temperature on the snow surface (Zuzel et al, 1975; Koivusalo et al, 2001) and variation in the melt factor, were considered in the SWAT model. This kind of arrangement intends to have more concentrated temporal distribution of snowmelt, and proportion of snowmelt in June to September was 76.8%. This feature of the SWAT model matched the natural snowmelt process more flexibly than the current MIKE SHE model and explained the huge seasonal change of stream runoff in the Yarkant River (Chen et al, 2006; 2010). But these kind of lumped parameters in each elevation band are hard to calibrate or validate. In practical, it might trigger the problem of overparameterization.

For the output of snow storage, although the annual volume in different elevation zones was similar between the SWAT and MIKE SHE models, the semi-distributed structure of the SWAT model strongly decreased the spatially distributed information. The MIKE SHE model produces the complete grid output with significant spatial variation. By the MIKE SHE model, it was found that the snowpack at approximately 4500 m could melt from July to September, although the snow cover above 5500 m showed a continuously increasing trend throughout the entire year. The fully distributed model presents the advantages in spatial distribution of outputs.

For all the spatial outputs of the hydrologic components, the MIKE SHE model showed clearer correlation in spatial distribution with the corresponding factor. For example, MIKE SHE produced more information regarding evapotranspiration being closely related to land use and water availability. Based on the spatial and temporal distribution, MIKE SHE suggested an obviously seasonal change in the region with good plant coverage around the outlet, but little or no variation in the glacial region around the western ridge. Additionally, because of the definite hydrodynamic relationship between the grids, the slope conflux was implemented and the depression could intercept and store some water in this process. In this case, the larger water area caused more water evaporation in the MIKE SHE model. Some terrain was correctly described as depressions but some descriptions as depressions resulted from mistakes in the digital

processing. Therefore, field investigations can be helpful in correctly judging depressions. The comparison in chapter 2 revealed the effect of the model structure on evaporation; the MIKE SHE model produced more water evaporation, with a proportion of 35.5% compared with SWAT. However, it was difficult to estimate which was better without actual field investigation of the terrain. Maybe the evapotranspiration on the HRU or finer scale can connect to the hydrological simulation in different scale, and help to seize the actual evapotranspiration.

Evapotranspiration is the primary dissipation type in the mountain region, although it is also the least well known of the climatic elements (Axel, 2002). Direct measurements in the whole catchment are not possible and must be calculated by other measurement and estimated parameters. Therefore, the chosen algorithm would strongly affect simulated results. The Penman-Monteith method has been previously used in the SWAT model to satisfy the growth of plants, and soil evaporation has been subject to the difference between actual soil content and soil water content at field capacity and the wilting point. This limitation in calculation could be more appropriate in arid and semi-arid regions. However, the Kristensen-Jensen method used in evapotranspiration calculation in MIKE SHE did not include these parameters restrictions. Finally, in the Yarkant River basin, MIKE SHE produced more soil evaporation, with the ratio of 63.7% relative to SWAT.

The SWAT and MIKE SHE models have had widely successful applications in many fields of hydrologic study and have also performed well for hydrography at the Kaqun station in the Yarkant River basin modeling. Their performances for the description of some hydrologic components which were not calibrated were quite distinct. For a single hydrological modelling, some aspects of hydrological processes can accord with the physical truth, but not the complete processes. Generally, the integrated application of two different types of hydrological models could achieve a good complementation and overcome the deficiency of model structure and algorithm.

## **RQ2: How do remote sensing data perform in hydrological modeling?**

In addition to model structure and algorithm, input data is another primary uncertainty source in hydrological modeling (Fang et al, 2015). To reduce this uncertainty source, different new data sources were used in hydrological study, thereinto, RSD are the most important which have been widely applied in calibration and validation. In chapter 3, remotely sensed data, including precipitation, temperature and PET, were collected and applied in hydrological modeling. In conclusion, their application did not improve the accuracy of simulated results but achieved an acceptable output.

RSD have enriched the data sources of hydrological modeling, especially for understanding the hydrological processes of high-cold alpine catchments (Chen et al., 2014). The PUB has strongly suggested developing remote sensing applications in ungauged catchments (Tan et al, 2004). Among the input data, precipitation surely is one of the complex and crucial variables among hydrometeorology factors. Currently, there are many remotely sensed precipitation datasets that can be chosen; however, their applications in hydrological modeling are hard to evaluate because of sparse validation data (Kan et al, 2013). Therefore, the precision of the chosen TRMM data in the study area was assessed based on observations. Through detecting of TRMM on actual rainy days, we found that TRMM overestimated many drizzle days when the daily volume of precipitation was lower than 0.3 mm. Based on this finding, LOCI can be chosen to correct the TRMM data from the precipitation frequency and volume.

Normally, the bias corrections of precipitation are complex because of many interlaced issues such as volume, frequency, intensity, and probability distribution. Different correction methods have focused on the different issues (Claudia et al, 2012; Fang et al, 2015). Therefore, determining the dominant problem of raw data is the precondition for effective bias correction. Based on the detection of TRMM in the Yarkant River basin, too many drizzle days are the dominant problem; after correction by LOCI, the correlation coefficients with the observations at a monthly scale were greatly improved.

Alternatively, the remotely sensed temperature and PET can be used in hydrological modeling after simple processing. The processed RSD were used to drive the MIKE SHE model, and their simulated discharge hydrography at the Kaqun station was evaluated by statistical coefficients. Compared with the SBD model, no improvement was found; all the applications of RSD resulted in merely acceptable simulation. This finding strongly indicates that RSD has difficulty determining the physical truth of meteorological factors with respect to spatial and temporal distributions.

It was difficult to use field investigation to clarify the actual situation of the hydrologic components in the untraversed region. The accuracy of RSD is still nebulous and direct applications may thus be in doubt. However, reference to field reality can also be achieved from RSD, which facilitates the understanding of hydrological processes.

### **RQ3: What are the responses of hydrologic components to forcing data?**

Interpolated SBD for precipitation and temperature are too piecemeal in the Yarkant River basin because of the very steep terrain. Spatial RSD reveals more rational

distribution characteristics with obvious isolines. However, the differences in spatial distribution between SBD and RSD cannot be explained by the flow hydrography. In chapter 3, after the significant impacts of input data on outputs were defined, more attention was paid to the responses of hydrological processes to input data. The snow in covered areas and storage volume allowed the interpretation of differences between SBD and RSD (precipitation and temperature), and transpiration was used in the PET data.

The hydrologic cycle is a quite complex and uncertain system in nature (Christiaens et al, 2002; Gallart et al, 2007); moreover, the relationships between inputs and outputs are highly nonlinear in hydrologic simulations (Kang et al, 2013). Therefore, which hydrologic component reflected the differences in input data in the hydrological processes? To answer this prerequisite problem, ANOVA was applied to test the significant impact of input data to outputs. ANOVA is a collection of statistical models used to analyze the significance between an impact factor and experimental results (Michael et al, 2005). The significant impacts of three kinds of input data (precipitation, temperature and PET) to hydrologic components were defined by ANOVA with three factors with fixed effects.

To study hydrological processes, chapter 2 focused on the effect of different input data. Compared with interpolated SBD, TRMM overestimated the precipitation in the high mountain region (above 6400 m), with a ratio of 12%, and caused more snow storage in this region, with a ratio of 12%. Similarly, the underestimation of TRMM in the 5000-5700-m zone resulted in less snow storage. The volume changes of precipitation and snow storage corresponded well. However, this simple correspondence cannot be directly extended to temperature; the change in remotely sensed temperature caused re-judgements of parameters in auto-calibration. The smaller DDF and higher TMT resulted in less snowmelt at elevations under 4300 m and more snow-covered areas with very thin depths. At 5000-5700 m, the snowpack was hard to melt and snowfall became the dominant factor in the volume of snow storage; the higher TMT and higher remotely sensed temperature in this region resulted in much less snow storage. Additionally, the higher remotely sensed PET also caused smaller transpiration because of the changed parameters.

When only one hydrologic component was studied in hydrologic simulations, very similar outcomes could be gained by different driving data after calibration. In the calibration processes, some biases may have been introduced in other hydrologic components that strongly affected the description of hydrological processes. To clarify

the effect of input data on hydrological processes, when one kind of input data is changed, the responses of the corresponding hydrologic components that are significantly sensitive to this input data must be analyzed. Moreover, an optimized set of parameters for one hydrologic component may be non-optimal for others.

#### **RQ4: What are the effects of climate change on the hydrological processes?**

According to the report from the IPCC (IPCC, 2013), climate change has undoubtedly influenced water resources in most parts of the world. At a global scale, 7% of the population would be exposed to a 20% decrease in renewable water resources for each degree of warming. Moreover, climate change has strongly altered the seasonal distribution of stream flow in snow-recharged regions. The IPCC estimated the global change tendency; however, climate change and its influences are still not adequately known in some parts of the world such as Central Asia (IPCC, 2013).

Hydrological processes variations under climate change in the 21<sup>th</sup> century in the Yarkant River basin were investigated in chapter 4 based on chapter 2 and chapter 3, which provided a good foundation for hydrological modeling study. The average ensemble change signals of precipitation and temperature were extracted from 21 GCMs; the moderate increase of precipitation was found to be from stronger extreme precipitation events, and temperature rose by 0.31-0.38°C/10a under RCP4.5 and 0.34-0.58°C/10a under RCP8.5. These change signals were used to add historical observations to calculate the future meteorological data. Finally, the changes in hydrological processes were analyzed by coupling the MIKE SHE model.

Most study of future climate change on a regional scale is based on GCM data. GCMs have provided change tendencies for future periods (Taylor et al, 2012), and GCMs from different institutes have shown huge deviations in future climate change; the average ensemble of several GCMs could be used to mitigate this uncertainty (Teng et al, 2012; Ghosh et al, 2012). Therefore, the scenario runs (in future periods) were compared with the equivalent control runs (in the history period) to extract the change signals and investigate future climate change at a regional scale. Additionally, the climate change focused on the variation tendency in long-term sequences, which means that each extracted change signal should include situations with different probabilities. In chapter 4, this study attempted to incorporate climate change in the 21<sup>st</sup> century based on dividing the future period into four parts of 20 years; the change signal for each future period could include situations with a probability of 0.05.

For precipitation, the Delta method ignores the frequency and intensity change and only focuses on the volume change (Onyutha et al, 2016). The QPM method considers the overall frequency change and the intensity perturbation at quantiles; this method successfully catches extreme precipitation and has achieved good application (Liu et al, 2011; Willems et al, 2011; Ntegeka et al, 2014). To decrease the uncertainties caused by randomly adding or subtracting precipitation events when a new data series is generated, this method was modified by assigning the frequency changes in the different precipitation intensity ranges. The average ensemble of 21 GCMs indicated that the precipitation would moderately increase, the increased part would be from the stronger extreme precipitation in winter, and the precipitation in summer would moderately decrease.

Dissimilar with the precipitation, temperature warming under the different emissions pathways largely differs between RCP4.5 and RCP8.5. At the end of this century, the warming could stabilize at 0.31 C/10a for RCP4.5, whereas it could persistently increase to 0.59 C/10a for RCP8.5. These increasing speeds in the Karakoram region are considerably larger than the mean global values (IPCC, 2013).

For hydrological process changes at the catchment scale under the future climate scenarios, note that each hydrologic component's alteration is not independent in the hydrologic system. From the water balance point of view, which is the basic control equation of the hydrological model, the redistribution of different hydrologic components and their transformations can be understood. In the Yarkant River basin, the precipitation slightly increased in volume; nonetheless, warming greatly altered the forms and most snowfall could change to rainfall. Moreover, warming enhances the snowmelt and brings it forward in time. However, all the growing available water resources could not supply the downstream region because of the greater rising dissipation.

The changes in hydrological processes in the Yarkant River basin under climate change were drastic; the transformation of different hydrologic components was strengthened, and the distribution could also reflect changes such as the retreat of the permanently snow covered area, stronger spring and early summer snowmelt, a reduced late summer snowmelt, and forward and stronger extreme discharges (with a probability lower than 0.08). All these changes suggest the development of downstream oases to confront the changing water situation, and new plans to adapt to severer water utilization and security are needed.

## 5.2 Critical reflections on methodology

The hydrological processes of high alpine catchments in arid regions are taken as the only theme in this dissertation. To clarify this topic, relative efforts were implemented from hydrological modeling, remote sensing applications and climate change. The methods used determined if the questions could be answered or not. Some critical aspects are presented in this section concerning the current methodologies in this dissertation to suggest potential improvements.

In Chapter 2, the joint application of the SWAT and MIKE SHE models was used to investigate the hydrological processes and analyze the effects of model structures and algorithms. In most catchment hydrological models, there are still many nature processes that are not involved in hydrological modeling or are hard to quantify or validate, such as frozen soil and glaciers. It may be a significant drawback to use a no open-source model. In this dissertation, the results from SWAT and MIKE SHE modeling indicated that they were insufficient in simulation in some aspects of the hydrologic cycle. Consequently, combining models may improve the understanding of hydrological processes in high-cold mountain catchments. The Variable Infiltration Capacity (VIC) model (Liang et al, 1994) has been suggested. VIC is a macroscale hydrological model that computes full water and energy balances. As such, it shares several basic features with the other land surface models that are commonly coupled to GCMs. In VIC, some important hydrologic cycles are included, such as frozen soil (Cherkauer and Lettenmaier, 1999) and blowing snow (Bowling et al, 2004). Moreover, the Cold Regions Hydrological model (CRHM), which was developed as a modular object-oriented modeling framework to simulate the hydrologic cycle of cold regions by a multi-disciplinary research group from various institutes in Canada (Pomeroy et al, 2007; Zhou et al, 2014), has also been suggested. CRHM focuses on the specific hydrologic cycle and can be effectively used to test snowdrift, glaciers and frozen soil simulations.

Comparisons of snow storage and actual evapotranspiration (among SWAT, MIKE SHE and MODIS) were implemented at four time points. The comparisons could reveal the general seasonal variation tendency but missed fine-scale details such as at monthly scales. Therefore, comparisons at fine time scale could enrich the understanding in temporal distribution.

RSD was the concern in chapter 3. Unfortunately, RSD applications have failed to make progress in discharge hydrography simulation at the Kaqun station; perhaps the bias

corrections are insufficient. On the one hand, the benchmarks of observations are too sparse and the heterogeneity of the Yarkant River basin is too strong. There is an assumption that the RSD remain stable when the corrected coefficient is interpolated into the entire catchment; however, the detected errors of TRMM at Tashkurgan station cannot well represent the truth in high mountain regions. On the other hand, LOCI scaling focused on volume and frequency correction but failed to correct the probability distribution, which may be a potential reason for the weak hydrography simulation at Kaqun station.

When the responses of hydrologic components to input data were analyzed, only one element was chosen (snow storage to precipitation and temperature, and transpiration to PET). However, as shown in Table 3-6, each input data type has significant impact on multiple hydrologic components. How would the deviations between different levels affect other sensitive elements? This question was missed in the research objectives. The study of the different responses of hydrologic components to input data could possibly optimize our understanding of hydrologic cycle.

In Chapter 4, the modified QPM and Delta were used to extract the variation signals of climate change. First, only the sustainable and high emission scenarios (RCP4.5 and RCP8.5) were selected to investigate the “average” and “high” levels in climate change. However, the other scenarios (RCP2.6 and RCP6) were ignored. Second, this research objective paid more attention to the average ensemble of 21 GCMs; their uncertainties were just briefly introduced. The huge uncertainties among GCMs and their effect in hydrological modeling would be much more notable in the 21st century. Third, because of fewer rainy days in arid regions, the frequency change was not very remarkable, the significance of advances of the modified QPM relative to initial QPM are hard to state, therefore, more applications and comparisons in the humid regions with more rainy days and frequency changes are also needed to clarify the advances.

In the analysis of the permanently snow-covered area, the permanent snowpack was simply defined as the timing of the least snow storage in the year. Strictly speaking, there could be a few deviations relative to the nature truth determined by this judgement. Moreover, the resolution of grids in the MIKE SHE model is 2 km, this size is enough for such large scale catchment in hydrological modeling, but still too big for determining the location of the snow line; therefore, this kind of work was not included in the research objective.



### **5.3 Recommendations for future work**

#### **5.3.1 Future work on model integration**

In Chapter 2, the integrated results from the SWAT and MIKE SHE model make a progress in understanding of hydrological processes. However, the two models were run independently, which means that more time was needed to execute each model. After we have determined the effects of model structure and algorithm on the different hydrologic components, a more appropriate integrated module can be developed. An integrated model can be implemented in a more effective way and given more available references to similar studies (Smith et al, 2012; 2013). In this way, an optimized integrated model can be used to study hydrological processes in the high-cold mountain region.

#### **5.3.2 Future work on diversified RSD**

Remote sensing data have constituted the major data resource for hydrologic studies in catchments with sparse gauges. With the diversified development of RSD, more and more data can be obtained. To check the precision and scale matching of hydrological models, comparisons and cross-verifications among more RSD need to be conducted. Based on the deviations of different RSD, suitable bias-correction methods need to be used to improve the accuracy of results with high confidence. The future work on RSD would not be confined to existing data sets but would also include more complex hydrologic components, such as soil moisture content, evaporation and snowpack depth, that need to be calculated based on newly achieved remotely sensed data.

#### **5.3.3 Future work on attribution analysis**

We have determined the sharp changes in hydrological processes under the climate changes discussed in chapter 4, and attribution analysis of the hydrologic component changes is strongly suggested because we have seen the significant impacts of input data on hydrologic components discussed in chapter 2. In the Yarkant River basin, the range of temperature was more dramatic than the variation of precipitation; however, the responses of hydrologic components to meteorological factors were different, with change in some factors having more impact on the hydrological processes. Moreover, human activities such as land use change must directly act on mountain regions in the future. The impact factors will be more complex, and it will be necessary to quantitatively distinguish their impacts. However, most present attribution analyses of climate change are historical (Jiang et al, 2011; Li et al, 2016) and rainfall-runoff is given statistically.

## References

- Axel, T. (2002). Seasonal and spatial variation of evapotranspiration in the mountains of Southwest China. *Journal of Mountain Science*. 20(2): 385-393. Dio: 10.16089/j.cnki.1008-2786.2002.04.001.
- Barthel, R., Reichenau, T. G., Krimly, T., Dabbert, S., Schneider, K., Mauser, W. (2012). Integrated Modeling of Global Change Impacts on Agriculture and Groundwater Resources. *Water Resources Management*. 26(7): 1929-1951. Doi: 10.1007/s11269-012-0001-9.
- Bowling, L. C., Pomeroy, J. W., Lettenmaier, D. P. (2004). Parameterization of blowing snow sublimation in a macroscale hydrologic model. *Journal of Hydrometeorology*. 5(5): 745-762. Dio: 10.1175/1525-7541.
- Braithwaite, R. J. (1995). Positive degree-day factor for ablation on the Greenland ice sheet studied by energy: balance modeling. *Journal of Glaciology*. 41(137): 153-16.
- Chen, Y., Takeuchi, K., Xu, C., Chen, Y., and Xu, Z. (2006). Regional climate change and its effects on river runoff in the Tarim Basin, China. *Hydrologic Processes*. 20(10): 2207-2216. doi: 10.1002/hyp.6200.
- Chen, Y., Xu, C., Chen, Y., Li, W., and Liu, J. (2010). Response of glacial-lake outburst floods to climate change in the Yarkant River basin on northern slope of Karakoram Mountains, China. *Quaternary International*. 226(1-2): 75-81. doi: 10.1016/j.quaint.2010.01.003.
- Chen, R. S.; Kang, E. S.; Ding, Y. J. (2014). Some knowledge on the parameters of China's alpine hydrology. *Advances in Water Science*. 25(3): 307-317.
- Cherkauer, K. A. and Lettenmaier, D. P. (1999). Hydrologic effects of frozen soils in the upper Mississippi River basin. *Journal of Geophysical Research*. 104(D16): 19599-19610.
- Christiaens, J., Feyen, J. (2002). Constraining soil hydraulic parameter and output uncertainty of the distributed hydrologic MIKE SHE model using the GLUE framework. *Hydrologic Processes*. 16(2):373-391.
- Claudia, T., Jan, S. (2012). Bias correction of regional climate model simulations for hydrologic climate-change impact studies: Review and evaluation of different methods. *Journal of Hydrology*. 456-457:12-19. doi:10.1016/j.jhydrol.2012.05.052.
- Fan, Y., Chen, Y., Liu, Y., Li, W. (2013). Variation of baseflows in the headstreams of the Tarim River Basin during 1960–2007. *Journal of Hydrology*. 487: 98-108. doi: 10.1016/j.jhydrol.2013.02.037.
- Fan, Y., Chen, Y., Li, X., Li, W., Li, Q. (2014). Characteristics of water isotopes and ice-snowmelt quantification in the Tizinafu River, north Kunlun Mountains, Central Asia. *Quaternary International*. doi: 10.1016/j.quaint.2014.05.020.
- Fang, G., Yang, J., Chen, Y., Xu, C., De Maeyer, P. (2015). Contribution of meteorological input in calibrating a distributed hydrologic model in a watershed in the Tianshan Mountains, China. *Environmental Earth Sciences*, 74(3), 2413-2424. doi:10.1007/s12665-015-4244-7.

- Fang, G. H., Yang, J., Chen, Y. N., Zammit, C. (2015). Comparing bias correction methods in downscaling meteorological variables for a hydrologic impact study in an arid area in China. *Hydrology and Earth System Sciences*, 19(6), 2547-2559. doi:10.5194/hess-19-2547-2015.
- Gallart, F., Latron, J., Llorens, P., Beven, K. (2007). Using internal catchment information to reduce the uncertainty of discharge and base flow predictions. *Advances in Water Resources*. 30(4): 808-823. Dio: org/10.1016/j.advwatres.2006.06.005
- Gayathri, K. D., Ganasri, B. P., Dwarakish, G. S. (2015). A review on hydrologic models. *International Conference on Water Resources, Coastal and Ocean Engineering (ICWRCOE 2015)*. Aquatic Procedia 4: 1001-1007.
- Ghosh, S., and Katkar, S. (2012). Modeling Uncertainty Resulting from Multiple Downscaling Methods in Assessing Hydrologic Impacts of Climate Change. *Water Resources Management*, 26, 3559-3579, doi:10.1007/s11269-012-0090-5.
- Hock, R. (2003) Temperature index melt modeling in mountain areas. *Journal of Glaciology*. 282: 104-115.
- Hock, R. (2005). Glacier melt: A review on processes and their modeling. *Progress in Physical Geography*. 29(3): 362-391.
- IPCC, 2013. Climate change 2013: The Physical Science Basis. Contribution of Working Group I to the Fifth Assessment Report of IPCC. Cambridge University Press, Cambridge, United Kingdom and New York, USA.
- Jiang T, Chen YD, Xu C, Chen X, Singh VP. 2007. Comparison of hydrologic impacts of climate change simulated by six hydrologic models in the Dongjiang Basin, South China. *Journal of Hydrology*. 336: 316–333. Dio: 10.1016/j.jhydrol.2007.01.010.
- Jiang, S. H., Ren, L. L., Yong, B., Singh, V. P., Yang, X. L., Yuan, F. (2011). Quantifying the effects of climate variability and human activities on runoff from the Laohahe Basin in northern China using three different methods. *Hydrologic Processes*. 25: 2492-2505. Dio: 10.1002/hyp.8002
- Kan, B. Y., Su, F. G., Tong, K., Zhang, L. L. (2013). Analysis of the application of four precipitation datasets in the upper reaches of the Yarkant River, the Karakorum. *Journal of Glaciology and Geocryology*. 35(3):710-722.
- Kang, E. S., Chen, R. S., Zhang, Z. H., Ji, X. B., Jin, B. W. (2007). Some scientific problems facing researches on hydrologic processes in an inland river basin. *Advances in Earth Science*. 22(9):940-953.
- Kang, Y., Cai, H. J., Song, S. B. (2013). Study and application of complexity model for hydrologic system. *Journal of Hydroelectric Engineering*. 32(1): 5-10.
- Kienzler, P. M. and Naef, F. (2008). Subsurface storm flow formation at different hillslopes and implications for the old water paradox. *Hydrologic Processes*. 22(1): 104-116. doi: 104-116, 10.1002/hyp.6687.
- Koivusalo, H., Heikinheimo, M., Karvonen, T. (2001). Test of a simple two-layer parameterisation to

- simulate the energy balance and temperature of a snow pack. *Theoretical and Applied Climatology*. 70: 65-79.
- Krenke, A. N., Khodakov, V. G. (1996). On the correlation between glacier melting and air temperature. *Materialy Glyatsiologicheskikh Issledovaniy, Khronika, Obsuzhdeniya*. 12: 153-164.
- Li, B. F., Chen, Y. N., Xiong, H. G. (2016). Quantitatively evaluating the effects of climate factors on runoff change for Aksu River in north weatern China. *Theoretical and Applied Climatology*. 123(1-2): 97-105. Dio: 10.1007/s00704-014-1314-6.
- Liang, X., Lettenmaier, D. P., Wood, E. F., Burges, S. J. (1994). A simple hydrologicly based model of land surface water and energy fluxes for GCMs. *Journal of Geophysical Research*. 99(D7): 14415-14428.
- Liu, T., Willems, P., Pan, X. L., Bao, A. M., Chen, X., Veroustraete, F. and Dong, Q. H. (2011). Climate change impact on water resource extremes in a headwater region of the Tarim basin in China. *Hydrology and Earth System Science*, 15, 3511-3527. doi:10.5194/hess-15-3511-2011.
- Ma, J. Z., Wang, X. S., Edmunds, W. M. (2005). The characteristics of ground-water resources and their changes under the impacts of human activity in the arid Northwest China—a case study of the Shiyang River Basin. *Journal of Arid Enviroment*. 61(2): 277-295. Dio: org/10.1016/j.jaridenv.2004.07.014
- Michael, H. K.; Christopher, J. N.; John, N.; William, L. (2005). *Applied Linear Statistical Models*, in: McGraw-Hill Education, 2 Penn Plaza, New York, USA.
- Moradkhani, H., Sorooshian, S. (2008). General review of rainfall-runoff modeling: model calibration, data assimilation, and uncertainty analysis. *Hydrologic Modeling and the Water Cycle*. Springer. 291 p. ISBN 978-3-540-77842-4
- Ntegeka, V., Baguis, P., Roulin, E. and Willems, P. (2014). Developing tailored climate change scenarios for hydrologic impact assessments. *Journal of Hydrology*, 508, 307-321. doi:10.1016/j.jhydrol.2013.11.001.
- Onyutha, C., Tabari, H., Rutkowska, A., Nyeko-Ogiramoi, P. and Willems, P. (2016). Comparison of different statistical downscaling methods for climate change rainfall projections over the Lake Victoria basin considering CMIP3 and CMIP5. *Journal of Hydro-environment Research*, 12, 31-45. doi:10.1016/j.jher.2016.03.001
- Pomeroy, J. W., Gray, D. M., Brown, T., Hedstrom, N. R., Quinton, W. L., Granger, R. model: a platform for basing model structure on physical evidence. *Hydrologic Process*. 21(19): 2650–2667.
- Roger, C. B., Noah, P. M., Thomas, H. P., Michael, D. D., Robert, R., Jeff, D. (2006). Mountain hydrology of the western United States. *Water Resources Reserch*. 42(6):1-13.doi:10.1029/2005WR004387.
- Smith, M. B., Koren, V., Zhang, Z. (2012). Results of the DMIP 2 Oklahoma experiments. *Journal of*

- Hydrology. 418: 17-48
- Smith, M. B., Koren, V., Zhang, Z. (2013). The distributed model intercomparison project–Phase 2: Experiment design and summary results of the western basin experiments. *Journal of Hydrology* .507: 300-329.
- Swarowsky, A., Dahlgren, R. A., O'Geen, A. T. (2012). Linking Subsurface Lateral Flowpath Activity with Streamflow Characteristics in a Semiarid Headwater Catchment. *Soil Science Society of American Journal*. 76(2): 532. doi: 10.2136/sssaj2011.0061.
- Tan, G., Xia, J., Li, X. (2004). Hydrologic prediction in ungauged basin. *Journal of Glaciology and Geocryology*. 26(2): 192-196.
- Taylor, K. E., Stouffer, R. J., Meehl, G. A. (2012). An Overview of CMIP5 and the experiment design. *Bulletin of the American Meteorological Society*. 93: 485-498. doi:10.1175/BAMS-D-11-00094.1, 2012.
- Teng, J., Vaze, J., Chiew, F. H. S. (2012) Estimating the Relative Uncertainties Sourced from GCMs and Hydrologic Models in Modeling Climate Change Impact on Runoff. *Journal of Hydrometeorology*, 13(1): 122-139.
- Verseveld, W. J., McDonnell, J. J., Lajtha, K. (2009). The role of hillslope hydrology in controlling nutrient loss. *Journal of Hydrology*. 367(3-4): 177-187. doi: 10.1016/j.jhydrol.2008.11.002.
- Willems, P., and Vrac, M. (2011). Statistical precipitation downscaling for small-scale hydrologic impact investigations of climate change. *Journal of Hydrology*, 402, 193-205. doi:10.1016/j.jhydrol.2011.02.030.
- Williams, W. D. (1999). Salinisation: A major threat to water resources in the arid and semi-arid regions of the world. *Lakes & Reservoirs: Research and Management*. 4: 895-91.
- WMO. (1986). Intercomparison of models for snowmelt runoff. Operational Hydrology Report. 23: (WMONo.646)
- Yang, D., Herath, S., Musiak, K. (2000). Comparison of different distributed hydrologic models for characterisation of catchment spatial variability. *Journal of Hydrologic Procedia* 14(3): 403-416.
- Zhang, Q., Xu, C. Y., Tao, H., Jiang, T. (2010). Climate changes and their impacts on water resources in the arid regions: a case study of the Tarim River basin, China. *Stochastic Environmental Research and Risk Assessment*. 24(3): 349-358. Dio: 10.1007/s00477-009-0324-0.
- Zhou, J., Pomeroy, J. W., Zhang, W., Cheng, G. D., Wang, G. X., Chen, C. (2014) Simulating cold regions hydrologic processes using a modular model in the west of China. *Journal of Hydrology*. 509: 13-24. Dio: 10.1016/j.jhydrol.2013.11.013.
- Zuzel, J. F., Cox, L. M. (1975). Relative importance of meteorological variables in snowmelt. *Water Resources Research*. 11(1): 174-177



# CHAPTER 6

## General conclusion

---

*The main findings of this dissertation on understanding hydrological processes are concluded in this chapter. According to the research objectives, they are given in a logical way to deepen understanding. The general conclusion is given in the last paragraph.*

Because of the great importance of mountainous water resources in arid and semi-arid regions, the hydrological processes of the alpine catchment were inspired to take as the theme of this dissertation. In practical, the Yarkant River basin was chosen as study area. Four research objectives focus on the hydrological modelling work in mountainous region, and four methodologies were used to overcome the challenges of understanding mountainous hydrological processes. Based on research outcome, GCM was coupled to investigate the future changes of hydrological processes under the climate change scenarios.

In order to overcome the restriction of model structure and algorithm by single hydrological model and the insufficient gauged observation for calibration, the joint application of the SWAT and MIKE SHE models in chapter 2 affirmed that either SWAT or MIKE SHE individually could solely deal with all aspects of the hydrological processes, even with the conventional well-calibrated results. Regarding to stream flow, MIKE SHE model fails to simulate the lateral flow, although the model better performed the base flow simulation. Through integration of the simulated results of the two models, we became aware of the constitution of stream runoff in the Yarkant River, to which surface runoff, soil lateral flow, and groundwater contributed approximately 40%, 40% and 20%, respectively. The SWAT model accounted for the temperature on the snowpack surface and the change of the snowmelt factor in snowmelt simulation, suggested the more feasible temporal pattern of snowmelt that 76.8% was concentrated on June to September. The fully distributed MIKE SHE model revealed the clearer snow storage in spatial distribution. It indicated that the snowpack began to gradually shrink from April and expanded to approximately 4500 m in July; the area above 5000 m was permanently covered by solid water. The simulated water body and soil evaporation in the MIKE SHE model was higher than in the SWAT model; however, MIKE SHE produced a clearer spatial evapotranspiration change basing on land use distribution pattern. When the SWAT and MIKE SHE models were combined, their deficiencies in structure and algorithm can be complemented by each other and a better understanding of hydrological processes in the Yarkant River basin was obtained from their integrated results.

The work in reducing uncertainty of input data, RSD including modeling performance and effects on hydrological processes were studied in chapter 3. TRMM was revealed a low-precision detection of rainy days in the Yarkant River basin. The major error was caused by the overestimation of low intensity rainy days. After the problem was detected, LOCI was successfully used to correct the biases in TRMM data. However, its



application in modeling has little effect to improve the simulation results. The LST data produced similar results as TRMM.

Furthermore, by defining the significant impact of input data on outputs in ANOVA, snow storage was chosen to analyze the influence of the differences between SBD and RSD. ANOVA demonstrated that the overestimation and underestimation of TRMM in some partial regions directly caused increased and decreased snow storage in the local region. In addition, when after the transformation of remotely sensed temperatures were used to replace interpolated gauging data in the MIKE SHE model, the main parameters of snowmelt were re-adjusted by auto-calibration, which resulted in a larger snow covered area in the low-middle mountain region and less snow storage volume in the high mountain region. Under the total water balance control in MIKE SHE, when the bigger PET was used to drive model, smaller actual evapotranspiration has been obtained because of re-adjusted parameters in auto-calibration.

Current understanding mainly aims to good future predictions. Therefore, chapter 4 focused on the changes of hydrological processes under future climate change. The investigation of climate change in the Yarkant River demonstrated that the growth in precipitation was moderate and mainly contributed by heavy rain in winter. The warming trend was much stronger than the average global level. It is suggested there are large deviations between RCP4.5 and RCP8.5 after 2060. The warming trend in mountainous regions was lower than in plain regions. After coupling with the hydrological model, results indicated that hydrological processes would be sharply altered by climate change. Increased evaporation dissipation would cause the shrinking of snow storage in high mountain regions and reducing of available water for downstream regions. The variations in permanent snow storage in different elevation bands are quite dissimilar. For the period 2060-2079, the permanent snow covered area below 5600 m could completely vanish and the snow covered area could lift by 600 m. The snow in the 5600-6400 m elevation range could be greatly reduced but little change would occur above 6400 m. Warming would also bring earlier and greater snowmelt, and the spring and early summer stream flow could also be increased following with these variation tendencies. Stronger and more frequent future flood events could occur.

Hydrological processes in alpine catchment of arid and semi-arid region were studied in this dissertation. Chapter 2 and chapter 3 focused on the main challenges in hydrological modeling, and chapter 4 investigated the effects of climate change. It was concluded that the joint application of multiple models can overcome the uncertainties of model structures and algorithms from a single model, and their integrated results

could improve the understanding of entire hydrological processes. After calibration, the uncertainties of input data were hided and could not appear in the hydrography. But its influence on the other hydrological components is significant. The inter-relationships between “effected” and “caused” can be well determined by statistical ANOVA. Hydrological processes were strongly altered under climate change, and the transformation among different forms of water resources could be cause the redistributed of hydrological components in temporal and spatial.

---

## Summary

---

In arid and semi-arid regions, the water resources from mountains dominate the development of oases in downstream. An accurate understanding of the mountainous hydrologic cycle plays a positive role in sustainable water resources management. However, because of the steep topography, a more complex hydrologic cycle, and sparse gauging with low representativeness for mountain regions, hydrological modeling becomes more difficult to handle in high-altitude mountainous catchment. The Yarkant River basin originating from the North Slope of Karakoram was taken the study area in this research work. Based on joint application of multiple hydrological models, remote sensing data and statistical models, the hydrological processes were analyzed. Additionally, the alterations of the hydrologic cycle and the redistribution of hydrologic components were investigated under climate change. The main objectives of this dissertation included the following:

(1) By the joint application of the SWAT and MIKE SHE models, the effects of model structure and algorithms on the hydrological processes were analyzed in terms of runoff, snow and evapotranspiration. The results showed that without multiple objectives calibrations, a single model only can successfully obtained some parts of the natural hydrologic cycle, but not the entire process. The complementarity of the SWAT and MIKE SHE models could overcome most model structural and algorithmic uncertainties and assist in understanding integrated hydrological processes.

(2) Combining with remote sensing data and statistical model, the responses of different hydrological components to input data were analyzed. Taking observations as a benchmark, precision checking and bias corrections were implemented firstly. The corrected TRMM, land surface temperature (LST) of and global potential evapotranspiration (PET) have little efforts to improve the simulation performances at Kaqun station's hydrography. However, on the premise of statistical hypothesis testing implemented by analysis of variables (ANOVA), their significant effects on different hydrological components were investigated Compared with model forcing by interpolated station data, the spatial deviations of snow storage in different elevation bands were more obvious in the TRMM driving model. In the LST driving model, there were larger snow coverage in the low-middle mountain region and less snow in the high mountain region. Additionally, remotely sensed PET driving model produced less transpiration because of the re-adjusted parameters in the auto-calibration.

---

(3) Coupling with the GCMs, the hydrological processes under future climate change scenarios were analyzed. The average ensemble change signals of 21 GCMs in precipitation and temperature were extracted, the modified quantile perturbation method (QPM) and the Delta method were applied to add these change signals into historical observations, then, the variations of hydrological processes under climate change were studied though coupling with the well-calibrated MIKE SHE model. The results suggested that the increased extreme precipitation in winter led to the moderate growth of annual precipitation volume. The warming in the mountain region was slower than in the plains region; moreover, large deviations were revealed between RCP4.5 and RCP8.5 scenarios after 2060. At the end of this century, warming values of  $0.31^{\circ}\text{C}/10\text{a}$  and  $0.59^{\circ}\text{C}/10\text{a}$  were predicted to occur under RCP4.5 and RCP8.5, respectively. Under the climate change, increasing evaporation dissipation would lead to decreasing snow storage in the higher altitude mountain region and likewise with regard to available water in the downstream region. The alterations of snow strong are quite different in elevation bands, the permanent snowpack area below 5600 m would completely vanished in 2060-2079, and the snow storage in 5600-6400 m would be reduced dramatically, however, there is little or no changes in the above 6400 m region. Warming could cause a stronger spring and early summer stream runoff and a reduced late summer flow due to the snowmelt change in temporal distribution. Furthermore, both the frequency and the intensity of the flood would be enhanced. In Karakoram region, more researches are needed about the transient water resources system and the worsening of flood threats in future.

The entire hydrological processes on the catchment scale were concentrated in this paper, and some innovations were brought out to overcome the main challenges. The joint application of multiple models provided a good suggestion to multi-factors evaluation of hydrological model in scarce gauging catchment. ANOVA successfully defined the significant relationships between “effects” and “caused” in hydrological processes, and help to understand the intervallic influences of input data on different hydrological components. The QPM was effectively optimized by considering the frequency changes in the different precipitation intensity ranges. This study makes a progress and supports a reference in high-altitude mountainous hydrological processes and climate change’s influences study.

---

## Samenvatting (Dutch Summary)

---

In droge regio's zijn waterbronnen in de bergen de voornaamste factor voor de ontwikkeling van stroomafwaartse oases. Een goed begrip van de hydrologische cyclus in de bergen is cruciaal voor een duurzaam management van de watervoorraden. De steile topografie, een complexe hydrologische cyclus en een onnauwkeurige schatting met een lage representativiteit voor bergstreken bemoeilijken echter de hydrologische modellering.

Voor deze thesis werd het Yarkant rivierbassin afkomstig van de noordelijke helling van het Karakoramgebergte gekozen als case study. De hydrologische processen werden geanalyseerd door een gezamenlijke toepassing van meerdere hydrologische modellen, remote sensing data en statistische modellen. Bovendien werden de veranderingen in de hydrologische cyclus en de distributie van de hydrologische componenten onderzocht rekening houdend met de invloed van klimaatverandering. De hoofddoelstellingen van de thesis omvatten:

- (1) Door de gemeenschappelijke toepassing van de SWAT en MIKE SHE modellen werden de effecten van modelstructuur en algoritmes op hydrologische processen onderzocht op vlak van afstroming, sneeuw en verdamping. De resultaten toonden aan dat bij afwezigheid van meerdere kalibraties, het gebruik van enkelvoudige modellen slechts delen van de natuurlijke hydrologische cyclus op een correcte wijze kunnen modelleren, maar niet het volledige proces. Simultaan gebruik van de SWAT en MIKE SHE modellen kan de meeste modelstructurele en algoritmische onzekerheden opvangen en kan helpen om inzicht te krijgen in de geïntegreerde hydrologische processen.
- (2) Door het gebruik van waarnemingen als referentie werd de nauwkeurigheid van de modellen geverifieerd en indien nodig gecorrigeerd. Gebruik van de MIKE SHE modellering leidt tot aanvaardbare resultaten voor de verbeterde TRMM, de landoppervlakte-temperatuur (land surface temperature of LST) van MODIS en globale potentiële evapotranspiratie (potential evapotranspiration of PET), maar leidde niet tot een nauwkeurigere simulatie van de hydrografie in Kaqun. ANOVA werd aangewend om de significante impact van de inputvariabelen op de efficiëntie van hydrologische systemen te kennen. De resultaten tonen aan dat de verschillende neerslag- en temperatuurgegevens een belangrijk effect zouden hebben op het sneeuwbehoud; in vergelijking met een model gebaseerd op geïnterpoleerde stationsgegevens modelleert het TRMM-gebaseerd model de ruimtelijke afwijking van de sneeuwopslag in verschillende hoogtebanden correcter. Het LST-gebaseerde model modelleerde ruimere met sneeuw bedekte gebieden in de lage en midden-hoge berggebieden en minder sneeuw in de hoge berggebieden. Aanvullend hadden verschillende PET-waarden een

---

significante invloed op de verdamping en produceerden ze minder verdamping in het teledetectie PET-gebaseerde model.

- (3) De gemiddelde gecombineerde verandering van neerslag- en temperatuursignalen van 21 GCM's werden bepaald door de gewijzigde kwantiele verstoringsmethode (modified quantile perturbation method of QPM) en de Delta methode. Na het toevoegen van historische waarnemingen voor de periode 1986-2005 werden de variaties in hydrologische processen onder klimaatverandering bestudeerd en gelinkt met het correct gekalibreerde MIKE SHE model. De resultaten toonden aan dat de verhoogde extreme neerslag in de winter leidde tot een gematigde stijging van het jaarlijks neerslagvolume. De opwarming in het berggebied ging trager dan op de vlaktes; bovendien werden grote afwijkingen tussen de RCP4.5 en RCP8.5 scenario's na 2060 aangetoond. Op het eind van deze eeuw worden de warmtewaarden van 0.31°C/10a en 0.59°C/10a voorspeld bij respectievelijk de RCP4.5 en RCP8.5 scenario's. Bij de scenario's van klimaatverandering worden de transformaties van verschillende vormen van waterbronnen verwacht de distributie van hydrologische componenten te veranderen. De toegenomen verdamping zou leiden tot een verminderd sneeuwbehoud in hoge bergstreken en minder beschikbaar water in de stroomafwaartse regio's. De sterke veranderingen in sneeuw varieerden voor verschillende hoogteposities.

Het gebied van permanente sneeuw onder de 5600 m zou volledig verdwijnen in de periode 2060-2079 en significante verminderingen kunnen voorkomen op hoogtes tussen 5600 en 6400 m; echter weinig of geen wijzigingen zouden plaatsvinden boven de 6400 m. Met betrekking tot de rivierafvloeiing kan opwarming een sterkere lente, een vroege zomer en een verminderde late zomerstroming veroorzaken door de smeltverandering in de distributie in de tijd. Bovendien zou de frequentie en intensiteit van de overstromingen versterkt worden en de ontstane instabiele waterbronnen en gestegen onveiligheid door overstromingen zou meer aandacht moeten krijgen.

De hydrologische processen in een bergverzamelbekken werden systematisch bestudeerde en enkele vernieuwingen werden benadrukt om de belangrijkste uitdagingen het hoofd te bieden. Eerst werd de gezamenlijke toepassing van meerdere modellen geïmplementeerd om bij te dragen aan het onderzoek naar hydrologische processen. Daarna werden de significante relaties tussen de input en output in het hydrologisch systeem bepaald met behulp van ANOVA. Uiteindelijk werd de QPM geoptimaliseerd door de frequentiewijzigingen in de verschillende bereiken van de neerslagintensiteit in overweging te nemen.

---

## 摘要 (Chinese Summary)

---

在干旱区，山区流域水资源对下游绿洲区的发展具有支配作用，而准确理解山区水循环过程对下游可持续地水资源管理具有十分积极的作用。然而由于极端地形变化、复杂水文过程以及实测站点稀缺等因素，使得山区流域水文过程模拟的难度加大。本文选取了发源于喀喇昆仑山北坡的叶尔羌河流域为例，通过多水文模型的联合应用、遥感技术以及统计分析模型，对高海拔山区流域水文过程进行了分析。进一步通过与 GCM 的耦合，对不同的未来气候变化情景下水循环过程的转变，水文要素的再分布等进行了探讨。研究主要包括了以下几个方面的工作：

(1) 通过 SWAT 和 MIKE SHE 模型的联合应用，从径流、积融雪以及蒸散发水文要素方面分析了模型结构和模型算法对水文过程的影响。结果表明，在缺少多目标的率定情况下，单一模型只能在某些水文要素上取得可行的模型结果，而不能对整体水文过程进行准确描述。整合多模型联合应用的模拟结果，可以减少模型结构和算法的不确定影响，从而提高对流域水文过程的认识。结合遥感数据以及相关研究的交叉验证，整体上明确了叶尔羌河流域的空间水循环过程。

(2) 借助遥感数据和统计模型，分析了输入数据不确定性对水文过程中不同水文要素的影响。首先以站点实测数据为基础，对遥感数据进行了精度验证和偏差校正。校正后的 TRMM, MODIS 以及潜在蒸散发数据在 MIKE SHE 的模拟中并没有提高对卡群站日径流过程的模拟精度。但是，进一步通过统计的多因子方差分析模型，确立了在复杂水文循环系统中“输入”与“输出”之间的显著性影响关系。借助这种显著性影响关系，分析得到了在 TRMM 驱动下，模型得到的积雪分布空间差异更加明显；在 MODIS 温度数据驱动下的模型在中低山区存在更多的永久性薄层积雪，高山区的储雪量减少；在模型的水量平衡控制下，遥感蒸散发驱动的模式在自动率定中通过参数调整，减小了实际的植被蒸腾作用。

(3) 通过 GCM 与水文模型的耦合，探讨了未来气候对研究区水文过程的影响。提取 21 个 GCM 中气候因子的变化信号，通过改进的百分位数波动法和 Delta 法，将变化信号与历史实测数据叠加后，得到未来的降水和温度数据，并用于驱动 MIKE SHE 模型，从流域水平衡角度分析了未来水文过程的变化情况。结果表明，因冬季极端降水的增强，未来叶尔羌河流域的降水呈现小幅度的增长趋势。未来情

---

景下，山区的增温小于平原区，而在 RCP4.5 和 RCP8.5 两种情况下，增温差异很大。到本世纪末，RCP4.5 的增温速度稳定在  $0.31^{\circ}\text{C}/10$  年，而 RCP8.5 将增加到  $0.59^{\circ}\text{C}/10$  年。未来气候变化情景下，叶尔羌河流域的水文过程将发生明显的变化，不同形式的水资源之间的转化改变了水文要素的分布。蒸发耗散的不断增加，使得山区的固体储水量和下游的可用水量减少。流域不同高程带的积雪量变化差异很大，5600m 以下的永久性积雪区将在 2060~2079 年消失，5600~6400m 区域积雪显著减少，6400m 以上基本没有变化。同时，增温导致的前期融雪增加，后期融雪量减少，在出山口卡群站也形成了前期径流增加，后期减少的年内径流过程。极端洪峰流量出现的频率增加，时间提前。未来叶尔羌河流域将面临更加不稳定的水资源情况以及更严峻的洪水安全问题。

本研究关注于流域尺度上水循环过程。针对高海拔山区流域水文过程模拟中的主要问题，开展的流域的模型联合应用，为缺资料地区，提供了有效的模型多要素评价方法；借助于统计分析模型，明确了复杂系统中“输入”与“输出”之间的显著性影响关系，以此确定了输入数据不确定性对不同水文要素的影响；在提取 GCM 降水变化中，通过明确不同分位数段的降水频率变化对百分位数波动法提出了有效地改进，减小了未来降水数据的不确定性。在高海拔山区流域水文过程及其气候变化影响研究方面取得了进展。



---

## Curriculum Vitae (Bibliography)

---

Jiao Liu was born in Chengdou (China) on the 2<sup>de</sup> of November, 1986. In 2009, he graduated from Xichang College and obtained his bachelor diploma of Engineering in the Water Conservancy Project. In 2013, he graduated from the North China University of Water Conservancy and Electric Power and obtained his master diploma of Engineering in Hydraulics and River Dynamics. In the same year, he began his doctoral education at the Xinjiang Institute of Ecology and Geography, University of Chinese Academy of Sciences, and pursued his doctorate at Ghent University.



From September 2013 until June 2017, Jiao worked at the Xinjiang institute of Ecology and Geography and Ghent University on the National Thousand Youth Talents Plan “The study on the hydrological modeling and stream runoff prediction in the scarcely gauged regions of the Traim River basin” (2013-2016).

Jiao has already contributed to several international conferences and is the author of several papers that have been published in leading international journals in the field of hydrology and water resources.